Harmonic Resonance in Power Transmission Systems due to the Addition of Shunt Capacitors

by

Hardik U. Patil

A Thesis Presented in Partial Fulfillment
of the Requirements for the Degree
Master of Science

Approved July 2015 by the
Graduate Supervisory Committee:

Gerald Heydt, Chair
George Karady
Raja Ayyanar

ARIZONA STATE UNIVERSITY

August 2015

ABSTRACT

Shunt capacitors are often added in transmission networks at suitable locations to improve the voltage profile. In this thesis, the transmission system in Arizona is considered as a test bed. Many shunt capacitors already exist in the Arizona transmission system and more are planned to be added. Addition of these shunt capacitors may create resonance conditions in response to harmonic voltages and currents. Such resonance, if it occurs, may create problematic issues in the system. It is main objective of this thesis to identify potential problematic effects that could occur after placing new shunt capacitors at selected buses in the Arizona network. Part of the objective is to create a systematic plan for avoidance of resonance issues.

For this study, a method of capacitance scan is proposed. The bus admittance matrix is used as a model of the networked transmission system. The calculations on the admittance matrix were done using Matlab. The test bed is the actual transmission system in Arizona; however, for proprietary reasons, bus names are masked in the thesis copy intended for the public domain. The admittance matrix was obtained from data using the PowerWorld Simulator after equivalencing the 2016 summer peak load (planning case). The full Western Electricity Coordinating Council (WECC) system data were used. The equivalencing procedure retains only the Arizona portion of the WECC.

The capacitor scan results for single capacitor placement and multiple capacitor placement cases are presented. Problematic cases are identified in the form of 'forbidden response. The harmonic voltage impact of known sources of harmonics, mainly large scale HVDC sources, is also presented.

Specific key results for the study indicated include:

- The forbidden zones obtained as per the IEEE 519 standard indicates the bus 10 to be the most problematic bus.
- The forbidden zones also indicate that switching values for the switched shunt capacitor (if used) at bus 3 should be should be considered carefully to avoid resonance condition from existing.
- The highest sensitivity of 0.0033 per unit for HVDC sources of harmonics was observed at bus 7 when all the HVDC sources were active at the same time.

ACKNOWLEDGEMENTS

I would like to express my sincere gratitude to my advisor Dr. Gerald T. Heydt, for his constant support and encouragement throughout this thesis. Without his patience, motivation, enthusiasm, positive attitude, incredible wisdom, and guidance the completion of this thesis would have been difficult. I could not have any better advisor and mentor for my thesis and I am forever grateful to him. I would also like to thank Dr. George Karady and Dr. Raja Ayyanar for their time and effort to be a part of my graduate supervisory committee.

I would also like to thank an industrial sponsor for the financial support they provided for this thesis. I would also like to thank Messrs. Jeff Loehr and Thomas LaRose for the engineering advice they provided. I am also thankful to Messrs. Brain Keel and Michael Chandler for the advice they provided. I am also grateful to Messrs. Ahmed Salloum and Parag Mitra for guiding me in the software that were used for this thesis.

Finally, and most importantly, I would like to sincerely and gratefully thank my parents, Mr. Ulhas Patil and Mrs. Milan Patil for their faith, unwavering love, continuous motivation and support. I would also like to extend my thanks to my friends and colleagues for their unending love and encouragement.

TABLE OF CONTENTS

Page

CHAPTER Page

CHAPTER Page

APPENDIX Page

LIST OF FIGURES

Figure Page

Figure Page

Figure Page

Figure Page

LIST OF TABLES

NOMENCLATURE

A	Equation Formed of Process Matrix H
A	Coefficient Matrix for Set of Equations
B	Equation Formed of Process Matrix H
B	Vector of Constants
b_1	First Constant in the Vector of Constants
CIGRÉ	International Council on Large Electric Systems
C	Capacitance, F
EHV	Extra High Voltage
F	Frequency, Hz
F	Fundamental Fequency, Hz
GE	General Electric
HVDC	High Voltage Direct Current
H	Process Matrix
H_{real}	Real Component of Process Matrix
H_{imag}	Imaginary Component of Process Matrix
h	Harmonic Order
h	Vector Valued Function of Vector Valued Argument
h_f	Harmonic Frequency, Hz
IEEE	Institute of Electrical and Electronics Engineer
I_{bus}	Column Matrix Showing Current Injection at the Bus
I_k^h	Current Injection at Bus k for Harmonic Order h
$I_{h,519}^{max}$	Maximum Current Injection Limit Imposed by IEEE Standard 519 at Harmonic Order h
ΔI	Change in Current Brought by Introduction of Shunt Capacitance at the Bus
$\Delta I(f)$	Fast Fourier Transform of ΔI

i	Bus Number
j	$\sqrt{-1}$
k	Bus Number
L	Inductance, H
L	Lower Left Triangular Matrix
L_{11}	Element in the First Row and First Column of the Lower Left Triangular Matrix L
MSCDN	Mechanically Switched Capacitor with Damping Network
N	Number of Shunt Capacitors in the Network
n	Number of Storage Elements
PCC	Point of Common Coupling
PDCI	Pacific DC Intertie
PSLF	Positive Sequence Load Flow
PSS/E	Power System Simulator for Engineering
P	Active Power Consumption of Load
Q	Reactive Power Consumption of Load
Q	Size of Shunt Capacitor
Q_{cap}	Size of Shunt Capacitor Bank
RC	Resistor-Capacitor
RL	Resistor-Inductor
RLC	Resistor-Inductor-Capacitor
RMA	Resonance Mode Analysis
R_{DC}	DC Resistance of Stator
R_S	Series Resistance in CIGRE Type C Load Model
R_h	Generator Resistance at Harmonic Order h
SWIS	South West Interconnected System
s	Laplace Variable

s	Slip of an Induction Motor
U	Upper Right Triangular Matrix
U_{nn}	Element in the n^{th} Row and n^{th} Column of the Upper Right Triangular Matrix U
V	Fundamental Frequency Voltage
V_{bus}	Column Matrix Showing Voltages at the Bus
V_k	Voltage at Bus k
V_k^h	Voltage at Bus k for Harmonic Order h
$V_{h,519}^{max}$	Maximum Voltage Limit Imposed by IEEE Standard 519 at Harmonic Order h
V_{11}	11^{th} Harmonic Voltage
V_{13}	13^{th} Harmonic Voltage
ΔV	Change in Voltage Brought by Introduction of Shunt Capacitance at the Bus
$\Delta V(f)$	Fast Fourier Transform of ΔV
$v_{real,i}$	Real Value of Voltage Measured at Bus i
$v_{imag,i}$	Imaginary Value of Voltage Measured at Bus i
WECC	Western Electricity Coordinating Council
W	Weighing Matrix
W	Matrix Product of Upper Right Triangular Matrix U and the Vector of Unknown Elements x
W_1	First Element of the Matrix W
W_2	Second Element of the Matrix W
W_n	n^{th} Element of the Matrix W
X_S	Series Reactance in CIGRE Type C Load Model
X_P	Parallel Reactance in CIGRE Type C Load Model
X_0	Generator Zero Sequence Reactance at 60 Hz
X_d''	Generator Subtransient Reactance at 60 Hz

X_2	Generator Negative Sequence Reactance at 60 Hz
x	Vector of Harmonic State
x	Vector of Unknown Elements
x_1	First Unknown Element of the Vector x
x_n	n^{th} Unknown Element of the Vector x
Y_{bus}	Bus Admittance Matrix
$Y_{cap,k}$	Admittance of Shunt Capacitor Bank at Bus k
Z_{bus}	Bus Impedance Matrix
$\lvert Z_{kk} \rvert$ or $\arg(Z_{kk})$	Absolute Value of Thévenin's Equivalent Impedance at Bus k
$Z(f)$	Impedance in Fourier Domain
$Z_{0(h)}$	Generator Zero Sequence Impedance at Harmonic Order h
$Z_{1(h)}$	Generator Positive Sequence Impedance at Harmonic Order h
$Z_{2(h)}$	Generator Negative Sequence Impedance at Harmonic Order h
Z_{kk}^{h}	Thévenin Impedance at Bus K for Harmonic Order h
$Z_{kk,h}^{max}$	Maximum Value of Thévenin Impedance at Bus k for Harmonic Order h
$Z_{kk,h}^{limit}$	Limiting Value of Thévenin Impedance at Bus k for Harmonic Order h
z	Thévenin Impedance at a Bus
z	Vector of Harmonic Measurements
$z_{real,i}$	Real Value of Impedance Measured at Bus i
$z_{imag,i}$	Imaginary Value of Impedance Measured at Bus i
σ	A Complex Root
ω	Frequency, Radians
ω_r	Rotor Speed
ω_s	Synchronous Speed
η	Measurement Error

Ω	Harmonic Set Including Fundamental
$(.)^T$	Transpose of a Matrix

Chapter 1: Resonance in power transmission systems

1.1 Objectives and goals of this study

The main objectives of this study are the calculations of resonant frequencies in a large electric power transmission system. The system used is an actual power system in southwest United States. There are two subgoals of this work:

> *Study goal A:* Evaluate the transmission system network impedance and determine if there are any areas where resonance conditions could exist today or where the addition of capacitor banks may create a resonance condition. This should form the basis of a system wide plan for dealing with the study of the harmonics when voltage support is added or system topology changes by identifying possible problem areas.
>
> *Study goal B:* Evaluate existing harmonic currents on the transmission system and identify where those harmonic sources are located. Determine if any identified sources may create problems in relation to Goal A, and if there are any ways of mitigating those harmonic sources.

The test bed system described in this thesis is a large scale system in Arizona. A large number of capacitors exist in the Arizona transmission system and more and being added to improve the voltage profile of the system. The addition of these new capacitors could create resonance conditions in the system. Also there exist few unidentified sources of harmonics in the system. These sources could interact with these new capacitors and cause severe disturbance in the system and may also lead to failure.

1.2 The phenomenon of resonance in electric power transmission systems

Resonance is a phenomenon that occurs in AC circuits where the magnitude of the driving point impedance in the circuit passes through an extremum (i.e., maximum or minimum). At the same instant, the phase angle of the driving point impedance also passes through zero indicating that the driving point impedance is totally resistive in nature. Resonance occurs in AC circuits due to the presence of energy storing components: inductors and capacitors. The resonance in an AC circuit occurs at a certain frequency or at several frequencies which are governed mainly by the amount of inductance and capacitance present in the circuit. For an AC circuit that has n number of storage elements have $n/2$ resonant frequencies where n is even or $(n\text{-}1)/2$ when n is odd. This observation is consequence of the fact that an n^{th} order linear ordinary differential equation has an n^{th} order characteristic equation, and when this characteristic equation has complex conjugate roots, those roots correspond to resonances. There are two types of resonances commonly observed in AC circuits the series resonance and parallel resonance. There exist simple methods to calculate resonant frequency for these simple circuits but for large networked circuits more complex calculations are needed. Transmission system components create an RLC circuit which can result in resonance. Shunt capacitor banks are placed in the transmission network to aid the voltage profile of the network. The addition of these capacitor banks affects the entire network and changes its resonant frequencies.

Many devices in power systems use DC power for its operation such as computers, communication equipment, some high efficiency lighting and DC motors that are used in large industrial plants. Rectifiers supply this power requirement. These rectifiers are the

main source of harmonics in power systems. In recent times there has been an increasing use of variable-speed drives which also contribute towards generation of harmonics. Also, high voltage DC (HVDC) systems may be used in transmission network. These HVDC converters are another source of harmonics in the system.

1.3 The literature of resonance in power systems

Any linear AC circuit can be represented by resistors, inductors and capacitors as they are the fundamental passive elements of the power system. Out these three elements, only an inductor and capacitor are called energy storage devices. An inductor stores its energy in the magnetic field while the capacitor stores energy as electric field between its two poles. Both circuit elements vary there impedance with the frequency of the system as $j2\pi fL$ and $\frac{1}{j2\pi fC}$ where f is the frequency, L is the inductance and C is the capacitance. When a number of capacitors, inductors, and resistors are combined, the model which describes this AC circuit is the sinusoidal steady state phasor model. This is equivalent to a high order differential equation. If the number of energy storage elements is n, the characteristic equation of that differential is an n^{th} order polynomial in the Laplace variable s,

$$f(s) = 0. \tag{1.1}$$

The roots of this characteristic equation are at complex conjugate poles, namely $s = \sigma \pm j\omega$. At these frequencies, the magnitude of the driving point impedance of a given bus in the circuit passes through extreme values, i.e. either maximum or minimum values. This phenomenon is called as resonance and the frequency at which this occurs is called the resonant

frequency of the system. Resonance analysis forms an important part of the process involved in shunt capacitive compensation in power transmission systems as occurrence of resonance in transmission systems can cause some problematic operating issues to occur.

Resonance can be a reason for malfunctions in the power system and can also lead to damage / loss of property in some cases [1]. Also the system operation can be affected by resonance. This makes it important to determine where resonance occurs in the system with the aim of mitigating resonance while designing the system. Resonance studies are carried out before making any changes to the system like adding new capacitor banks, increasing existing capacitor bank sizes or changing overhead transmission to underground transmission. A few of the methods used for estimation of harmonics and resonant frequencies are described here.

A. Estimation of harmonic resonant frequencies at a bus by using the current source method

The basic AC model [2] of a power system is

$$I_{bus}=Y_{bus}V_{bus} \tag{1.2}$$

$$V_{bus}=Z_{bus}I_{bus}. \tag{1.3}$$

The Z_{bus} and Y_{bus} matrices are the bus impedance and admittance matrices. Normally these matrices are evaluated at 60 Hz. For studies of resonance, these matrices are evaluated at other frequencies. References [3, 4, 5, 6, 7] discuss the properties of the bus impedance and admittance matrices.

It is possible to use Z_{bus} and Y_{bus} to evaluate the frequency response of a large scale interconnected system. This method uses the idea that the diagonal elements of the Z_{bus} are the Thévenin equivalent impedance at the bus with respect to the ground. In power systems, the capacitor banks are considered to be connected between the bus and the ground. No series capacitors are considered at this point. This configuration creates a case of parallel resonance. Examination of $|Z_{kk}|$ and / or $arg(Z_{kk})$ gives information about resonance at bus *k*. One approach is to allow frequency to 'scan' over a range of values at which the diagonal entries of Z_{bus} are evaluated. This type of analysis is performed for all the harmonics of interest and a frequency versus amplitude plot is created. The points where the extreme values are obtained are the point of resonance. If a maximum value is obtained then parallel resonance occurs at that frequency. If a minimum value is obtained then series resonance is observed at that frequency. In this method, the system bus impedance matrix is evaluated at each frequency. This is done by obtaining the system bus admittance matrix and then inverting the admittance matrix. The diagonal element that corresponds to the location of the desired bus in the Z_{bus} matrix is extracted at each frequency and it is stored. The results at all the desired frequencies are collected for all the desired buses and a subsequent frequency scan is plotted for each bus of interest.

B. Empirical estimation of system parallel resonant frequencies using capacitor switching transient data

Resonant frequencies can be evaluated by using short circuit impedance of the system at the bus where capacitor banks are added [8]. This is not possible for a practical system which has a large number of capacitor banks. This method uses the capacitor

switching transient data which is recorded from various locations in the transmission system as it provides accurate estimation of system parallel resonant conditions. The fast Fourier transform is performed on these data to obtain the spectra for transient waveforms of voltage and current for each phase. By observing the 'bumps' or lobes of same frequencies in both the current and voltage spectra give us the frequencies at which the system is likely to resonate.

An improvement over the method to that described above occurs in [9]. It also uses the capacitor switching transient data in order to estimate the resonant frequencies. In order to properly extract the transient data from the waveforms, the two sets of voltage and current waveforms are taken one when the capacitor is brought into service and other when it is kept offline. The effective transient data are then obtained by subtracting the offline data from the online data. This has the benefit of removing any harmonic content that existed in the waveforms. Fast Fourier transforms are performed on the effective transient data and the impedance estimation is performed as,

$$Z(f) = \frac{FFT\ of\ \Delta V}{FFT\ of\ \Delta I} = \frac{\Delta V(f)}{\Delta I(f)}. \tag{1.4}$$

The terms $\Delta V(f)$ and $\Delta I(f)$ may contain small values of non-resonant frequencies which can give large and misleading impedance estimates [8]. This issue is surpassed by setting such large impedance values to zero for the frequencies which satisfy the condition $\Delta I(f) < x\Delta I(60\ Hz)$, where x ranges between 5% and 15%. Another heuristic which uses voltage is

$$V(f) < xmax[\Delta V(60\ Hz)],$$

where x ranges between 5% and 25% [9].

C. State estimation of power system harmonics by using synchronized measurements

The harmonic state estimation is formulated as [10],

$$z=h(x)+\eta \tag{1.5}$$

where, z is the vector of harmonic measurements and x is the vector of harmonic state. In (1.5), η denotes the measurement error and h is a vector valued function of vector valued argument and h describes the process. The bus voltages are considered as system state. The phase voltage is expressed as,

$$Re\left\{ \sum_{i\epsilon\Omega} e^{j(i\omega t)} \left(v_{real,i}+jv_{imag,i}\right);\ \Omega:\ \text{harmonic set including fundamental}\right\}. \tag{1.6}$$

Here the terms $v_{real,i}$ and $v_{imag,i}$ are considered as state variables and one of this set exists for each harmonic. The measurements are obtained as $z_{real,i}$ and $z_{imag,i}$ and are expressed in the form,

$$Re\left\{\sum_{i\epsilon\Omega} e^{j(i\omega t)} \left(z_{real,i}+jz_{imag,i}\right);\ \Omega:\text{harmonic set including fundamental}\right\}. \tag{1.7}$$

From these measurements, the state variables can be obtained by using the relationship,

$$\begin{bmatrix} A & B \\ -B & A \end{bmatrix} \begin{bmatrix} x_{real} \\ x_{imag} \end{bmatrix} = \begin{bmatrix} H_{real}^T Wz_{real} + H_{imag}^T Wz_{imag} \\ H_{real}^T Wz_{imag} - H_{imag}^T Wz_{real} \end{bmatrix} \tag{1.8}$$

where, H is the process matrix which models the asymmetric control variables in the transmission system and W is the weight that is applied when the non-diagonal elements are zero. The elements A and B are given as,

$$A = H_{real}^T H_{real} + H_{imag}^T H_{imag} \tag{1.9}$$

$$B = H_{imag}^T H_{real} - H_{real}^T H_{imag}. \tag{1.10}$$

D. Harmonic current vector method

The harmonic current vector method [11] was devised so as to study the contribution of utility and the consumers to the harmonics in the system. In this method, the system to be studied is simplified by creating a Norton equivalent circuit for both the utility side and the customer side at the point of common coupling (PCC). Thus each side now has its own equivalent harmonic current source and harmonic impedance for one specific frequency. Thus, the Norton equivalent circuit needs to be recalculated for each and every frequency of interest. This method can also be used when there are periodically varying loads on the system and where switching capacitor banks are used. This is done by considering a constant impedance case and representing the customer side and utility side impedances under this situation as the reference. The variation in the impedance values on any side of the PCC is represented as change to the current source on that side. The harmonic

voltages and currents are measured only at the point of common coupling and the contribution from each side is found out by using the principle of superposition. The contributions from each side are then projected onto the current flowing through the PCC to obtain the contribution factors. Depending on the contribution factors, the rates to be imposed in case of violation of the harmonic limits are decided.

The harmonic current vector method is a very simple method but has one problem that is the customer and utility side impedances are required. It is easy to get these at power frequencies but their frequency characteristics are unknown. This can be very easily explained by considering a case where the customer has an RLC load which is does not have any harmonic source of its own. This load can simply cause high harmonic current amplification if supplied from the utility side with a harmonic current that has the same frequency as its series resonant frequency. The basic harmonic current vector method described above does not consider this case. This problem is overcome by making use of reference impedances [11, 12]. This replaces the utility side impedance and customer side impedance in the equivalent circuit with reference impedances on both sides. The difference between the actual impedance and reference impedance is transferred to an additional harmonic current source. The reference impedance is defined on the basis of measurements taken at the PCC. This results in the customer load resistive component to be introduced as the reference impedance. The customer load is represented as parallel connection of resistance and reactance and only the current through the reactance is transferred to the additional current source. If needed, the skin effect can also be considered. Thus the customer is treated as resistive load and any deviation causing harmonic amplification is shown as additional harmonic source. A similar approach is used when finding the reference impedance for the

utility side. The utility side impedance is generally considered as the impedance of the last transformer before the PCC. Following the later procedures as mentioned in the basic harmonic current vector method described above will give the rates to be imposed in case of violation of the harmonic limits.

1.4 Power system models at frequencies greater than 60 Hz

A. Transformers

The transformer model that is used in power flow studies can be used to a certain extent in harmonic analysis of the system. Though this model fails to consider some of the effects that occur at higher frequencies, it is generally found to be accurate for analysis up to 13^{th} harmonic. For higher frequencies, generally more complex models are used. Though it is not properly known which of the many models available serve the purpose the best, each of them has its own advantages and drawbacks. The power system transformer model, consist of both the winding series impedance and the shunt core impedance of the transformer coupled to an ideal transformer. The winding impedance on both the sides can be transferred to either of the two sides and added to the winding impedance on that side to create the effective series impedance of the transformer. The shunt core loss impedance can be represented on either of the two sides.

B. Overhead transmission lines

The modeling of overhead transmission lines and transmission lines has been documented over a wide range of frequencies in the literature. Typically a transmission line is modeled as a coupled equivalent-pi circuit [13]. But the series impedance per unit length

is frequency dependent due to the line inductance and the skin effect of the conductor. The series impedance values per unit length are calculated by using the physical construction of the line through established methods [14, 15]. In order to properly account for the frequency dependent components, calculation should be made for each concerned frequency. Long line effects are also needed to be considered if the line is very long or if the frequency is very high. It is a general practice to employ long line models if the line length exceeds 150/*h* miles where *h* is the harmonic order. It is also observed that for line that have lengths of 250 km for third harmonic and 150 km for fifth harmonic, transpositions are ineffective and can cause increased unbalance in the system [16]. The underground cables are also modeled very similar to an overhead transmission line. But in the case of underground cables, long line models apply when the length exceeds 90/*h* miles.

C. Rotating machines

The synchronous and induction machines are the AC rotating machines that are used in the power industry. The synchronous machines are generally used as generators while the induction machines finds application as motor. The rotating magnetic field in these machines has a speed that is significantly higher than rotor due to the stator harmonics [13]. Thus the machine impedance approaches the negative sequence impedance. In both these machines, we obtain the inductance in different ways but one fact that is the frequency dependence of the resistance may be important due to skin effect and eddy current losses. In cylindrical rotor synchronous machine, a negative current injection of order *h* in the stator results in generation of rotor flux having an order of *h*+1 [17]. This causes an induc-

tion of negative sequence voltage of order h in the stator. A similar case results with the injection of positive sequence current of harmonic order h, the only difference is that the induced rotor flux has an order of $h-1$. In salient pole synchronous machines, it is a very different case. A negative current injection of order h in the stator results in creation of two counter-rotating rotor fluxes having order of $h+1$. This causes induction of negative sequence voltage of order h and positive sequence voltage of order $h+2$ in the stator. Similar observations are made when positive sequence currents of harmonic order h are injected creates two counter-rotating fluxes of order $h-1$. This results in generation of positive sequence voltage of order h and negative sequence voltage of order $h-2$ in the stator. This then again goes on repeating for order of $h-2$ and higher in the stator. Thus the salient pole synchronous machine acts as generator of harmonics contrary to popular belief [13]. There is a very complex model given in reference [17] which describes the process that develops the model which takes into account the above mentioned harmonic generation phenomenon. A simple model which can used in harmonic analysis is as follows [18],

$$Z_{0(h)}=R_h+jhX_0 \quad h=3,6,9... \tag{1.11}$$

$$Z_{1(h)}=R_h+jhX_d'' \quad h=1,4,7... \tag{1.12}$$

$$Z_{2(h)}=R_h+jhX_2 \quad h=2,5,8... \tag{1.13}$$

where, X_0, X_d'' and X_2 are the generator zero sequence, subtransient and negative sequence reactances at fundamental frequency and the resistance at harmonic frequencies is given as,

$$R_h = R_{DC}\left[1 + 0.1\left(\frac{h_f}{f}\right)^{1.5}\right] \tag{1.14}$$

where, R_{DC} is the DC resistance of the stator, h_f is the harmonic frequency in Hz and f is the fundamental frequency.

A similar phenomenon is also known to occur in induction machines [18]. But an induction machine, the rotor speed has a slip s

$$s = \frac{\omega_s - \omega_r}{\omega_s} \tag{1.15}$$

where, ω_r is the rotor speed and ω_s is the synchronous speed. This slip affects the frequency of the flux as the multiplier $h-1+s$ times the baseband (60 Hz) frequency for positive sequence current injection of harmonic order h. The multiplier $h+1-s$ is applied for negative sequence current injection of harmonic order h. A simple model used in harmonic analysis of induction machine is given in reference [18].

D. System loads

The selection of the model for the load that is connected to the transmission system is very essential for the proper assessment of harmonic resonance magnitude of the system [13]. But there exist no generally applicable model that can define each and every load. So if detailed studies are supposed to be conducted then there is need to perform measurements and evaluations for every case. But there are still few simple load models which can be used for harmonic analysis. One of these simple models is the simple RL and RC circuits

as shown in Fig. 1.1 (a) and (b) [18]. The individual components in these two models can be calculated from the voltage, apparent power and power factor. Another simple model is the CIGRÉ type C load model as shown in Fig 1.1 (c). This model has been derived experimentally. This model can be used for bulk power loads and is valid between 5^{th} and 30^{th} harmonics. The parameters in this model can be obtained as,

$$R_s = \frac{V^2}{P} \tag{1.15}$$

$$X_s = 0.073 h R_s \tag{1.16}$$

$$X_p = \frac{h R_s}{6.7 \frac{Q}{P} - 0.74} \tag{1.17}$$

where V is the fundamental frequency voltage, P is the real power, h is the harmonic order and Q is the reactive power.

1.5 Case studies

For the purpose of discussing and illustrating the resonance phenomenon in power systems, it is useful to examine case studies. References [20] – [23] are a few samples (taken from the many examples) of case studies that have appeared in the literature. A few interesting cases are produced here for discussion.

A. *Resonance analysis in German transmission system*

Resonance analysis for the transmission system in Germany has been carried out

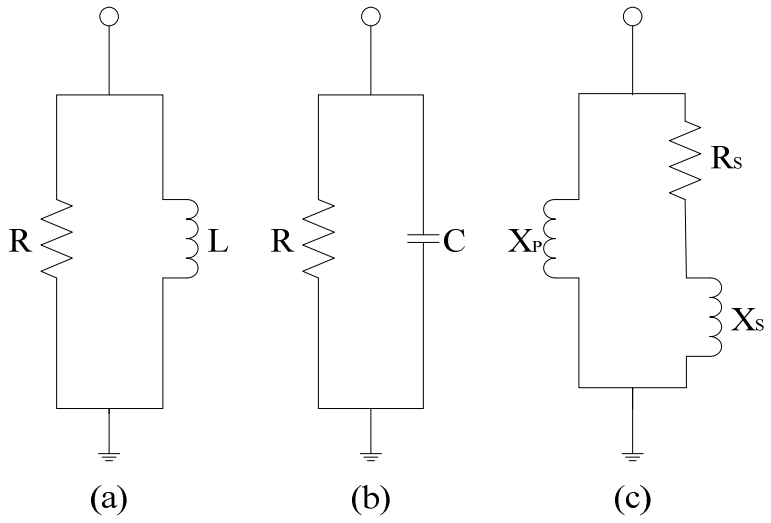

Fig. 1.1 Three Simple Load Models used for Harmonic Analysis
(taken directly from [18])

and documented in [20] by the Resonance Mode Analysis (RMA) method at different operating conditions. The extra high voltage (EHV) transmission network used for this analysis has 268 buses, 244 transmission lines, 8 two-winding and 17 three-winding transformers, 57 linear loads, 35 generators, 9 bus-bar connectors, 9 reactors, and 1 C-type capacitor bank with damping network (MSCDN). Two loading scenarios were considered. In the first scenario, system is operated under low load conditions in which most of the loads exhibit capacitive nature. All the reactors are connected in the network to balance the capacitive reactive power and the MSCDN is disconnected. In the second scenario, the system is operated under high load condition and the behavior of the load is inductive in nature. All the reactors are not needed and are thus turned off. But the MSCDN is turned on to supply reactive power. Also the switching scenarios (tests) of are different. The frequency scan modal impedance curves are plotted for both the cases for positive and zero

sequence components in [20]. The results of the simulations performed reflect that the system resonant behavior changes as the load behavior and power system elements switching conditions change.

B. Harmonic propagation in transmission system with multiple capacitor installations

As an example of published work on harmonics in a power transmission system, consider a case history from Australia. There has been rapid development in the South West Interconnected System (SWIS), the main transmission system in Western Australia in recent years [21]. New capacitor banks were installed to improve voltage profile and compensate for reactive power. These new capacitor banks created resonance conditions which then later affected the utility and customer equipment. Harmonic voltage and current measurements were taken at various buses in the transmission network. The fifth harmonic voltage at 132 kV Cannington terminal was found to exceed the limit prescribed by the Western Power technical requirements. Switching on the 132 kV capacitor bank connected to this bus causes an increased fifth harmonic current to flow in the capacitor banks. At certain times, it was observed that the capacitor bank was attracting an additional fifth harmonic current from the low voltage circuit through the substation transformer. Another bus Mason Road, was found to be the source of distortion caused at Cannington terminal. The fifth harmonic voltage at 132 kV level and current in the transmission line were found to exceed the limit specified by Western Power technical requirements.

C. Failure of 13.8 kV switchgear and loss of plant due to harmonic resonance

The Eurocan Pulp and Paper mill located at Kitimat, British Columbia, Canada is feed by BC Hydro and Alcan by a single 287 kV feeder [22]. This power is then converted

to 13.8 kV by using two separate transformers each rated at 50 MVA. The switchgear of this plant is arranged in such a way that power can be taken from either system independently. In order to facilitate this, a 13.8 kV standby incoming tie circuit breaker which is normally open is used after the transformer which connects BC Hydro system to the plant. In order to adjust for the plants power factor, a large bank of capacitors is used on the 13.8 kV bus. BC Hydro and Power Authority had noticed "occasional occurrences" of fifth harmonic voltage waveforms. The mill itself had 8 MW of paper machine thyristor DC drives. These drives are the main source of producing 5^{th}, 7^{th}, 11^{th}, 13^{th}, 17^{th}, 19^{th} and such other harmonics in the system. On 24^{th} June 1986, the standby incoming tie circuit breaker faced a major failure which resulted in a catastrophic fire that completely destroyed the mill. An investigation that followed found out that the system was resonating at 4.99 times 60 Hz for a total period of 4 minutes before the catastrophic failure.

D. Failure of 20 kV capacitor bank fuses

In the suburban regions of the city of Shiraz in Iran, exists a sub-transmission 63/20 kV substation [23]. The substation consists of two 40 MVA wye-grounded/delta transformers which are equipped with two 1200 A grounding transformers. On the 20 kV bus of this substation, four 2.4 MVAr capacitor banks are connected. This substation is feeding a steel rolling factory. The power authority that is Fars power grid experienced an outage of capacitor bank in this substation. This outage had occurred due to blowing up of the capacitor fuse. The investigation that followed into this revealed that the fuse link did not blow due to a problem with the capacitor bank. It was also observed that a large fifth harmonic distortion was present on the feeder when the steel rolling mill was operating. Further inves-

tigations proved that this caused a very high distorted current of the order of 3.2 times the fundamental current flowed through the fuse which caused it to melt in 15 seconds.

1.6 Sources of harmonics

Since the very beginning stages of the modern AC power systems, harmonic voltages and currents have been present [24]. The main reason for this is the battle between AC and DC systems. In the long term, AC systems have largely become standardized worldwide. The main sources of harmonics are inverters and rectifiers.

One industrial application of rectifiers is for the energization of DC motors. The main reason for survival of the DC machine is the controllability of the DC motor. Rectifiers are used to energize DC machine loads. These power converters use electronic switches. All harmonics producing devices are found to have one common trait that is they have a non-linear voltage-current operating relationship [25]. DC motors are mainly used in paper mills and other special applications where speed control is needed. There are many other applications which require DC. It is arguable that more than one-third of loads are electronically controlled, and many of these loads require DC.

A discussion of rectifiers as harmonic sources appears in [17]. Other sources of harmonics are documented in [27].

It is also found that the traditional electromagnetic devices also produce harmonics. One such device is the salient pole synchronous machine which is described above as a source of harmonic. Relating to transformers [25], inrush current that flows on energization

contains low order harmonics (e.g., 2^{nd}, 3^{rd}, 4^{th}). Also overexcited transformers exhibit harmonic voltages. Other industrial devices which result in harmonics are discussed in [28, 29].

1.7 Organization of the thesis

This thesis has been divided into six chapters. Chapter 1 gives a background on resonance occurring in transmission system. It talks about the various methods used for evaluating resonance, high frequency models of power system components, case studies and sources of harmonics. Chapter 2 discusses about the various software tools used for obtaining steady state AC response of the system. It also describes the test bed system used for analysis, method used for obtaining system impedance and admittance matrix and the calculation of driving point impedance at the bus. The discussion on frequency scan and capacitance scan is also included in this chapter.

In Chapter 3, the results for single capacitor bank placement and multiple capacitor bank placements cases are shown and discussed. In Chapter 4, the method for calculation of forbidden zones is described and the forbidden zones thus obtained are discussed. In Chapter 5, the impact that HVDC sources have on the system was evaluated. The conclusions and recommendations are listed in Chapter 6.

Appendix A describes the forward and backward substitution method in calculation of the value of x in $Ax=b$. Appendix B describes the Matlab code developed to perform harmonic analysis for single capacitor placement and multiple capacitor placement cases. Appendix C shows a few of the phase angle plots that were used to verify the resonance

point observed. Appendix D describes the code developed to evaluate the impact of HVDC sources on these buses.

Chapter 2 The calculation and analysis of resonance using commercial software tools

2.1 Pertinent commercial software tools

The electric power industry has produced a number of valuable software tools for the analysis of large scale transmission systems. The effort that has gone into the development of these tools is considerable. In these tools, components in the transmission system are modeled in some detail including such complications as multi-winding transformers, transmission line long line models, status of series and shunt capacitors, and generator models and status. Since this research focuses on transmission systems, and on the steady state AC response of these systems, the software tools that are appropriate include PSS/E [32], PowerWorld Simulator [33], PSLF [34], and Matlab. Because actual data were used, and those data were in PSLF format, this software tool was used. Also, the equivalencing and input / output capabilities of PowerWorld Simulator were used. In this chapter, some of the analysis details of these software tools are explained and applied to the harmonic analysis problem. Matlab was used for post-processing of results.

2.2 System data used

The system used here is the complete WECC transmission system. The details of this system are given in the Table 2.1. But for this thesis, only the transmission network in Arizona is looked at. Thus the entire WECC transmission network is equivalenced to retain only the Arizona transmission system. The details of the system after it is equivalenced is also given in Table 2.1.

Table 2.1 Test Bed System Data Description

Before equivalencing (full system)	Number of buses	21442
	Number of lines	17347
	Number of generators	3891
	Number of areas	21
After equivalencing	Number of buses	2770
	Number of lines	2035
	Number of generators	272
	Number of areas	1

2.3 The system impedance and admittance matrix from the system data

The system data exists in the GE Concorda PSLF software file format '.sav'. This system data consists of the entire WECC system. This system data contains information about the buses, generators, transformers, lines, loads, shunts, static var devices, taps, Qtable, interface, DC bus, DC line, DC converter, branch interface, motors, areas, zones, owners, interfaces, branch interfaces, transactions, Ztable and line conductors. This complete system data is then converted to '.epc' format by using PSLF software so that PowerWorld Simulator V17 can read this data. This system data is then equivalenced in order to retain the system for Arizona. This is done by inputting the area number of Arizona in the equivalencing interface of the PowerWorld Simulator V17. The result is that all of the buses in the WECC system outside Arizona are removed and the equivalent circuit is retained as shown in Figure 2.1 [30].

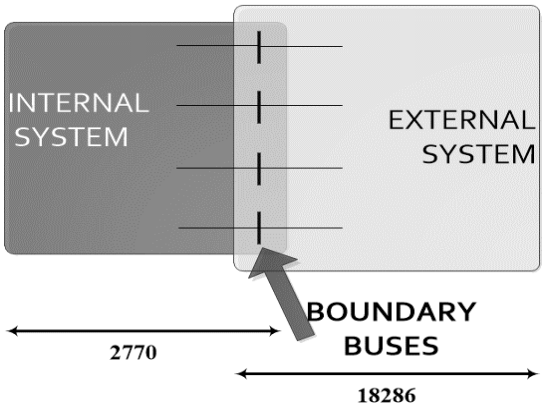

(a) Original system (number of buses shown)

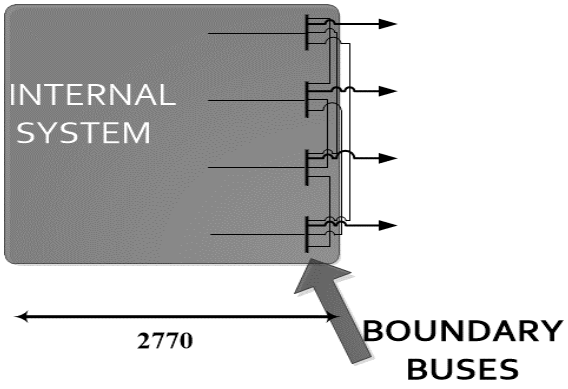

(b) Equivalenced system (2770 buses retained)

Fig. 2.1 The Original Network and its Equivalenced Network

Equivalencing a circuit is a reduction of the network external to that under study. This is not an approximation. Equivalencing is an exact representation of the external portion of the network. However, the external buses are no longer represented in detail in the model, namely the admittance matrix.

From the equivalenced circuit, the system bus admittance matrix is obtained. The

bus admittance matrix being modeled in PowerWorld Simulator V17 consists of only transmission lines, transformers, line shunts, switched shunts and bus shunts [31]. The generators are modeled as open circuits while the loads are modeled as short circuits to the ground. This Y_{BUS} that is obtained for the equivalent circuit is a sparse matrix and can be exported to both Microsoft Office Excel and Matlab. Fig. 2.2 shows a pictorial of the approach used.

2.4 Calculation of driving point impedance

The Y_{BUS} that was obtained by the above method was exported in to both Microsoft Office Excel and Matlab. The analysis was done using Matlab but the Y_{BUS} was exported to excel so as to know the position of the required buses in the Y_{BUS}. In Matlab, the few island buses in the system were removed and consequently the same was done in the Excel copy of Y_{BUS} to keep consistency. Then the Y_{BUS} was used to find voltages V in Matlab by forward/backward substitution,

$$V = Y \backslash I \tag{2.1}$$

At bus k, if an injection of 1.0 p.u. current is considered, the corresponding value of V_k at bus k will give the Z_{kk} at the bus. The Z_{kk} at bus k is the Thévenin equivalent impedance of the network at bus k.

Shunt capacitor banks are added at certain buses. This modifies the system Y_{BUS} at the diagonal elements that correspond to those buses. The location of these buses in the Y_{BUS} is found from the modified Excel file. In Matlab, the modified Y_{BUS} after the removal of the island buses, is modified at the diagonal elements. The modification of Y_{kk} is accompli-

shed by adding the capacitive admittance $Y_{cap,k}$. The capacitive admittance is,

$$Y_{cap,k} = \frac{jQ_{cap}}{|V_k|^2}. \tag{2.2}$$

The per unit value of the capcitive admittance is subtracted from the diagonal element of Y_{BUS} to give the modified Y_{BUS} which includes the shunt capacitors.

The Y_{BUS} obtained is correct for 60 Hz, but analysis is also required to be done for higher frequencies. This can be done by modifying the elements of the Y_{BUS}. Summing the elements in a row of the Y_{BUS}, gives the net admittance tie to ground at the artifact bus; and the negative of the off diagonal elements are the net admitance between the two buses. From these Y_{BUS} matrix entries, the primitive circuit impedances are obtained and the signs of their imaginary parts are examined. If the imaginary portion of the primitive circuit component impedance is positive, that circuit impedance is assessed to be inductive and therefore the corresponding reactance is the 60 Hz reactance multiplied by the harmonic order h. If the primitive circuit component reactance is negative, that reactance is assessed to be capacitive and the conversion to the higher frequency reactance is accomplished by dividing the 60 Hz value by h. These new impedance values described above are then again converted to admittance and replaced in the Y_{BUS}. While doing so, it is important to note that off diagonal elements are the negative of admittance between two buses and diagonal elements are the sum of the admittance between two buses and the net ground tie at that bus. The Y_{BUS} is then inverted to obtain the Z_{BUS} at the required frequency by the method discussed above.

2.5 Frequency scan

Frequency scan is very popular method that is been used to find resonances that occur in a circuit. A typical frequency scan for a parallel resonance condition is shown in Figure 2.3. Parallel resonance occurs in the system when the inductors and capacitors are connected parallel to each other. Under these circumstances, when resonance occurs, the system impedance reaches a maximum value. If there are multiple such resonant frequencies in the system, there will exist that many maxima each of which corresponds to one resonant frequency. The frequencies between which half the absolute magnitude of the Thévenin equivalent at the bus k, that is $\frac{1}{2}|Z_{kk}|$, defines the bandwidth as shown in Figure 2.3.

2.6 Capacitance scan

A frequency scan (i.e., a plot of driving point impedance magnitude versus frequency) is a useful method but this tool does not illustrate the impact of variation of the shunt capacitor value. This is not useful in studying the rating of capacitance bank and a concomitant assessment of the value that causes resonance. Also frequency scans are done for all frequencies, while in a power system, only integer multiples of baseband frequency are injected. Also frequency scans are done for all frequencies, while in a power system, only integer multiples of baseband frequency are injected. A capacitance scan has been used here for the purpose of analysis. Instead of keeping the rating of capacitance bank fixed as done in a frequency scan, frequency is kept fixed and the reactive power rating of capacitance bank (i.e., Q) is varied from zero to a suitable value. The magnitude of driving point Thévenin impedance $|Z_{kk}|$ is plotted versus frequency. The reactive power of the

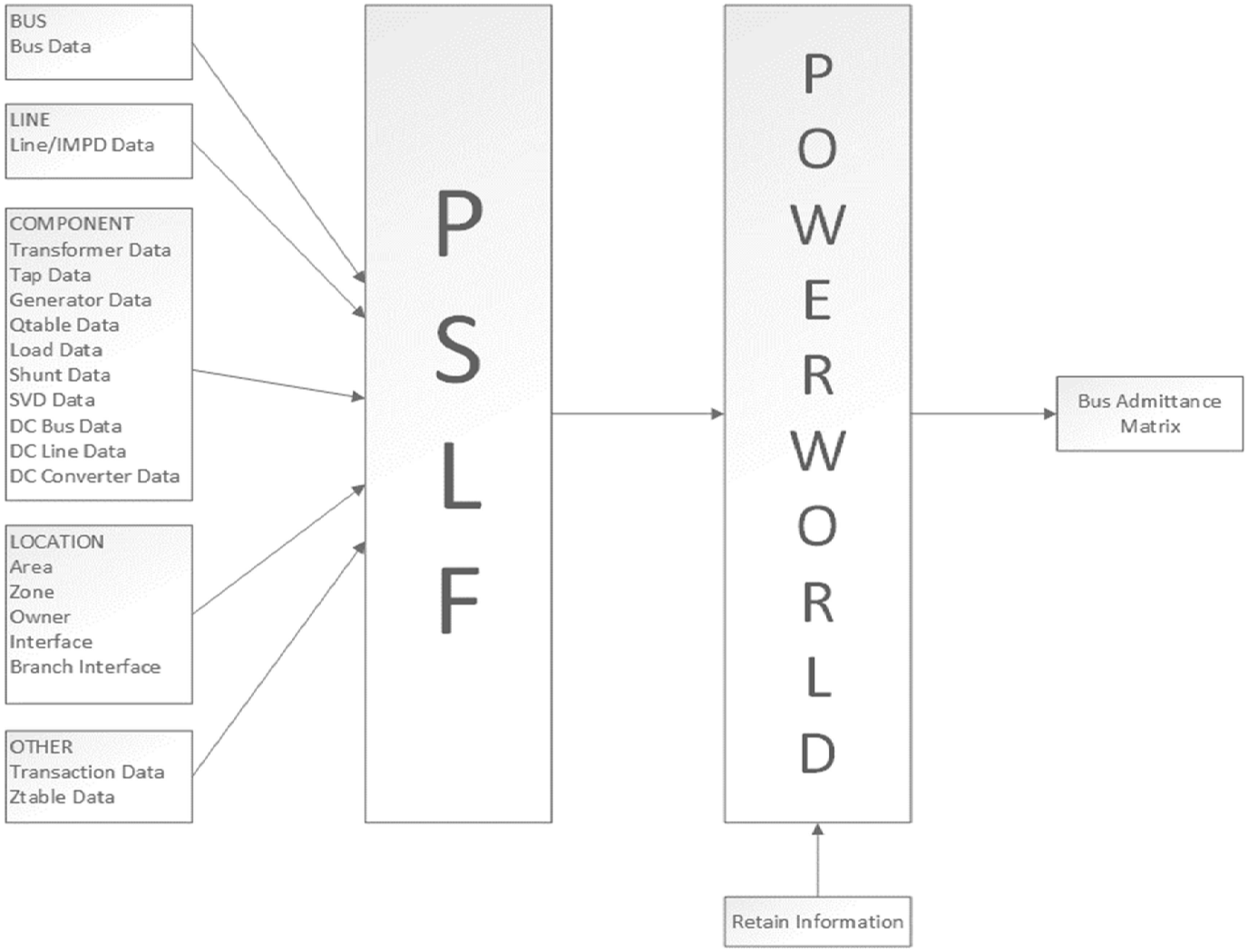

Fig. 2.2 The Flow for Obtaining The System Bus Admittance Matrix

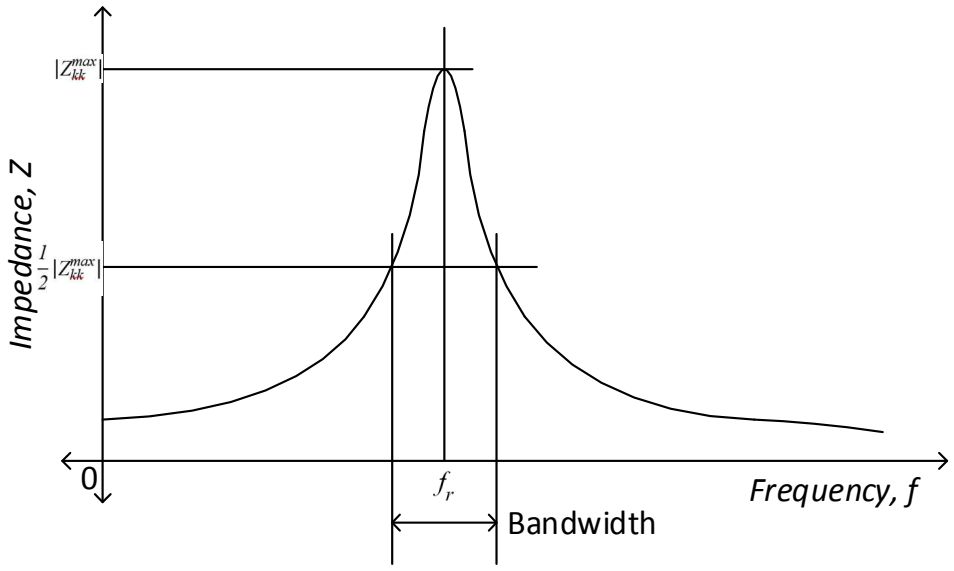

Fig. 2.3 A Typical Frequency Scan for Parallel Resonance

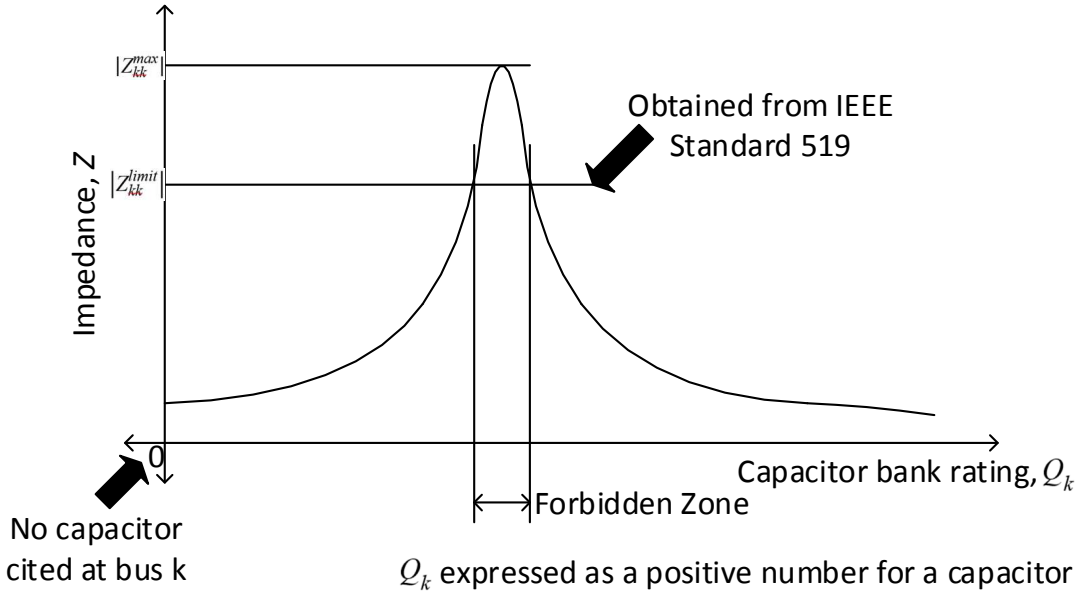

Fig. 2.4 A Typical Capacitance Scan

capacitor bank is expressed as a positive number for the sake of simplicity.

The driving point impedance at the capacitor siting bus is used to assess the resulting harmonic voltage magnitude at that bus. From the capacitance scan, the maximum value of $|Z_{kk}|$ is then multiplied by the maximum per unit value of current permissible as per the IEEE Standard 519. The resulting value of the $Z_{kk}I_k$ is a voltage and this voltage magnitude is the worst (maximum harmonic voltage) case scenario. This voltage is then compared to the maximum as per the IEEE Standard 519. Corresponding to the scenarios that exceed the IEEE 519 harmonic voltage limit, the value of $|Z_{kk}|$ are labeled in a band of forbidden values on a pictorial range of Q. If more than one frequency is being considered, similar analysis is needed for those frequencies. It may also be a case that for different frequencies, these forbidden zones may overlap. Fig. 2.4 shows this concept.

2.7 Summary

In this chapter, a software based method has been outlined for the analysis of a transmission system for harmonic resonance. The method is suitable for a large scale transmission system. Equivalencing is used to focus on a given area of a large interconnected system. The software tools PSLF, PowerWorld Simulator and Matlab are used to system planning data (in PSLF) which is subsequently equivalenced (by PowerWorld Simulator) and exported to Matlab.

The harmonic resonance analysis is accomplished using a capacitance scan. The basis of the analysis is the use of IEEE Standard 519 and its harmonic current and voltage

limits. Appendix B shows the Matlab code used to modify Y_{bus}, and create the capacitance scans.

Chapter 3 Analysis using planning case data

3.1 Explanation and presentation of results

In this chapter, the test bed described in Chapter 2 is used to assess the harmonic resonance impact of shunt capacitor placement. The analytical methods described in Chapter 2 are used for this assessment. The results are organized for two cases:

- Single shunt capacitor placement
- Multiple shunt capacitor placement.

3.2 Results for single capacitor placement

Analysis of the system was done by using the algorithm described in Chapter 2 coded in Matlab. The magnitude and phase angle plots were obtained for the driving point impedance at the buses at which the shunt capacitors are placed. The magnitude plots are shown here as arranged in Tables 3.1 and 3.2. A sampling of the phase angle plots are shown in the Appendix C. The phase angle plots were mainly used to verify the location of the resonance point. In this case, it was considered that the capacitor bank at the bus under consideration was the only newly added capacitor in the system. Ten buses are considered. The shunt capacitors other than at the ten artifact buses were considered to be in service in the base case.

Table 3.1 Listing of The Results for Figures 3.1 to 3.25

Figure	Bus	Harmonic order
3.1	1	1
3.2	1	5
3.3	1	7
3.4	1	11
3.5	1	13
3.6	2	1
3.7	2	5
3.8	2	7
3.9	2	11
3.10	2	13
3.11	3	1
3.12	3	5
3.13	3	7
3.14	3	11
3.15	3	13
3.16	4	1
3.17	4	5
3.18	4	7
3.19	4	11
3.20	4	13
3.21	5	1
3.22	5	5
3.23	5	7
3.24	5	11
3.25	5	13

Table 3.2 Listing of The Results for Figures 3.26 to 3.50

Figure	Bus	Harmonic order
3.26	6	1
3.27	6	5
3.28	6	7
3.29	6	11
3.30	6	13
3.31	7	1
3.32	7	5
3.33	7	7
3.34	7	11
3.35	7	13
3.36	8	1
3.37	8	5
3.38	8	7
3.39	8	11
3.40	8	13
3.41	9	1
3.42	9	5
3.43	9	7
3.44	9	11
3.45	9	13
3.46	10	1
3.47	10	5
3.48	10	7
3.49	10	11
3.50	10	13

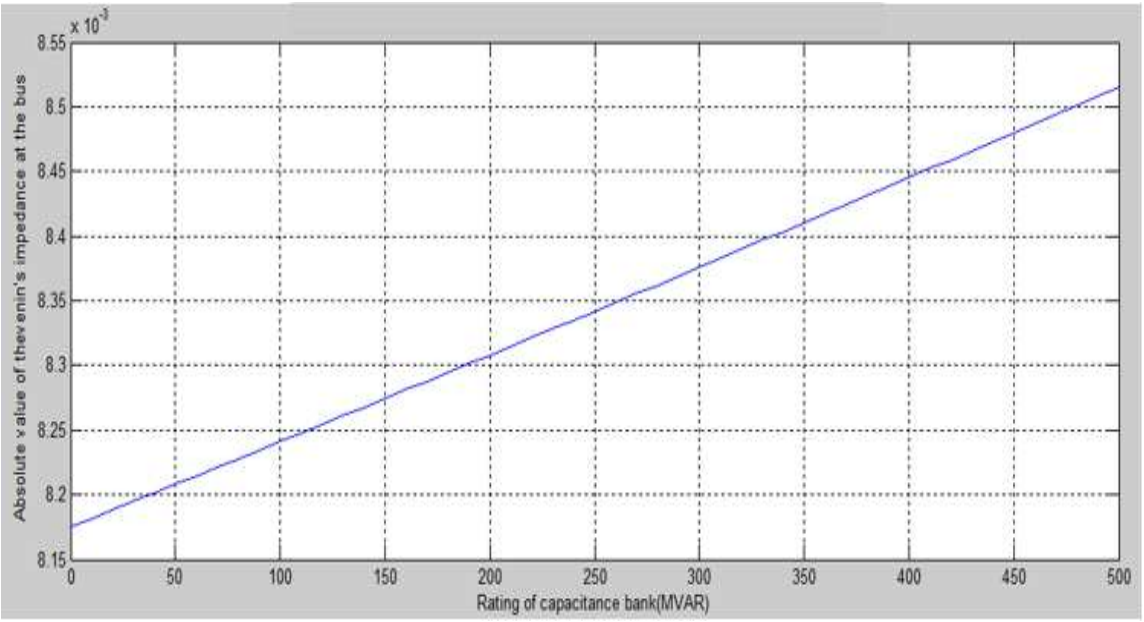

Fig. 3.1 Capacitance Scan at Bus 1 for Fundamental Frequency

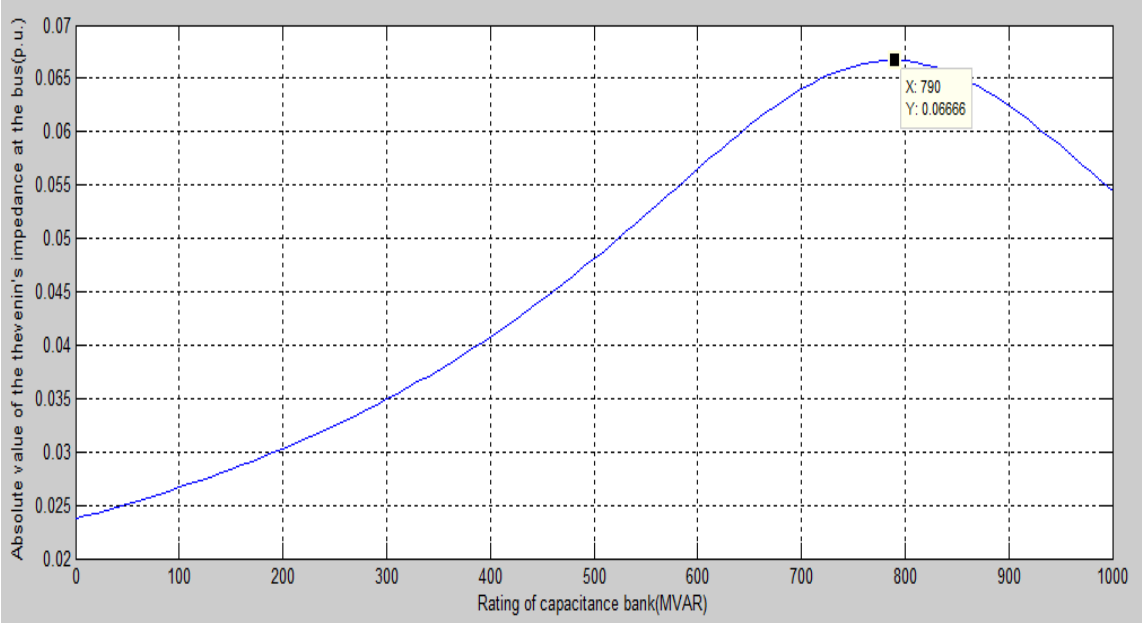

Fig. 3.2 Capacitance Scan at Bus 1 for Harmonic Order 5

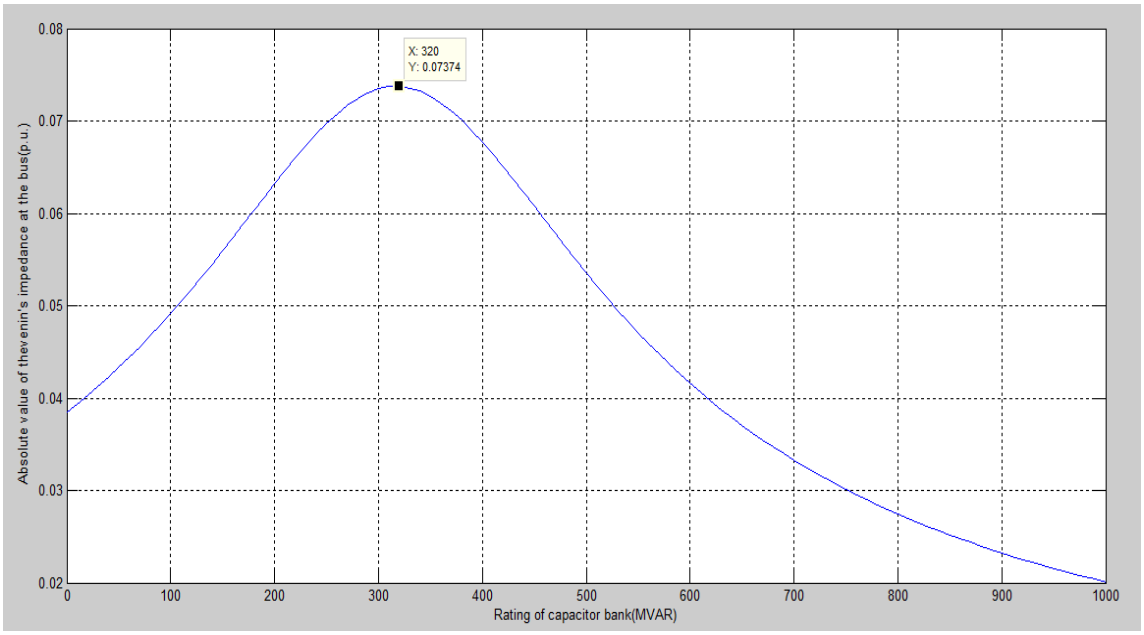

Fig. 3.3 Capacitance Scan at Bus 1 for Harmonic Order 7

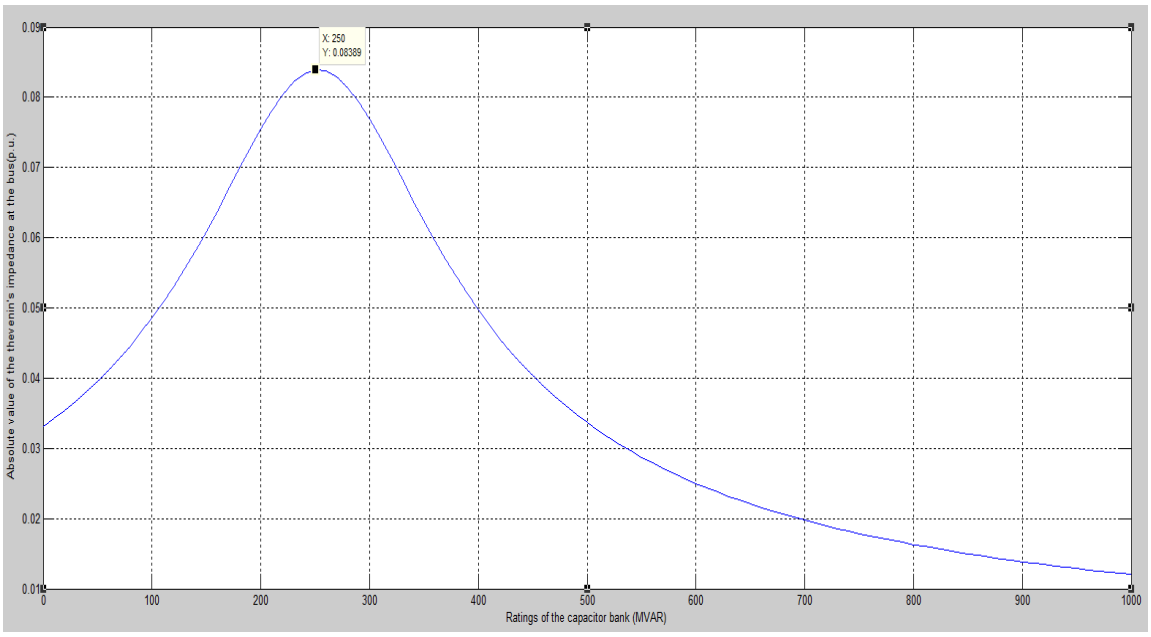

Fig. 3.4 Capacitance Scan at Bus 1 for Harmonic Order 11

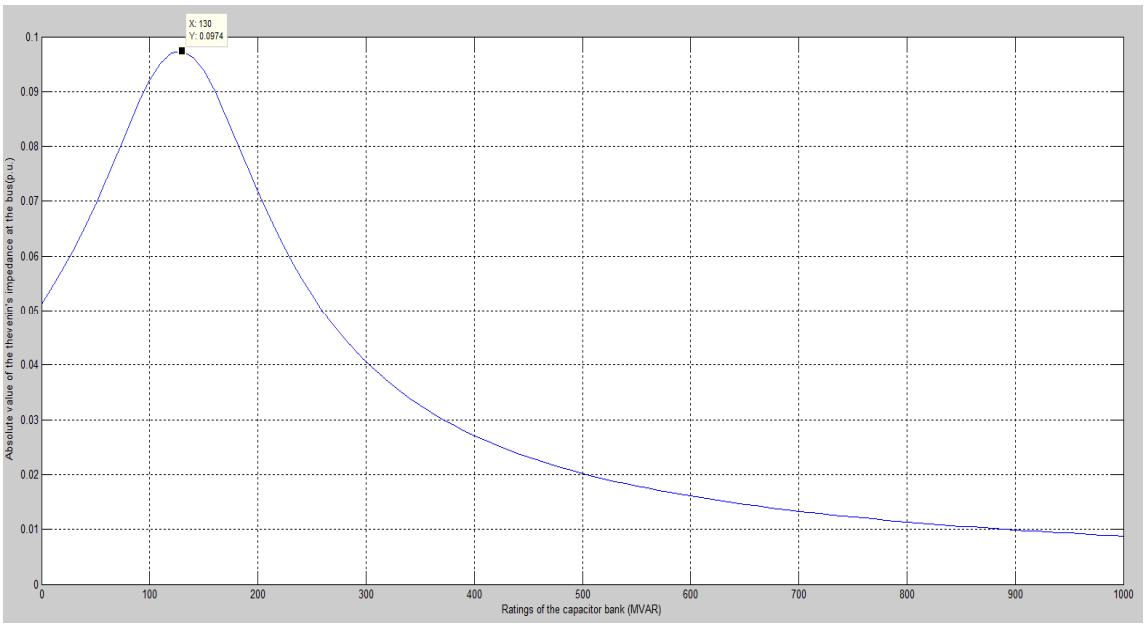

Fig. 3.5 Capacitance Scan at Bus 1 for Harmonic Order 13

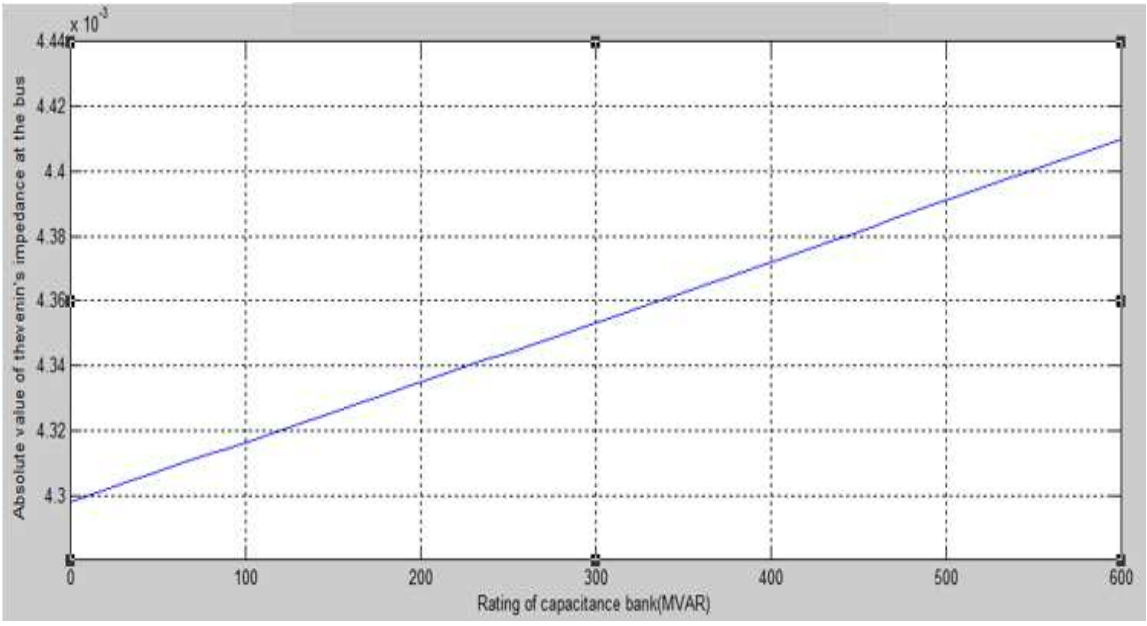

Fig. 3.6 Capacitance Scan at Bus 2 for Fundamental Frequency

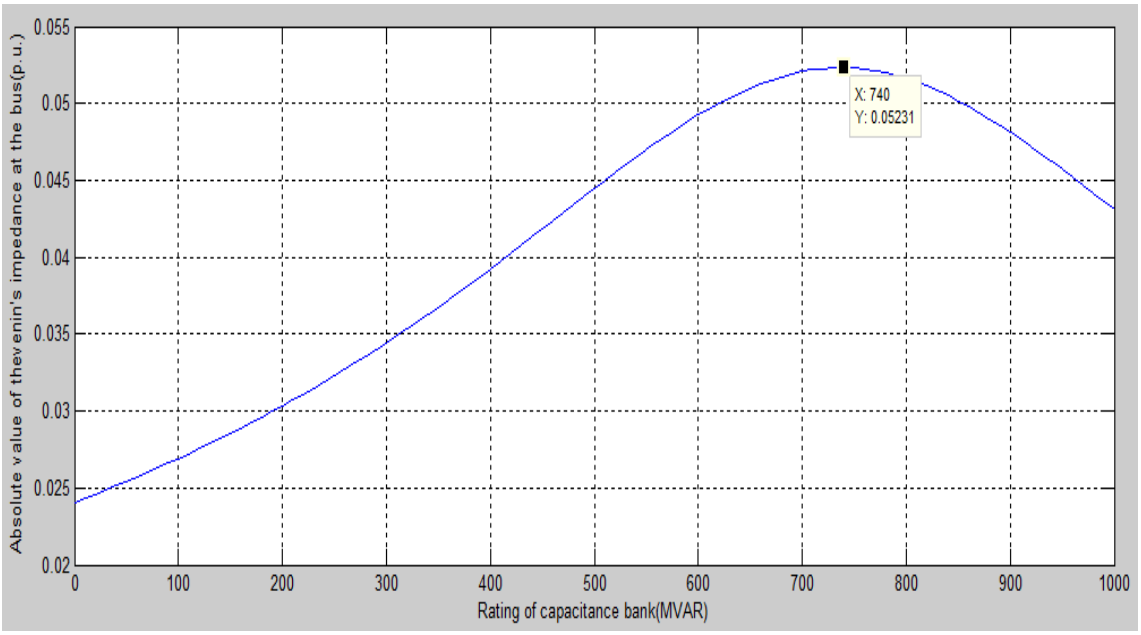

Fig. 3.7 Capacitance Scan at Bus 2 for Harmonic Order 5

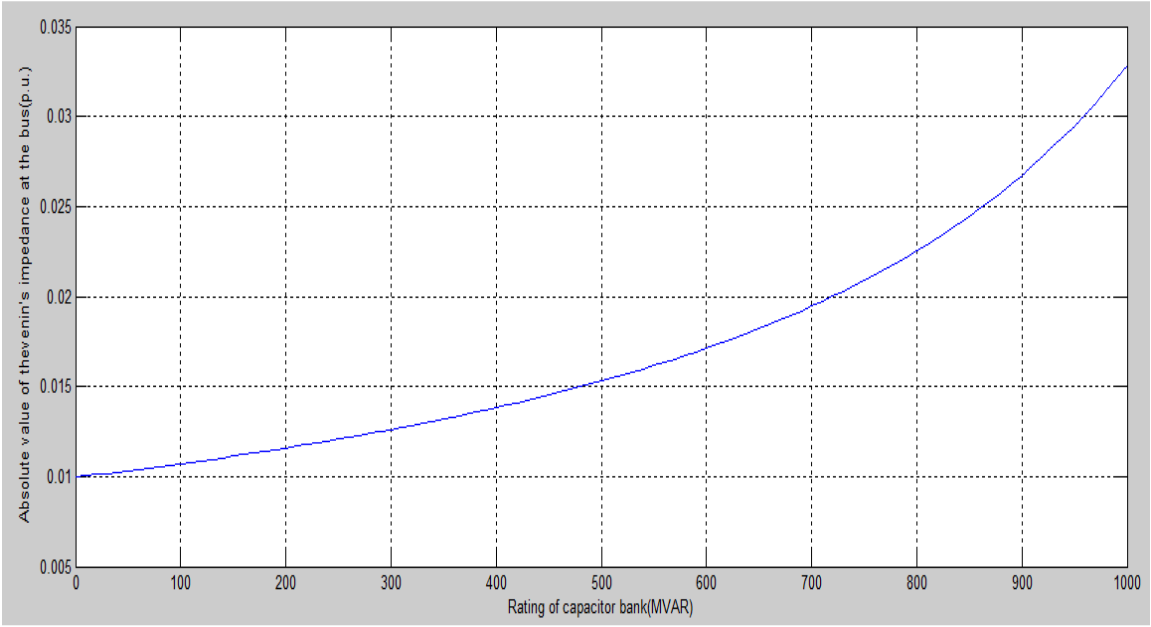

Fig. 3.8 Capacitance Scan at Bus 2 for Harmonic Order 7

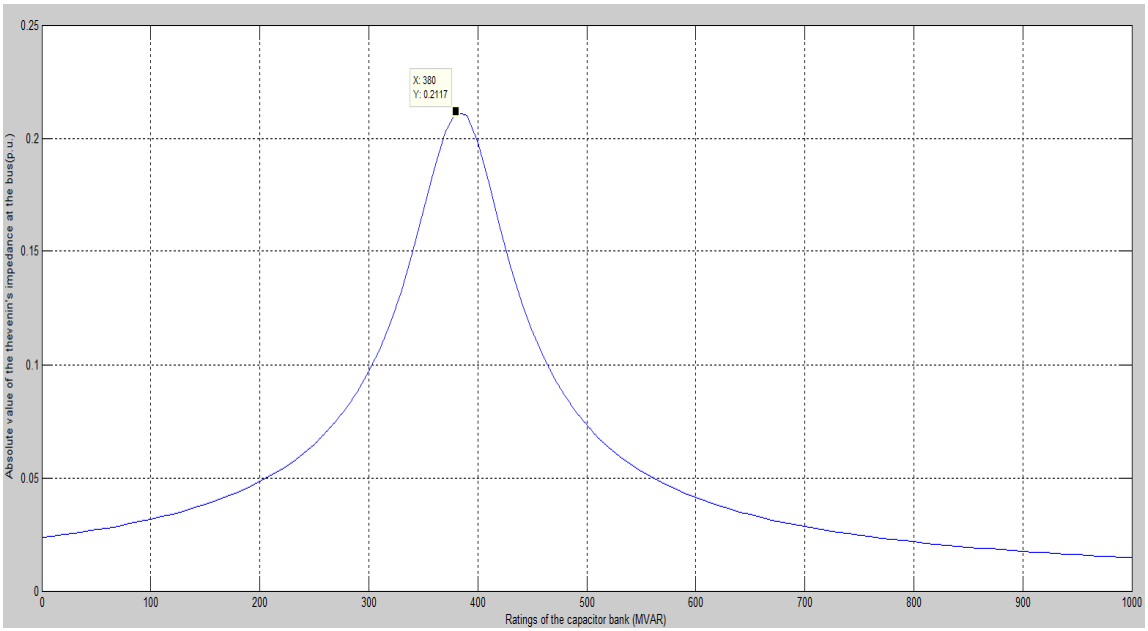

Fig. 3.9 Capacitance Scan at Bus 2 for Harmonic Order 11

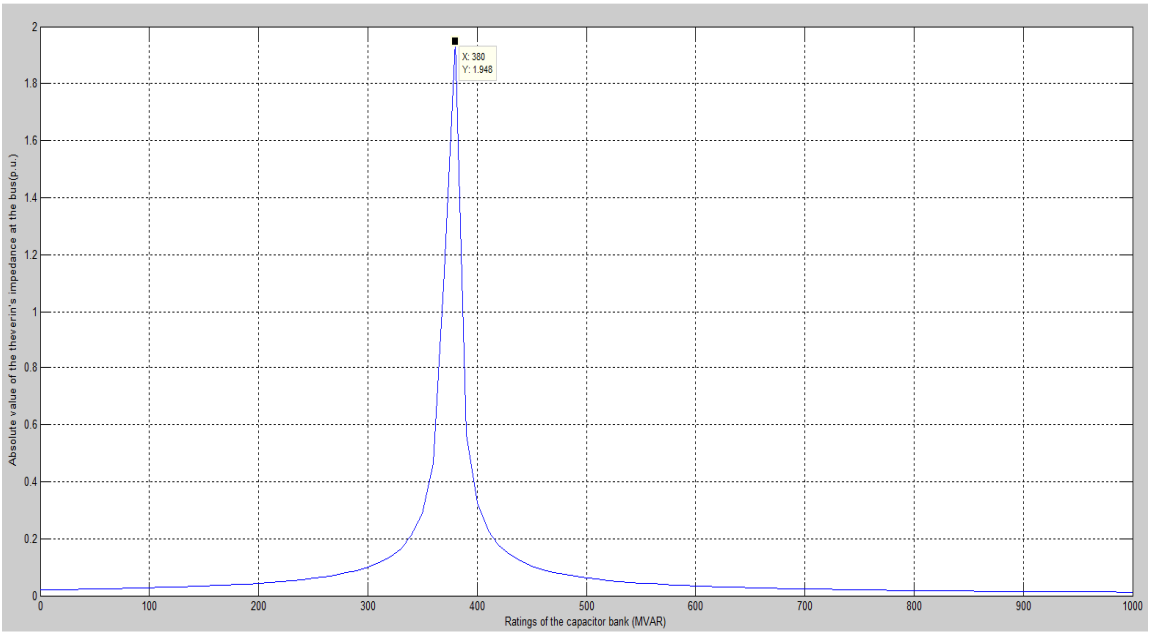

Fig. 3.10 Capacitance Scan at Bus 2 for Harmonic Order 13

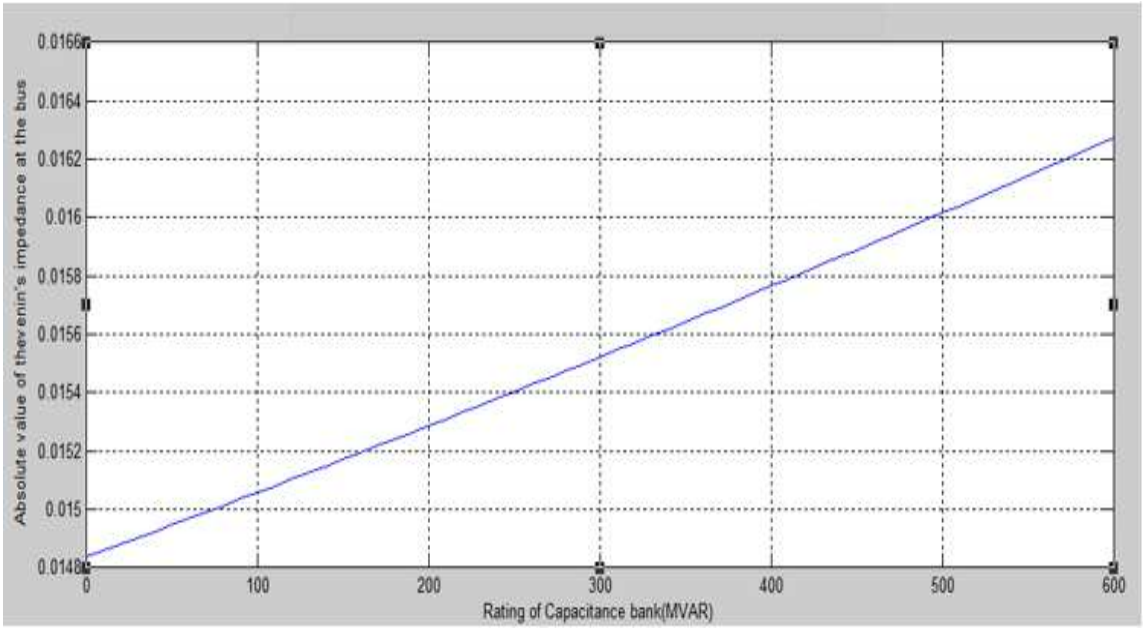

Fig. 3.11 Capacitance Scan at Bus 3 for Fundamental Frequency

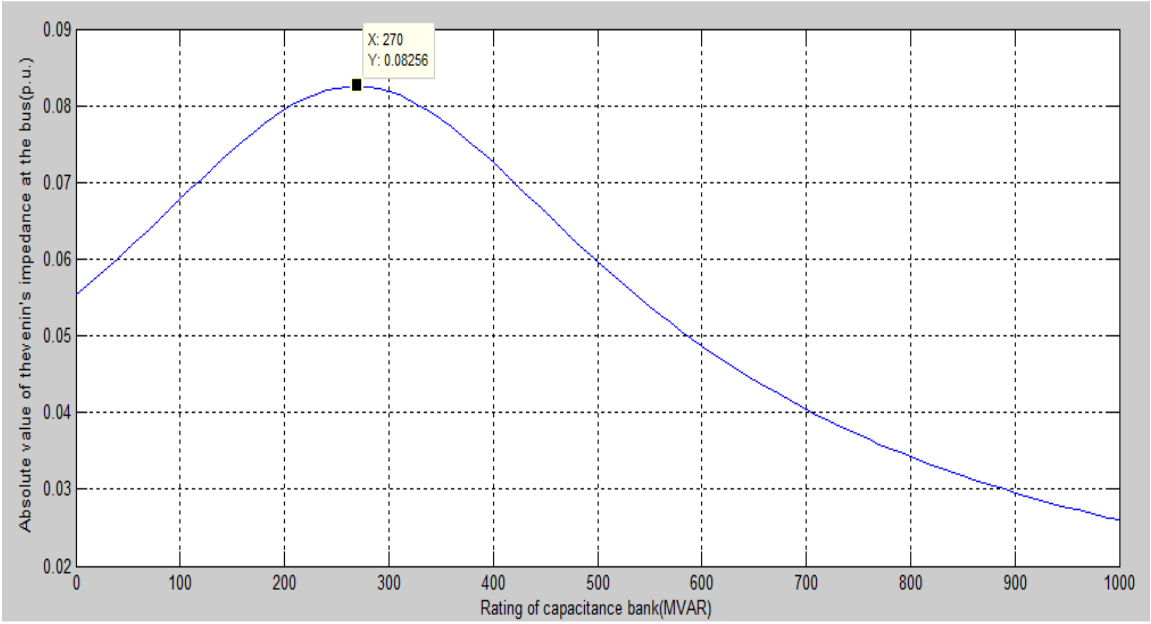

Fig. 3.12 Capacitance Scan at Bus 3 for Harmonic Order 5

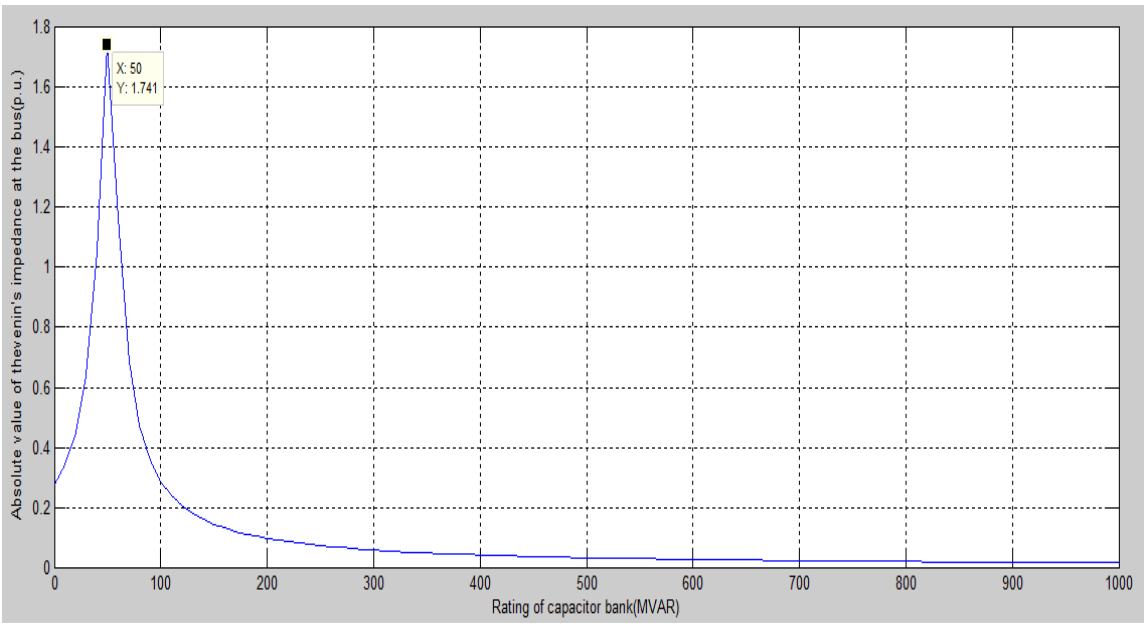

Fig. 3.13 Capacitance Scan at Bus 3 for Harmonic Order 7

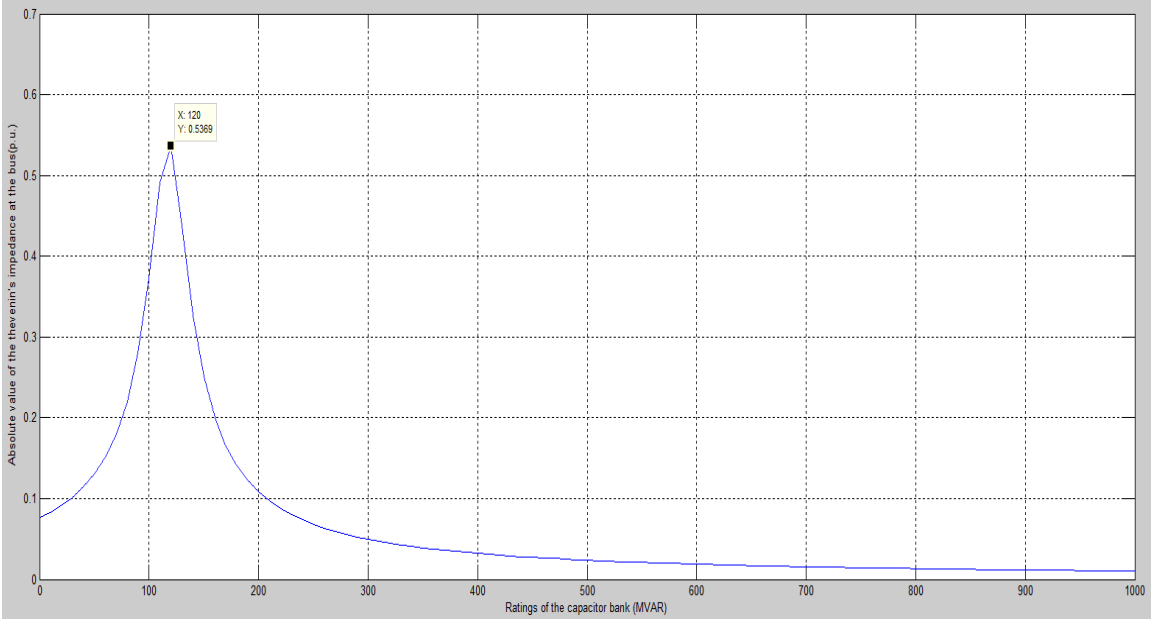

Fig. 3.14 Capacitance Scan at Bus 3 for Harmonic Order 11

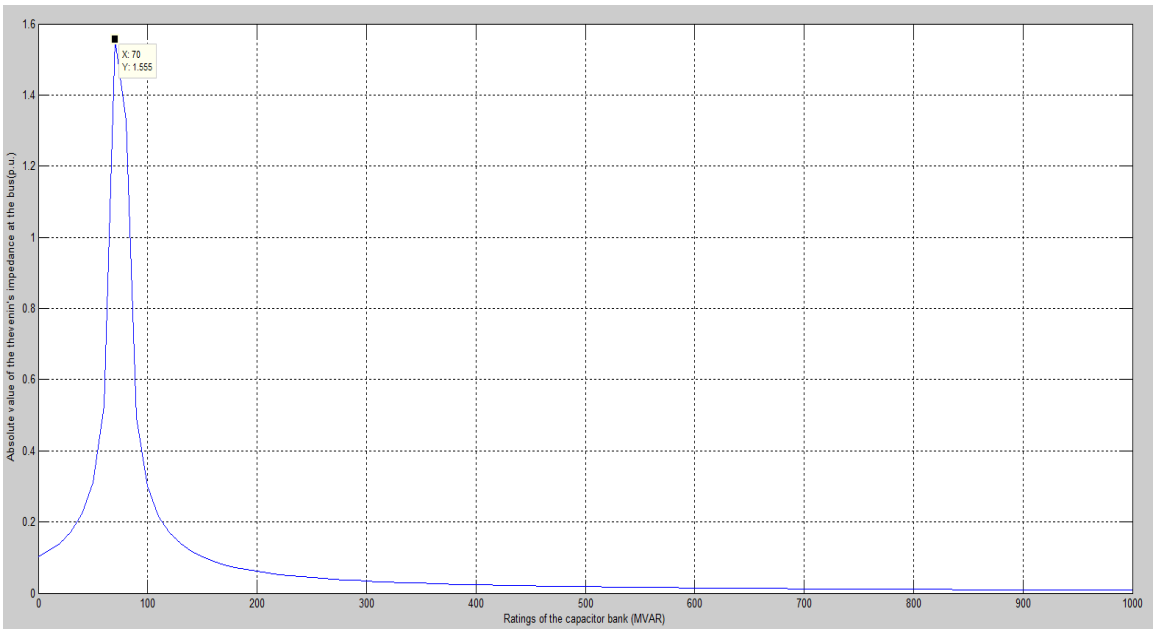

Fig. 3.15 Capacitance Scan at Bus 3 for Harmonic Order 13

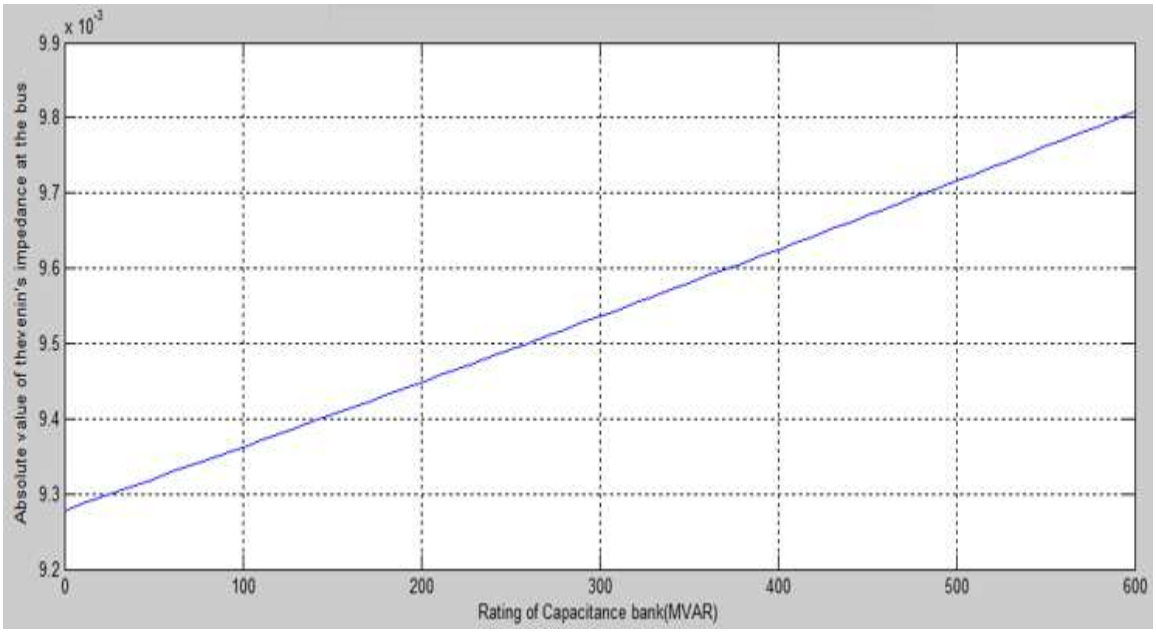

Fig. 3.16 Capacitance Scan at Bus 4 for Fundamental Frequency

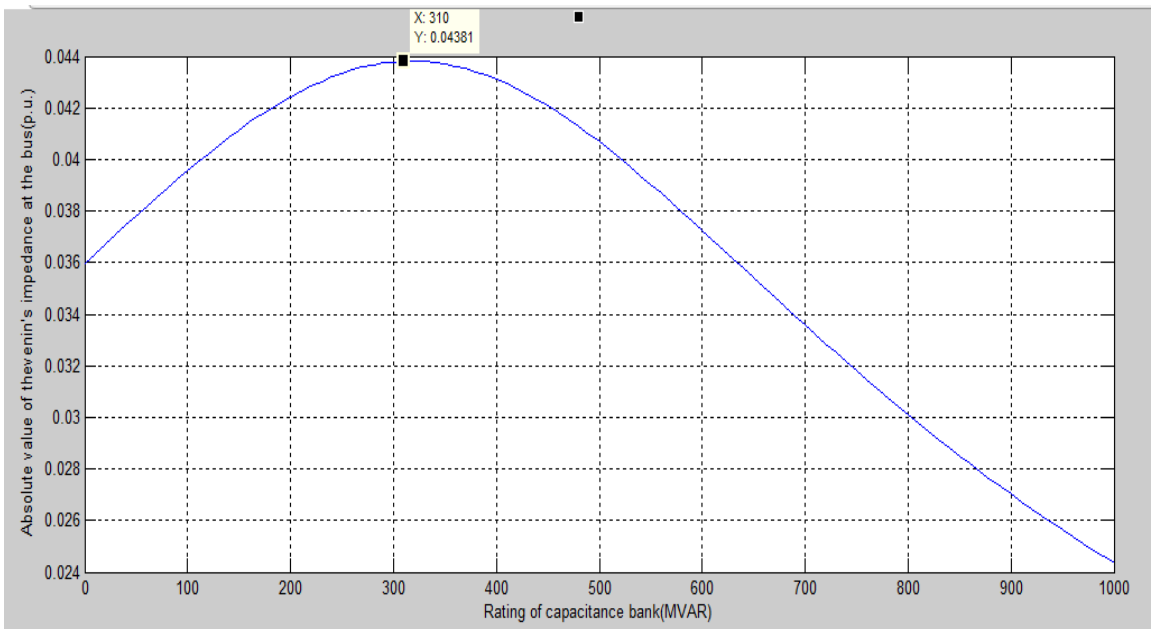

Fig. 3.17 Capacitance Scan at Bus 4 for Harmonic Order 5

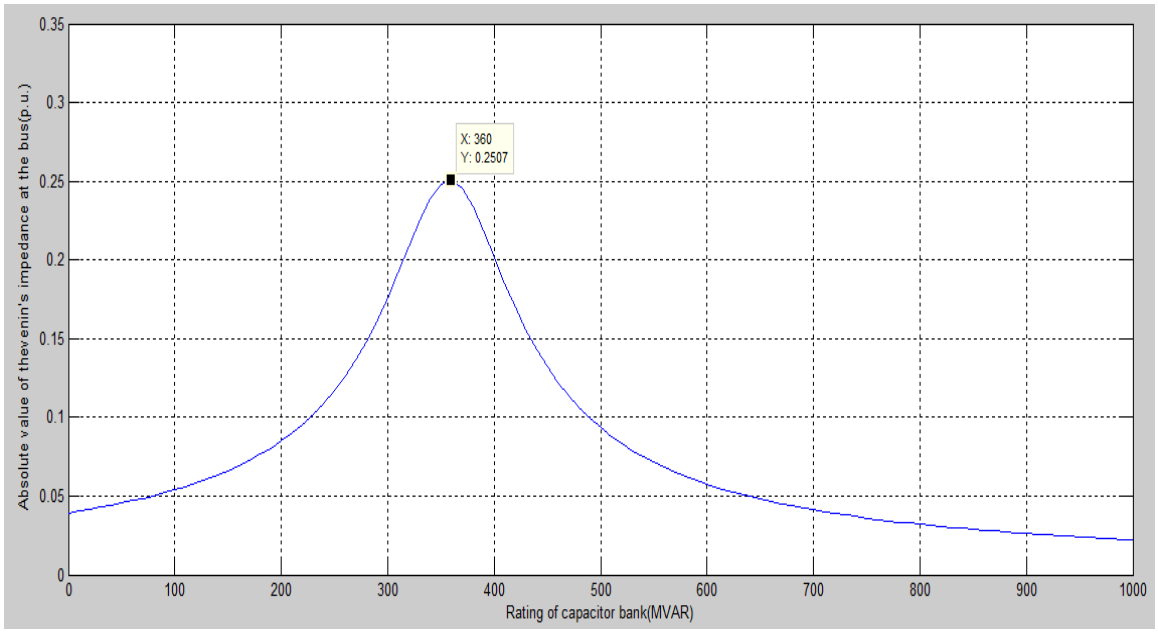

Fig. 3.18 Capacitance Scan at Bus 4 for Harmonic Order 7

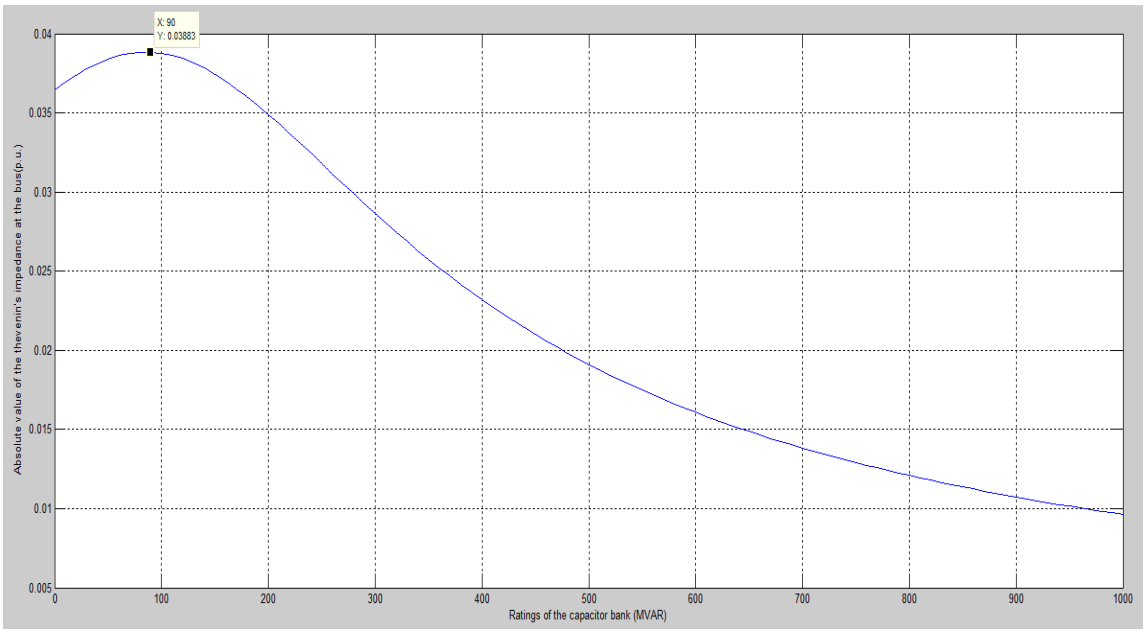

Fig. 3.19 Capacitance Scan at Bus 4 for Harmonic Order 11

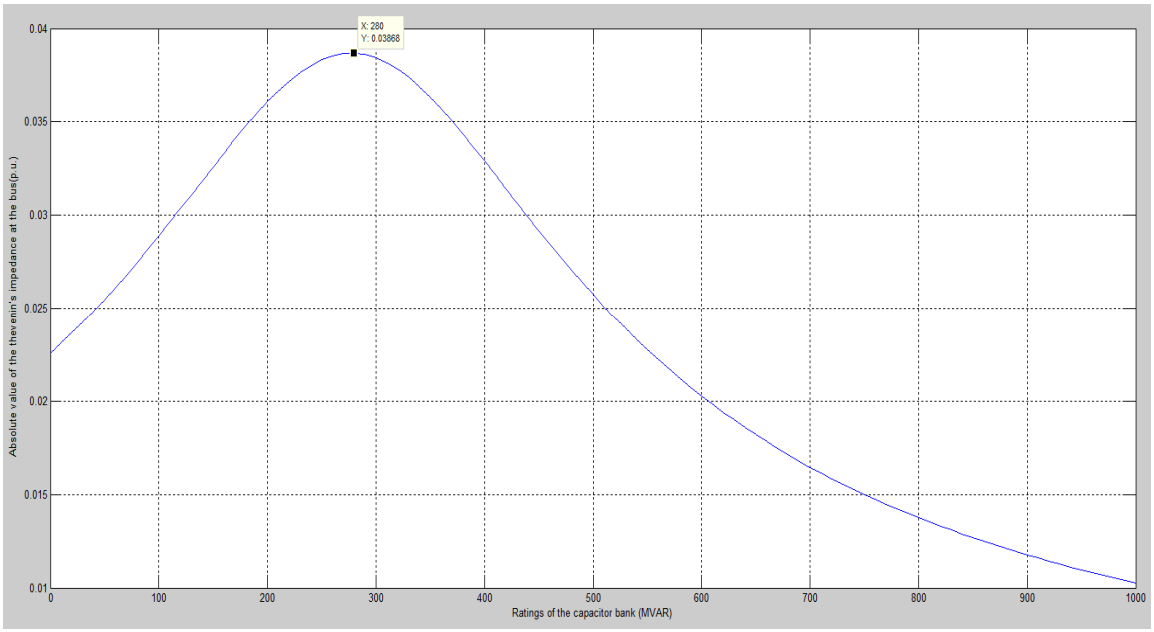

Fig. 3.20 Capacitance Scan at Bus 4 for Harmonic Order 13

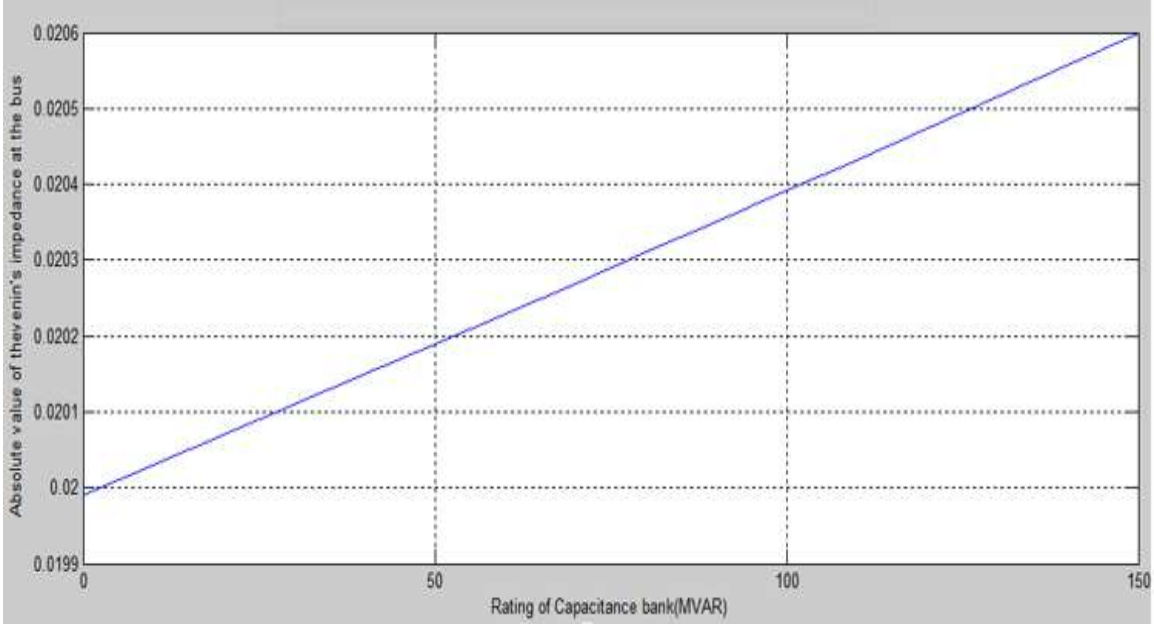

Fig. 3.21 Capacitance Scan at Bus 5 for Fundamental Frequency

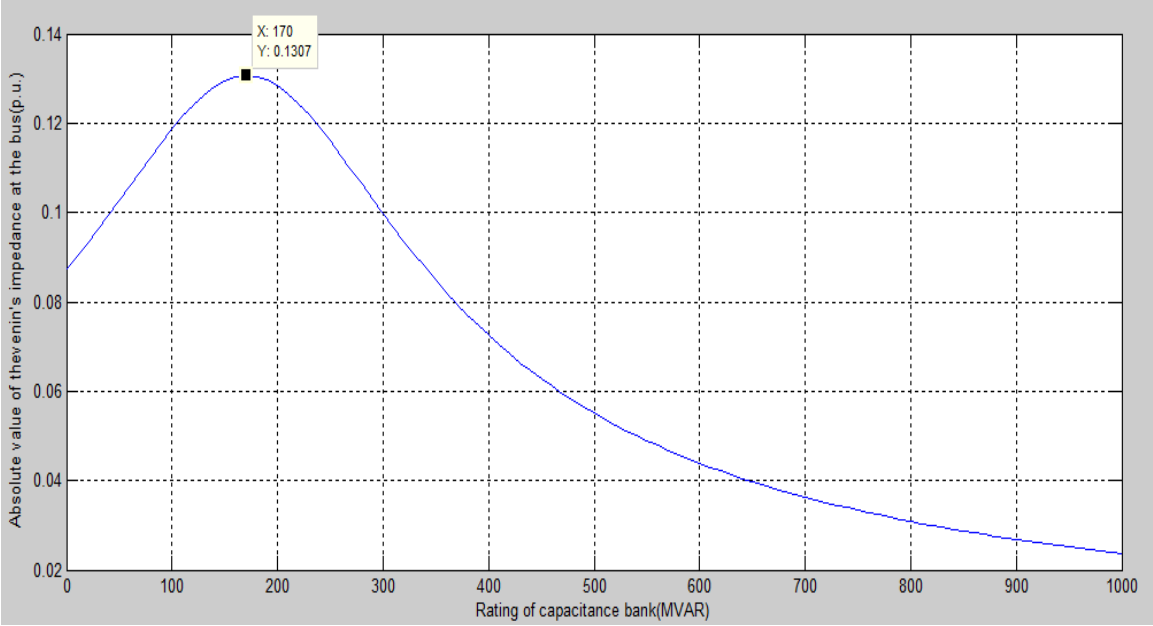

Fig. 3.22 Capacitance Scan at Bus 5 for Harmonic Order 5

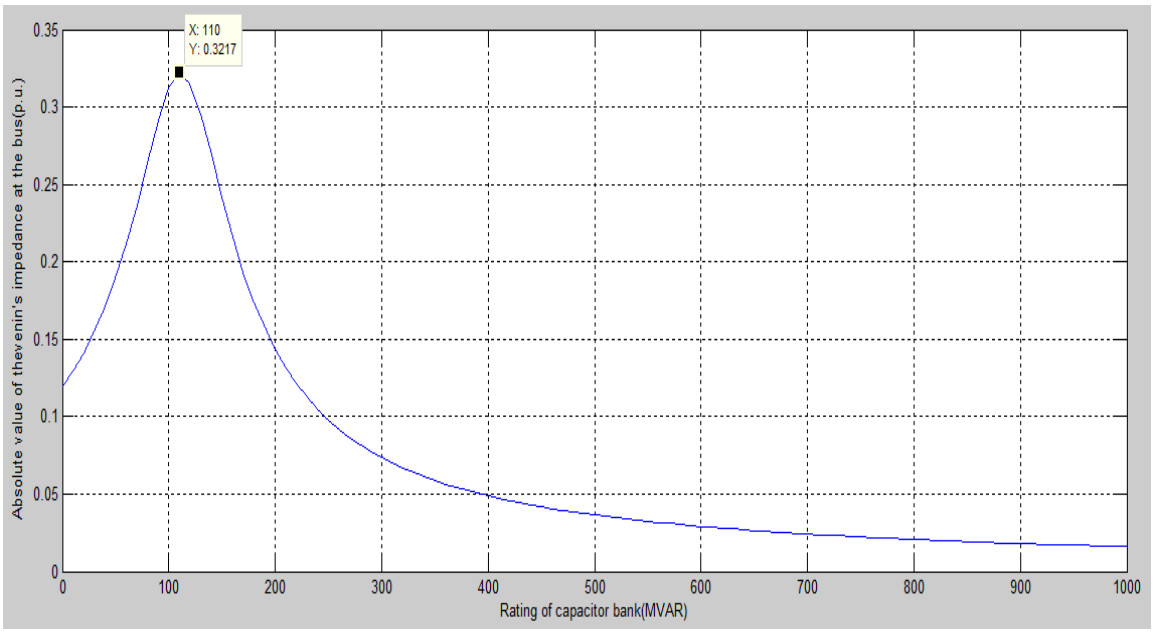

Fig. 3.23 Capacitance Scan at Bus 5 for Harmonic Order 7

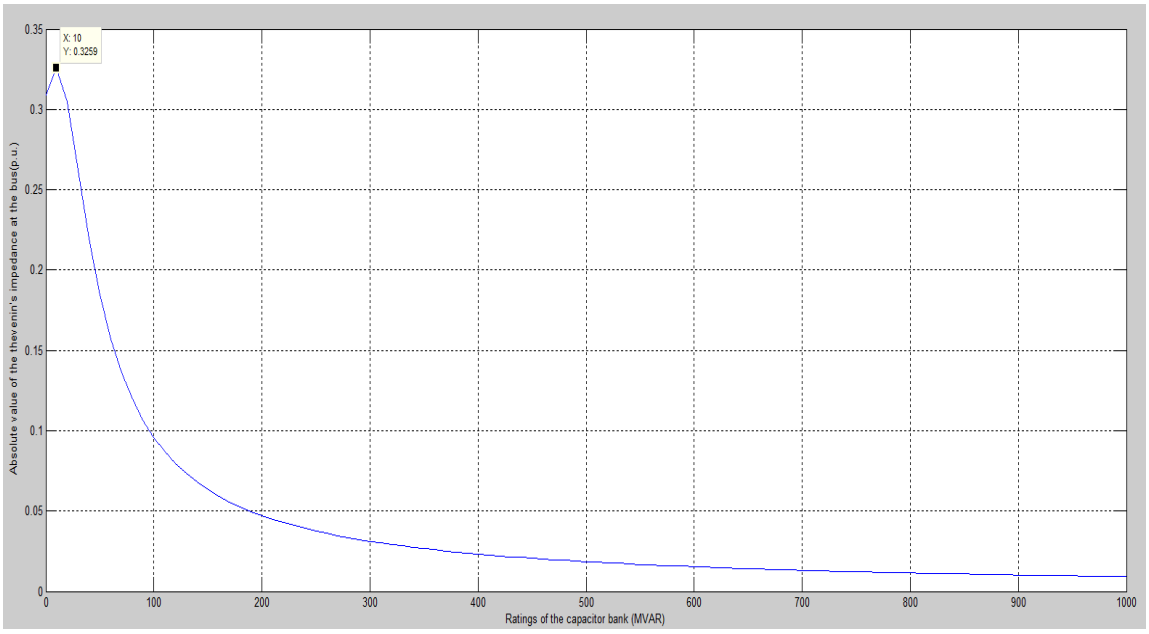

Fig. 3.24 Capacitance Scan at Bus 5 for Harmonic Order 11

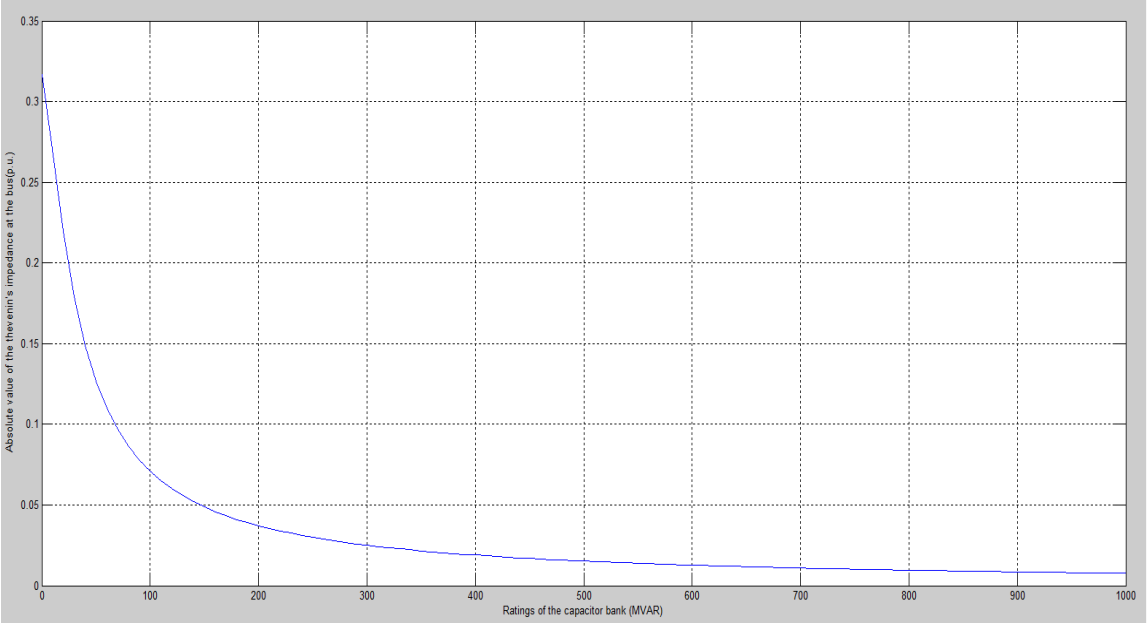

Fig. 3.25 Capacitance Scan at Bus 5 for Harmonic Order 13

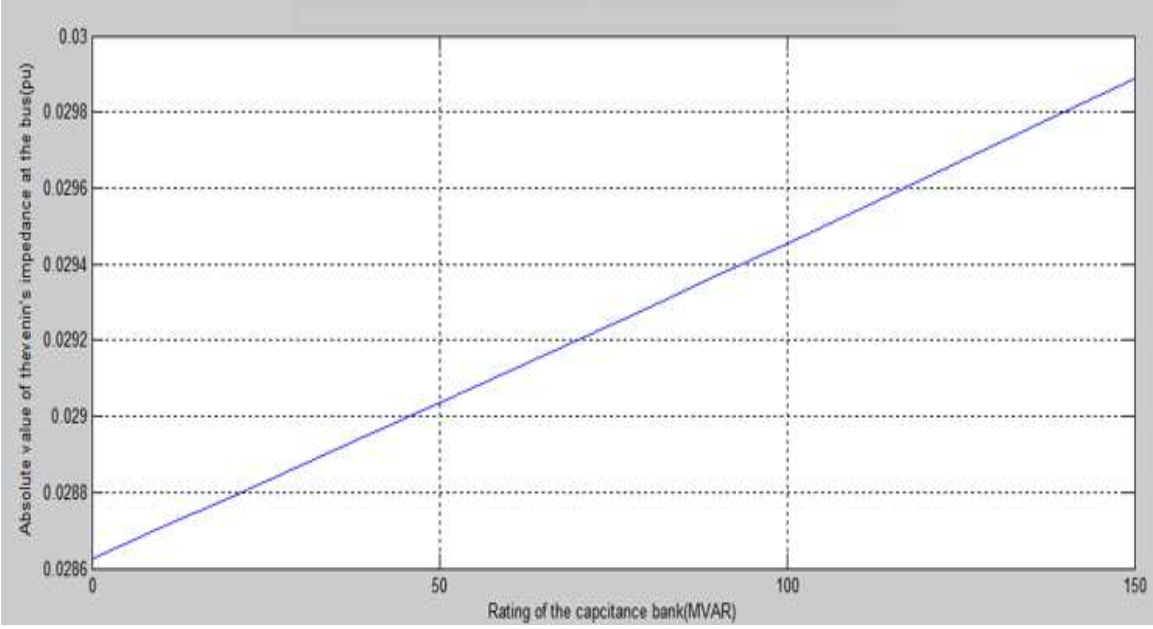

Fig. 3.26 Capacitance Scan at Bus 6 for Fundamental Frequency

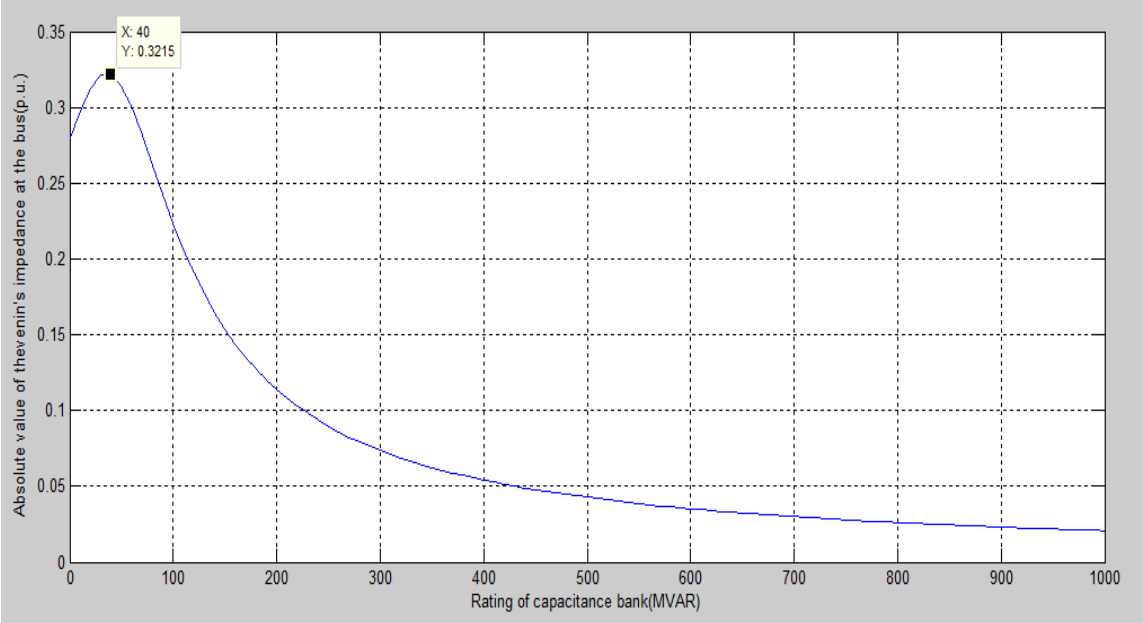

Fig. 3.27 Capacitance Scan at Bus 6 for Harmonic Order 5

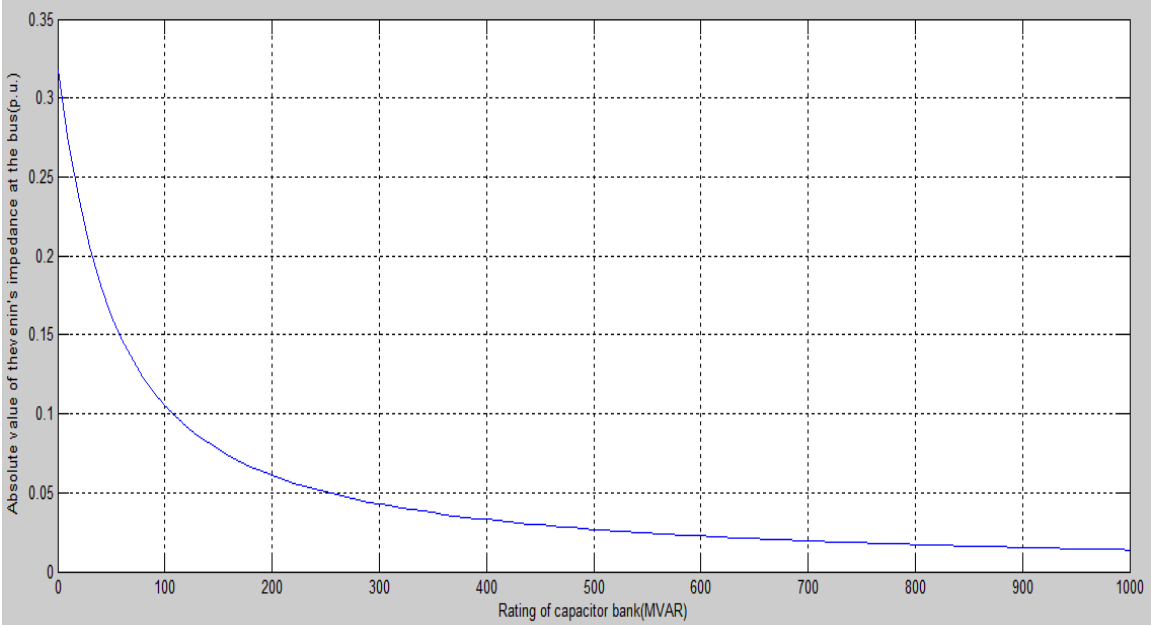

Fig. 3.28 Capacitance Scan at Bus 6 for Harmonic Order 7

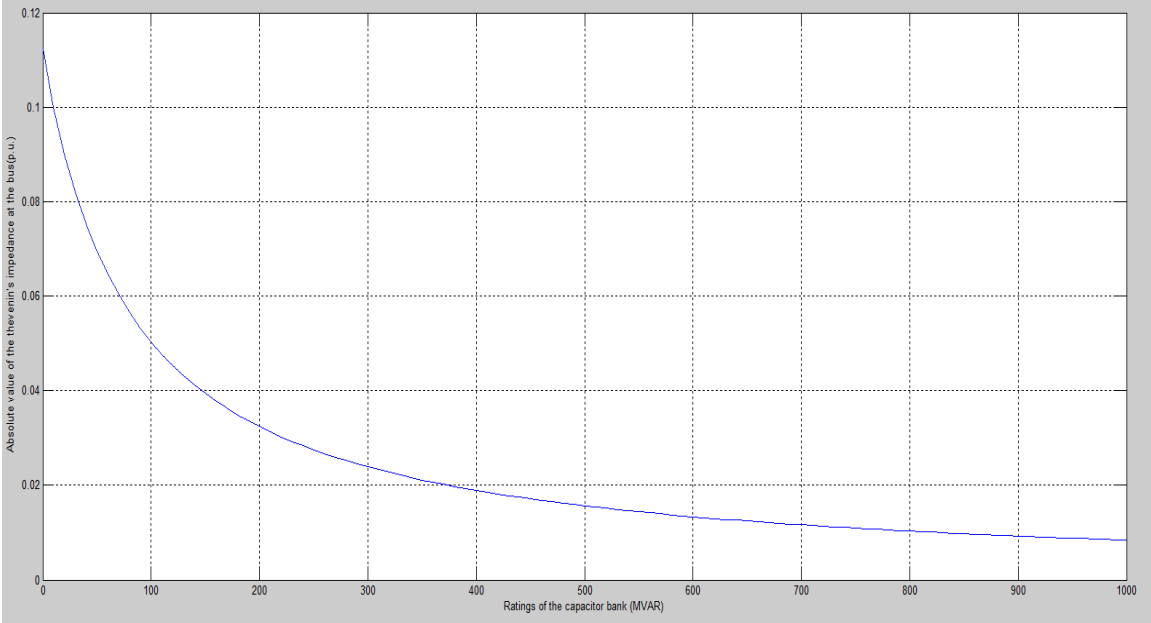

Fig. 3.29 Capacitance Scan at Bus 6 for Harmonic Order 11

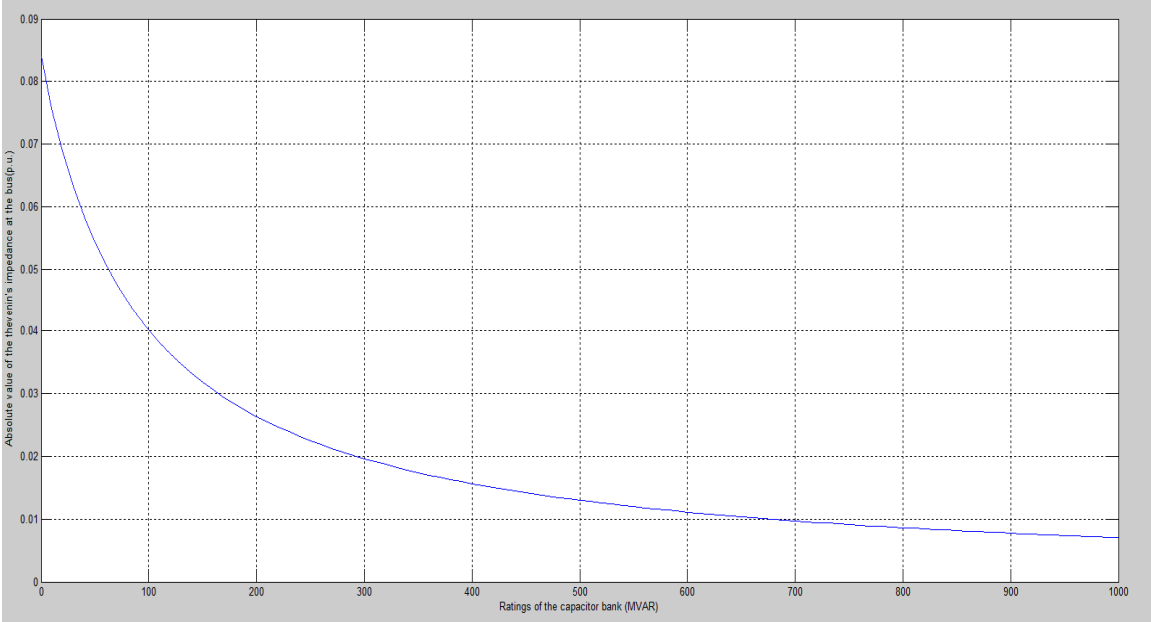

Fig. 3.30 Capacitance Scan at Bus 6 for Harmonic Order 13

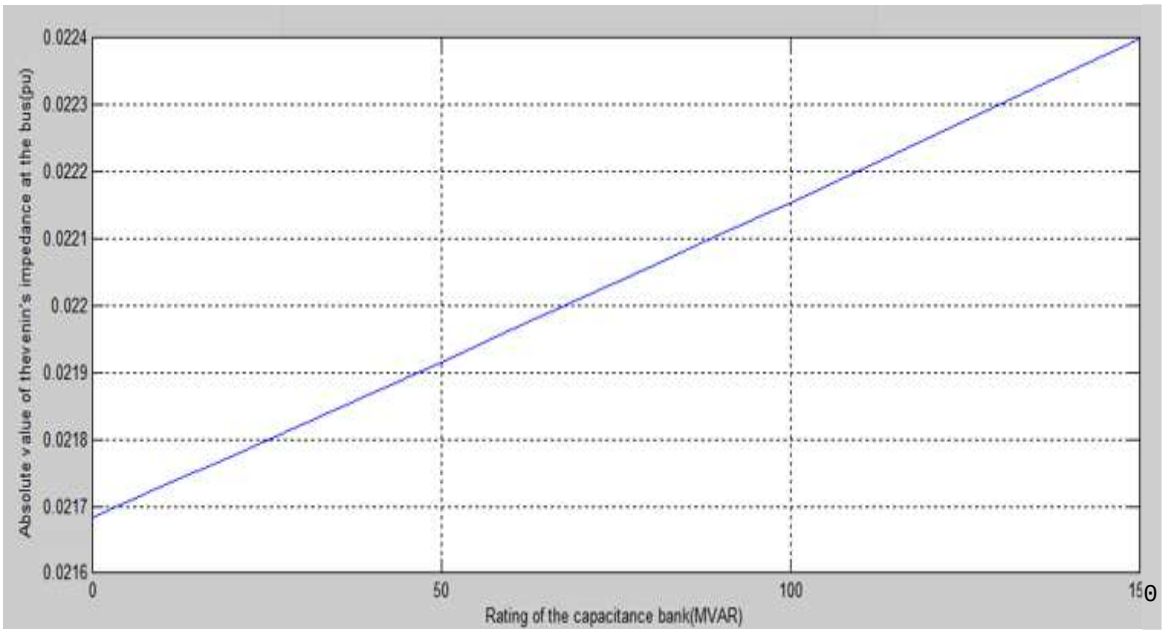

Fig. 3.31 Capacitance Scan at Bus 7 for Fundamental Frequency

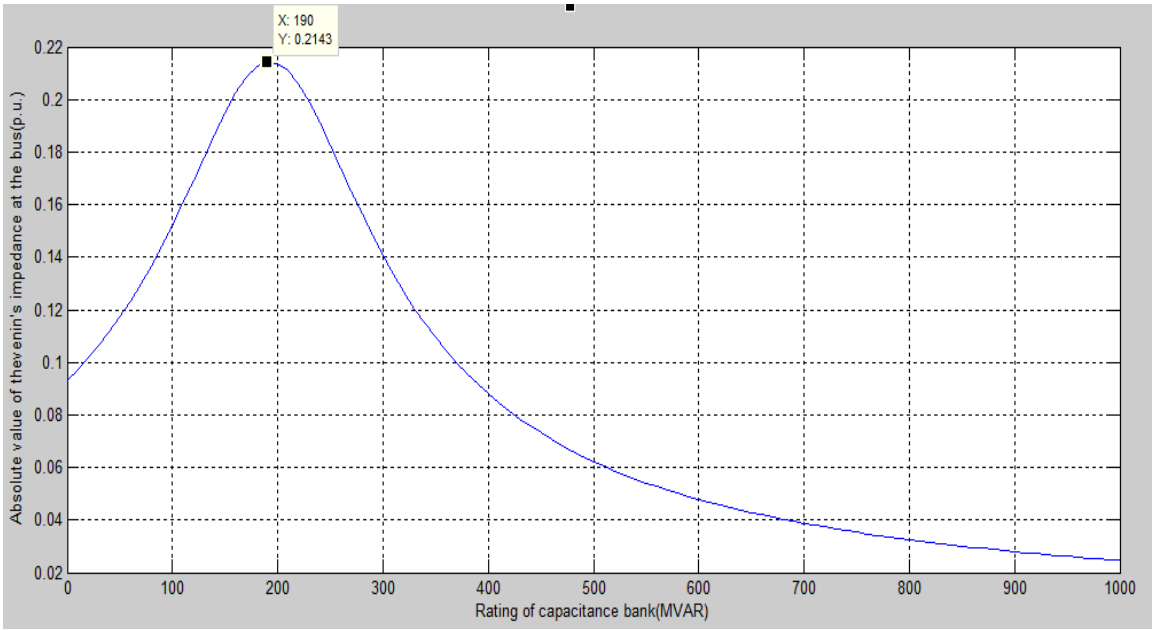

Fig. 3.32 Capacitance Scan at Bus 7 for Harmonic Order 5

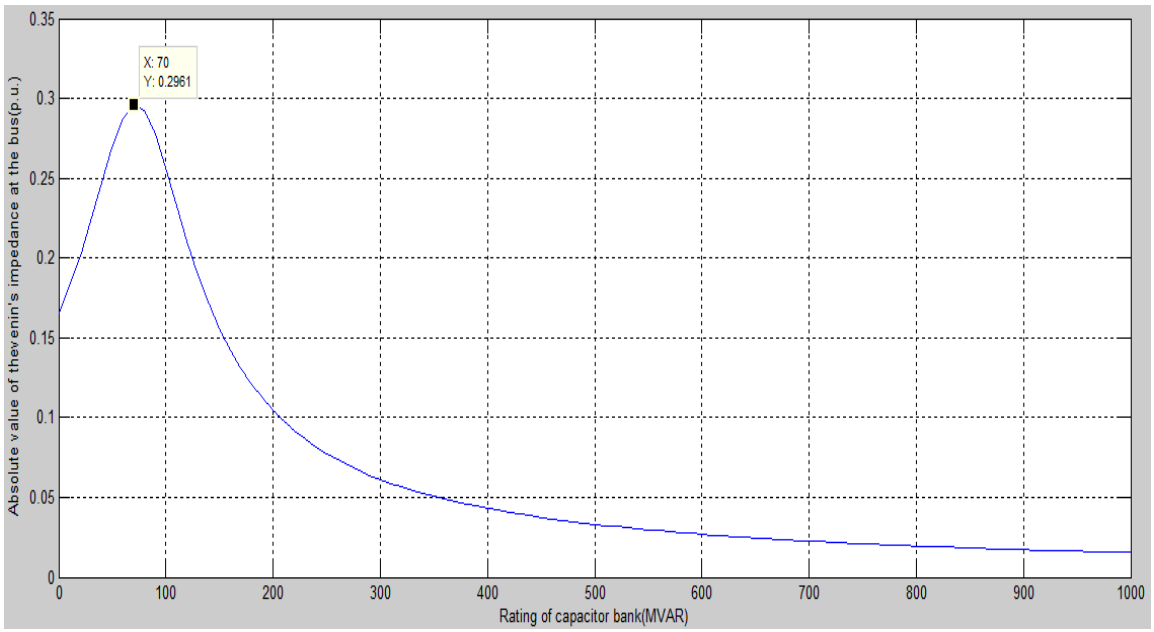

Fig. 3.33 Capacitance Scan at Bus 7 for Harmonic Order 7

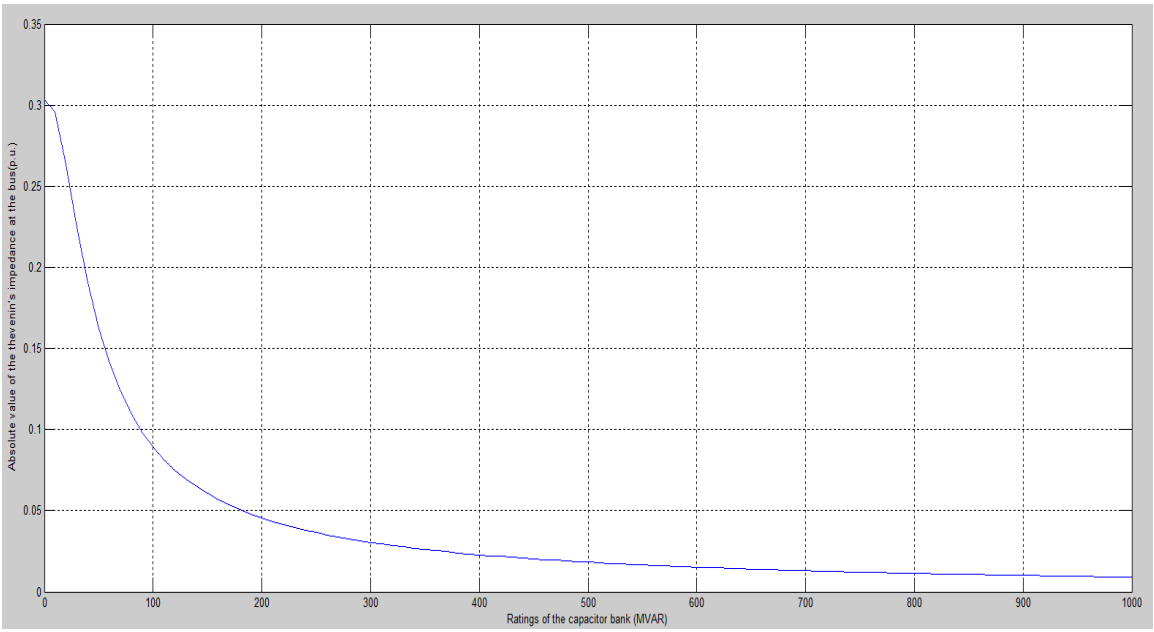

Fig. 3.34 Capacitance Scan at Bus 7 for Harmonic Order 11

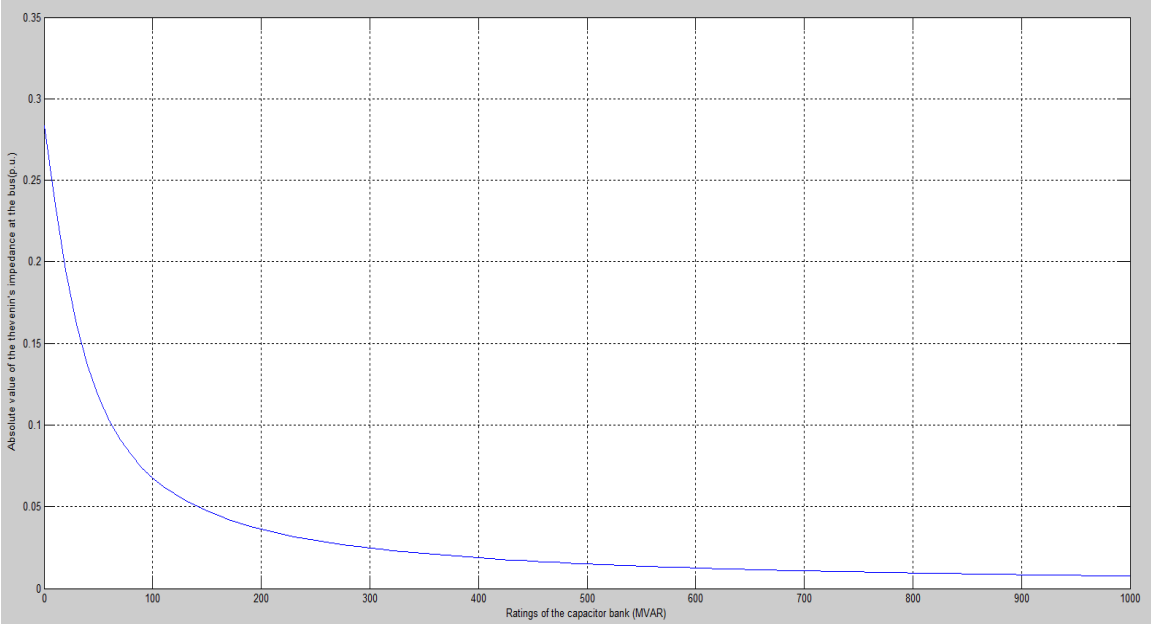

Fig. 3.35 Capacitance Scan at Bus 7 for Harmonic Order 13

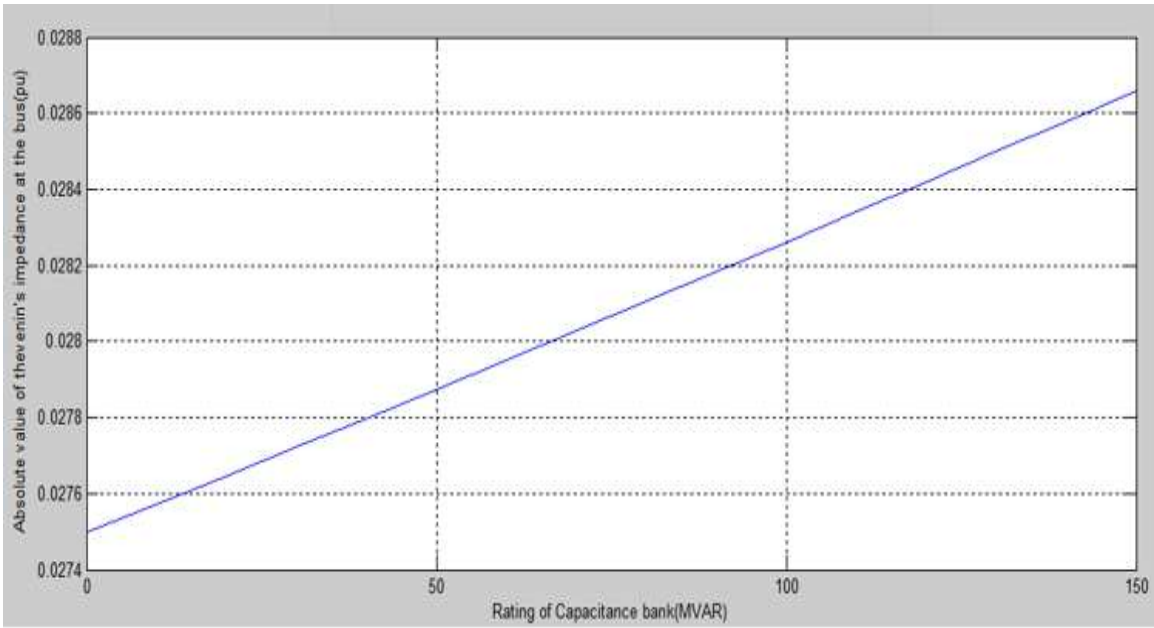

Fig. 3.36 Capacitance Scan at Bus 8 for Fundamental Frequency

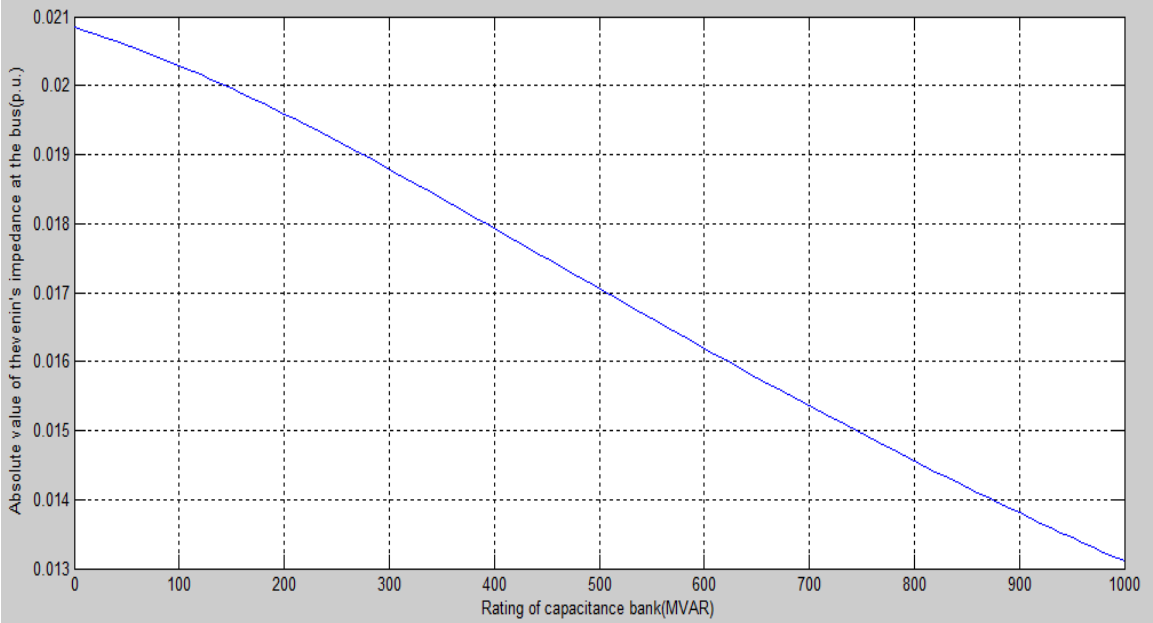

Fig. 3.37 Capacitance Scan at Bus 8 for Harmonic Order 5

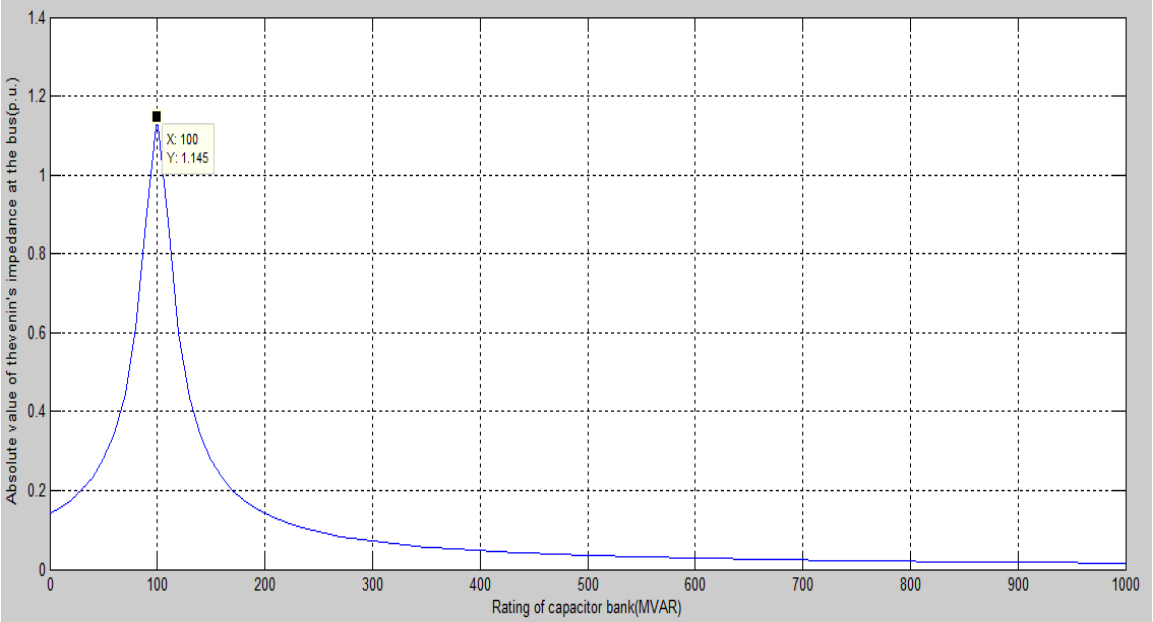

Fig. 3.38 Capacitance Scan at Bus 8 for Harmonic Order 7

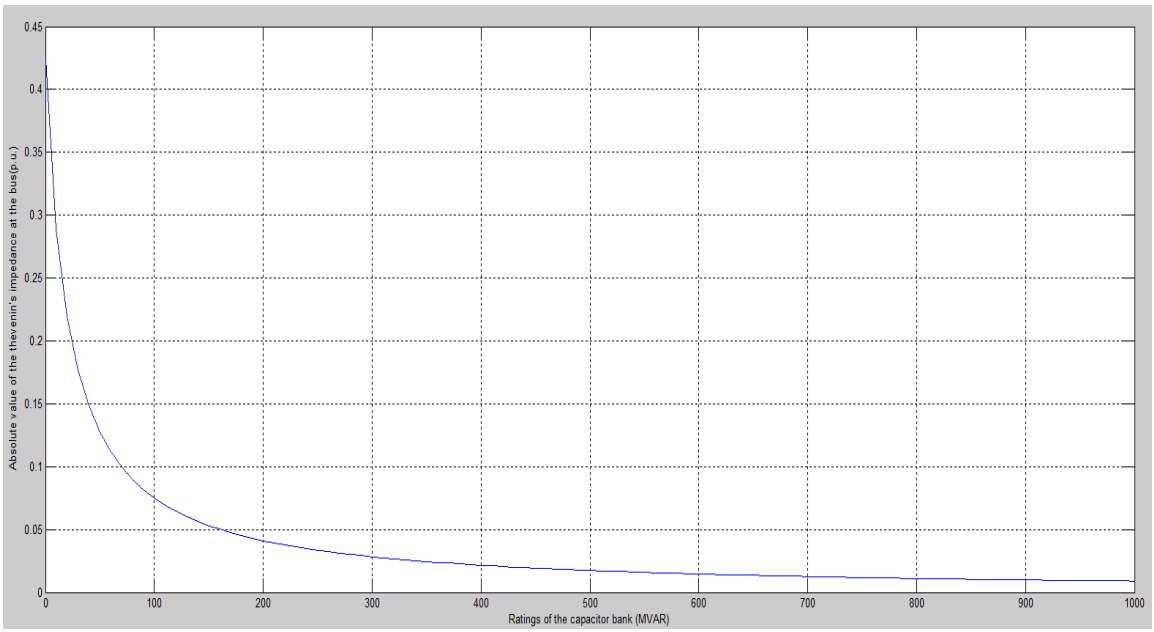

Fig. 3.39 Capacitance Scan at Bus 8 for Harmonic Order 11

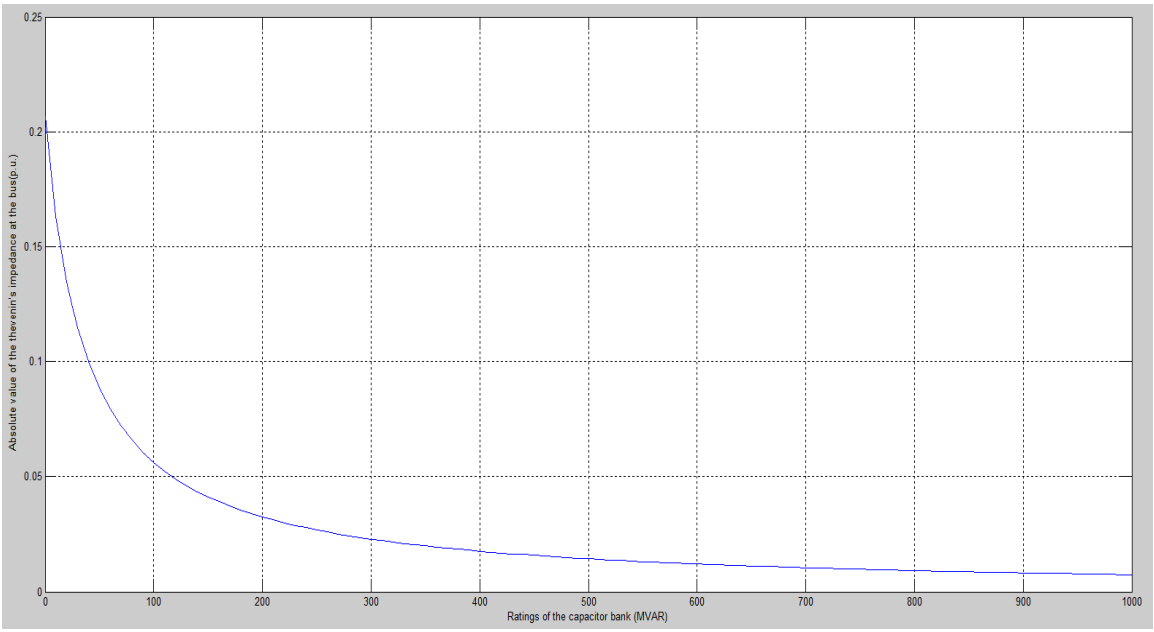

Fig. 3.40 Capacitance Scan at Bus 8 for Harmonic Order 13

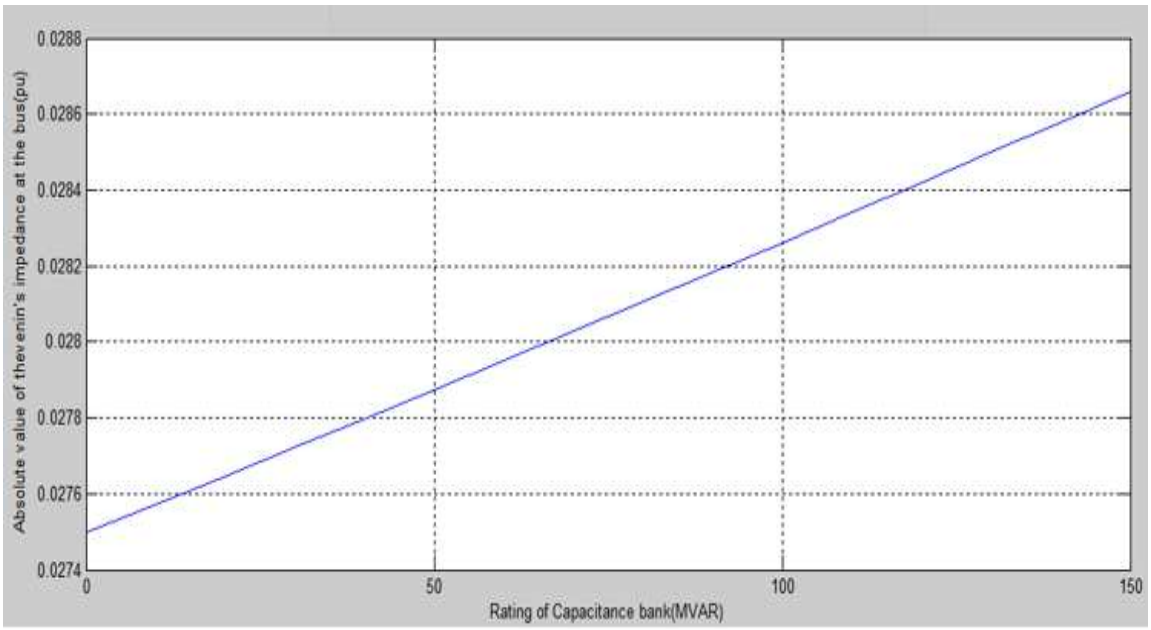

Fig. 3.41 Capacitance Scan at Bus 9 for Fundamental Frequency

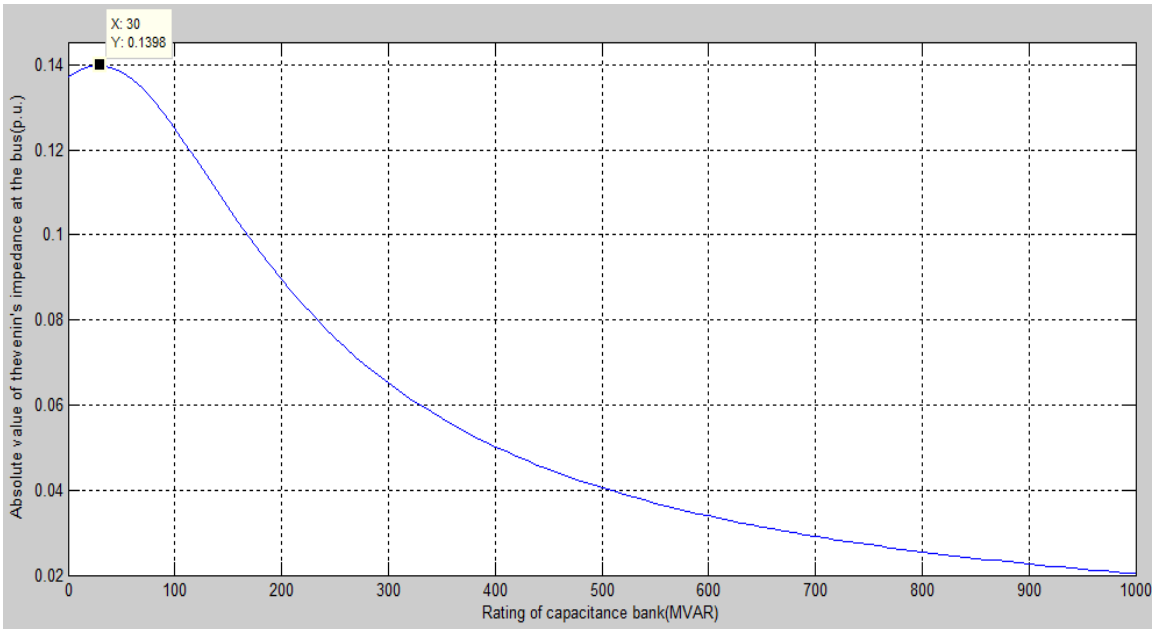

Fig. 3.42 Capacitance Scan at Bus 9 for Harmonic Order 5

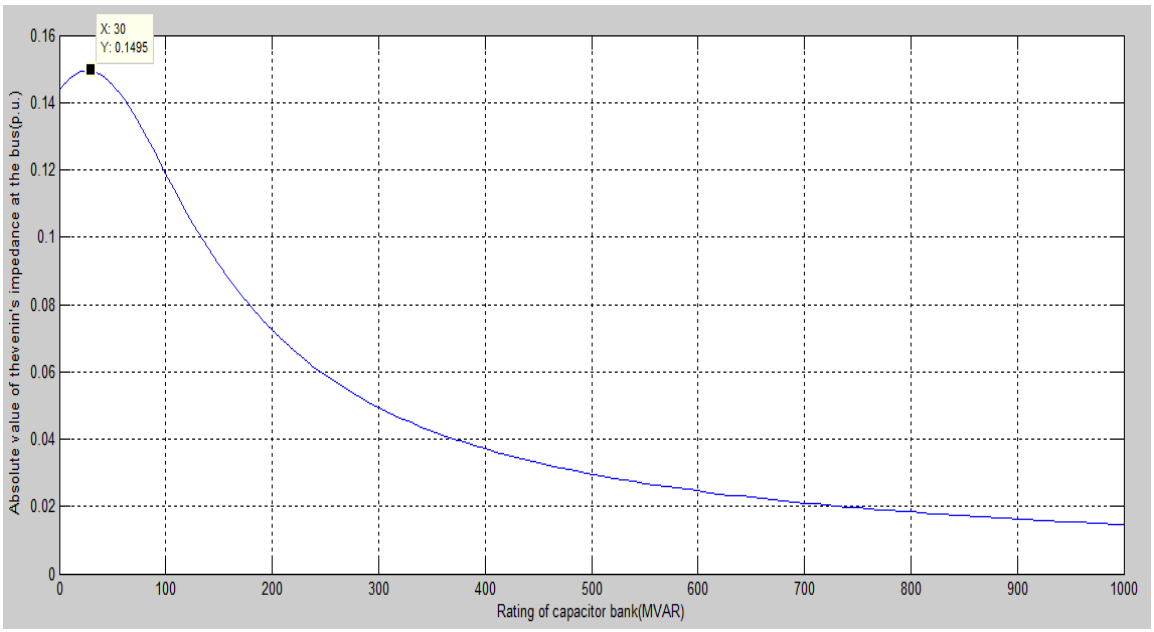

Fig. 3.43 Capacitance Scan at Bus 9 for Harmonic Order 7

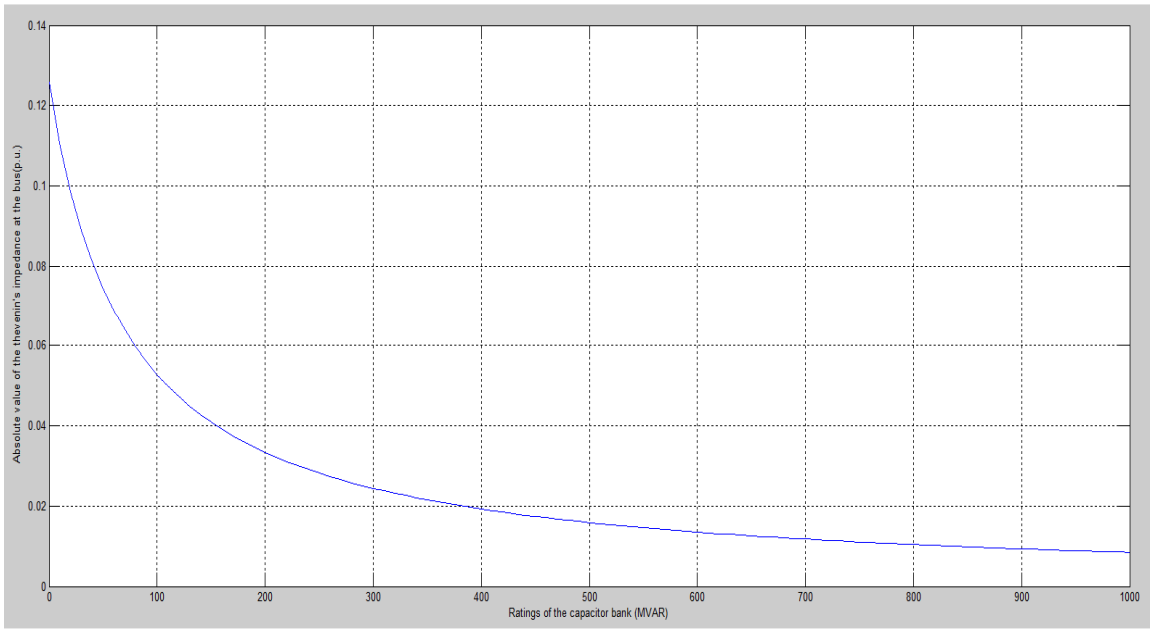

Fig. 3.44 Capacitance Scan at Bus 9 for Harmonic Order 11

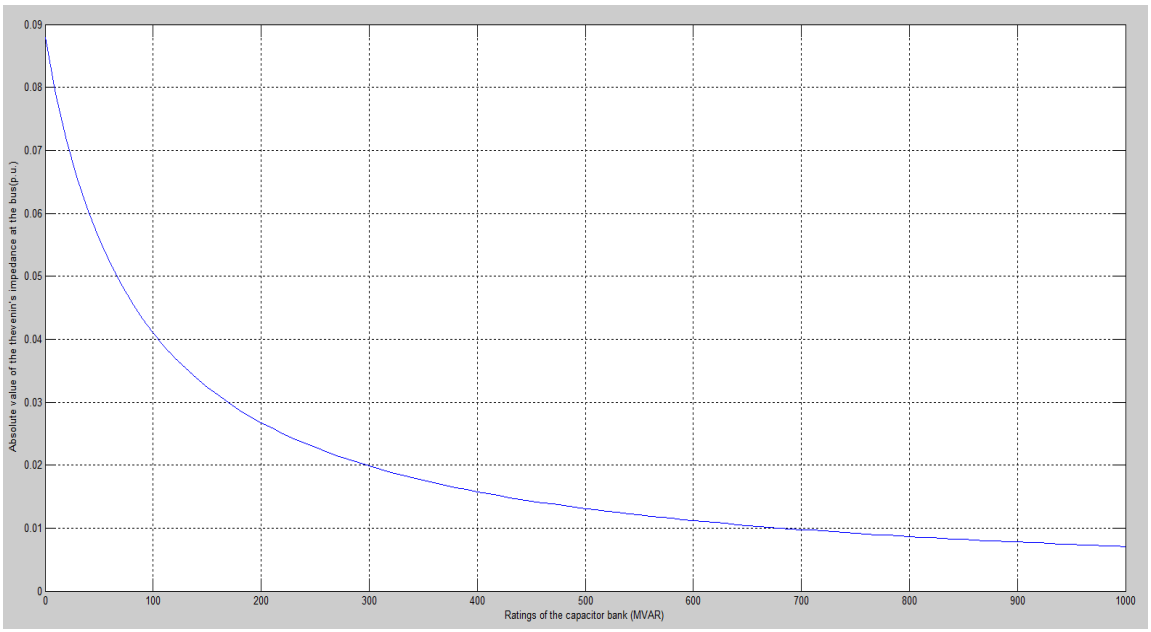

Fig. 3.45 Capacitance Scan at Bus 9 for Harmonic Order 13

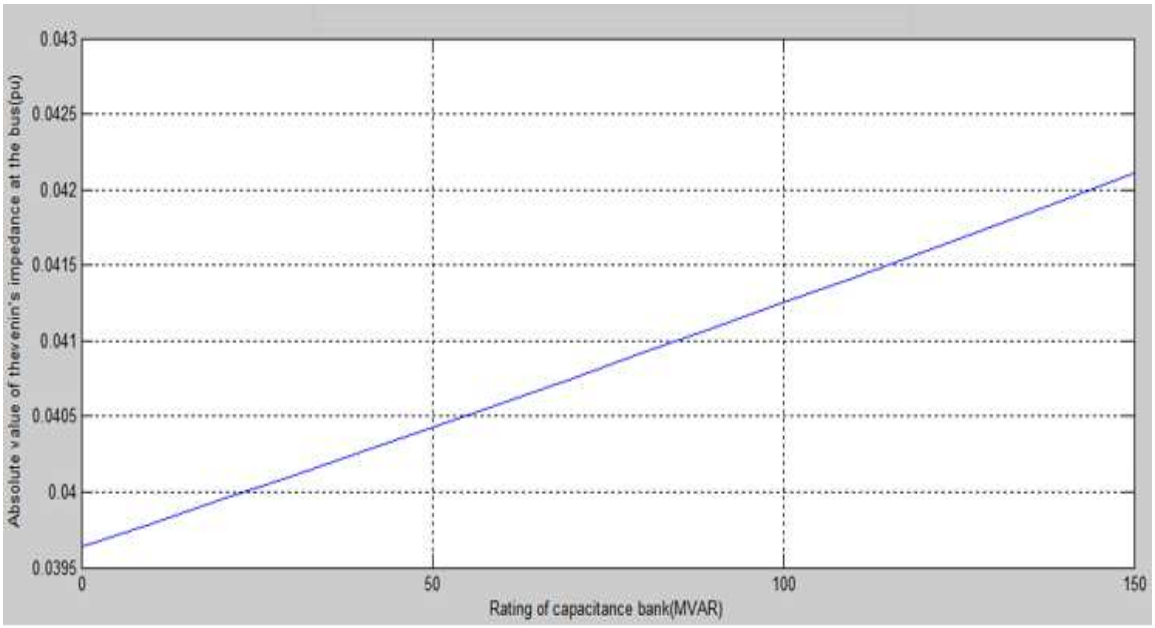

Fig. 3.46 Capacitance Scan at Bus 10 for Fundamental Frequency

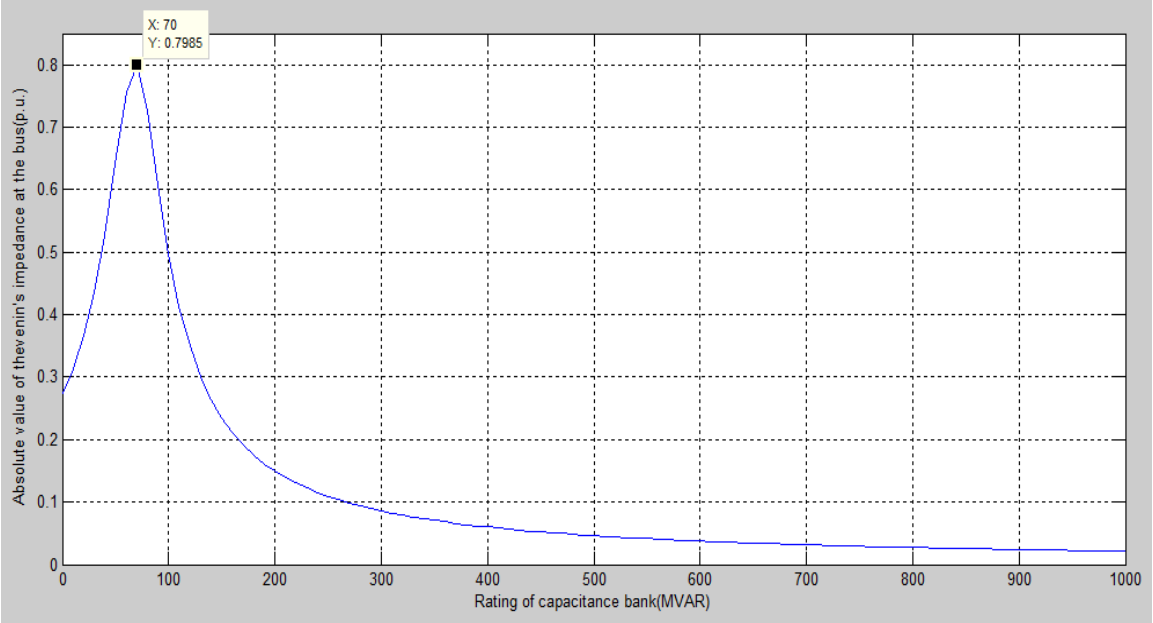

Fig. 3.47 Capacitance Scan at Bus 10 for Harmonic Order 5

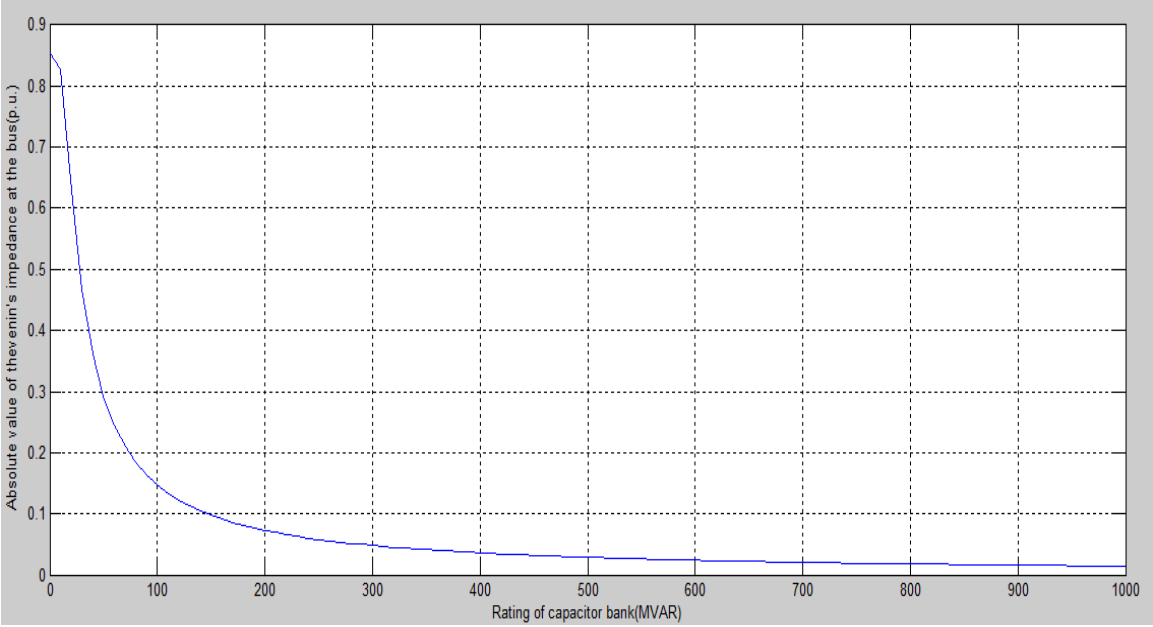

Fig. 3.48 Capacitance Scan at Bus 10 for Harmonic Order 7

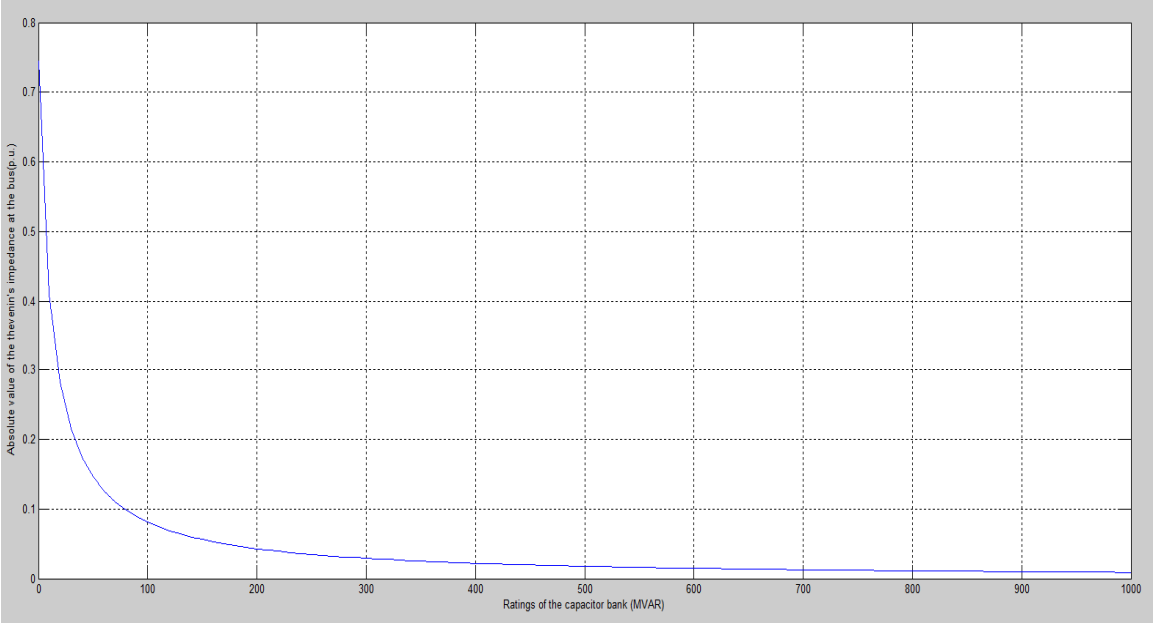

Fig. 3.49 Capacitance Scan at Bus 10 for Harmonic Order 11

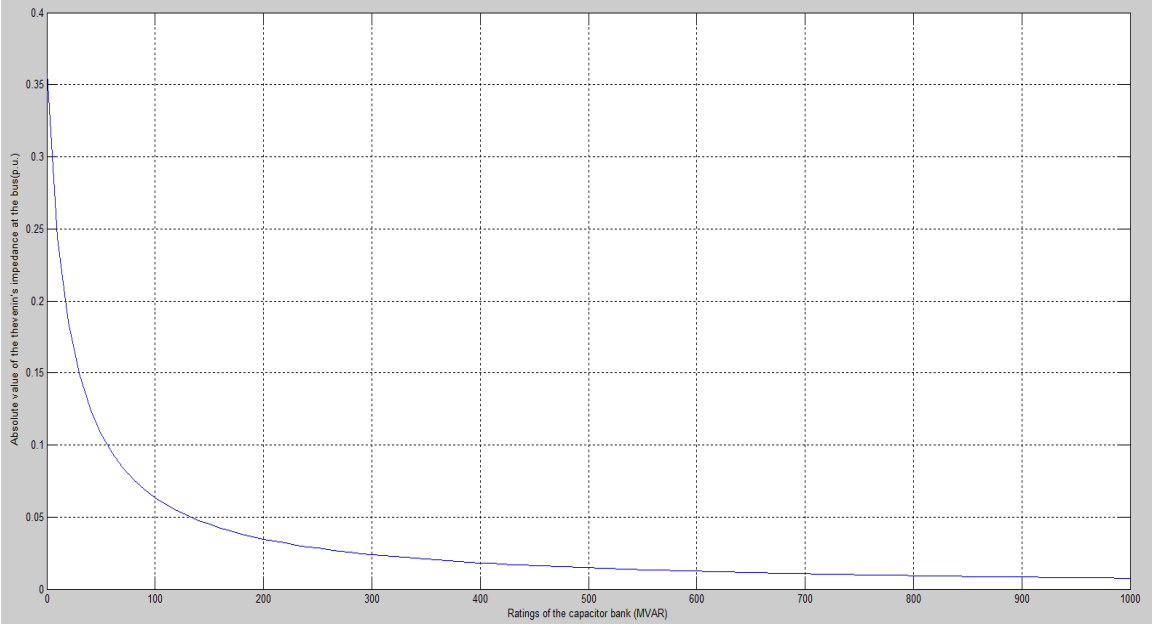

Fig. 3.50 Capacitance Scan at Bus 10 for Harmonic Order 13

3.3 Capacitance scans for the case of multiple shunt capacitor placement

The system under test has a large number of shunt capacitors. Depending on the number of shunt capacitor connected in the transmission network, the number of combinations of which capacitors are in service, and which are out of service is of the form 2^N. A few of these cases are considered as shown in the Table 3.3. In Table 3.3, the proposed shunt capacitor size is given as a single number, a maximum value. In fact, the capacitors are switched and the shunt capacitor may be smaller than the values shown in Table 3.3. The capacitor values are shown, as is the usual case in transmission engineering, in megavars (capacitive). In Table 3.3, the notation 'X' is used to denote which capacitors are ON. If the columns at the right contain a blank, then the corresponding capacitor is OFF. Since the buses 9 and 10 are being studied, in cases C, E and F, they are considered as fixed value capacitor bank only for case when they are not being studied. It means that for case C when bus 10 is being studied, bus 9 has a fixed value that is written in the column labeled proposed shunt capacitor. The Q values at bus 10 in this case will vary from 0 to 1000 MVAr. The notation 'X^1' is used to denote such cases.

The six cases shown in Table 3.3 are labeled Case A through Case F. The results of resonances found for these cases are shown in Tables 3.4 and 3.5.

3.4 Discussion of results

By looking at the results of single capacitor placement, it is evident that at the first four buses that resonance occurs only after addition of the shunt. These four buses have a rated voltage of 230 kV.

Table 3.3 List of the Various Cases Studied

Bus	Bus voltage	Proposed capacitor bank size	Original case	Case A	Case B	Case C	Case D	Case E	Case F
1	230 kV	150 MVAr	← No other capacitors sited→	X		X			
2	230 kV	300 MVAr		X		X	X	X	
3	230 kV	300 MVAr				X	X	X	
4	230 kV	300 MVAr				X	X		
5	69 kV	48 MVAr			X	X			X
6	69 kV	48 MVAr			X	X			
7	69 kV	48 MVAr				X			
8	69 kV	48 MVAr			X	X			
9	69 kV	48 MVAr				X^1		X^1	
10	69 kV	24 MVAr				X^1			X^1

X=Shunt capacitor at this bus is ON

X^1= Shunt capacitor has values 0 to 1000 MVAr when it is being studied

Table 3.4 Results of the Multiple Shunt Capacitor Cases

Case	Resonance checked at	$h = 5$	$h = 7$	$h = 11$	$h = 13$
Base	9	Q = 30 MVAr	Q = 30 MVAr	← No resonance observed →	← No resonance observed →
		$\|Z\|$ = 0.1398 pu	$\|Z\|$ = 0.1495 pu		
	10	Q = 70 MVAr	Q = 0 MVAr		
		$\|Z\|$ = 0.7985 pu	$\|Z\|$ = 0.85 pu		
A	9	Q = 30 MVAr	Q = 30 MVAr		
		$\|Z\|$ = 0.1396 pu	$\|Z\|$ = 0.15 pu		
	10	Q = 70 MVAr	Q = 0 MVAr		
		$\|Z\|$ = 0.7998 pu	$\|Z\|$ = 0.85 pu		
B	9	Q = 30 MVAr	Q = 30 MVAr		
		$\|Z\|$ = 0.1398 pu	$\|Z\|$ = 0.1495 pu		
	10	Q = 70 MVAr	Q = 0 MVAr		
		$\|Z\|$ = 0.7985 pu	$\|Z\|$ = 0.85 pu		
C	9	Q = 130 MVAr	Q = 30 MVAr		
		$\|Z\|$ = 0.1032 pu	$\|Z\|$ = 0.5799 pu		
	10	Q = 70 MVAr	Q = 0 MVAr		
		$\|Z\|$ = 0.8235 pu	$\|Z\|$ = 0.85 pu		
D	9	Q = 130 MVAr	Q = 30 MVAr		
		$\|Z\|$ = 0.1054 pu	$\|Z\|$ = 0.6577 pu		
	10	Q = 70 MVAr	Q = 0 MVAr		
		$\|Z\|$ = 0.8201 pu	$\|Z\|$ = 0.8526 pu		
E	9	Q = 50 MVAr	Q = 20 MVAr		
		$\|Z\|$ = 0.1412 pu	$\|Z\|$ = 0.1636 pu		
	10	Q = 70 MVAr	Q = 0 MVAr		
		$\|Z\|$ = 0.8214 pu	$\|Z\|$ = 0.8558 pu		
F	9	Q = 30 MVAr	Q = 30 MVAr		
		$\|Z\|$ = 0.1399 pu	$\|Z\|$ = 0.1495 pu		
	10	Q = 70 MVAr	Q = 0 MVAr		
		$\|Z\|$ = 0.7985 pu	$\|Z\|$ = 0.854 pu		

Note: Q corresponds to the capacitor causing resonance

At bus 2, the seventh order resonance occurs off the considered range of Q. The other buses are all rated 69 kV. At these buses, for harmonic orders 11 and 13, the driving point impedance has already become capacitive.

Inspection of Figures 3.21-3.50 (for the 69 kV buses studied) indicated the following:

- At bus 8, the resonance at seventh harmonic is particularly sharp (low damping) and the $|Z_{kk}^{7}|$ is high, thus indicating the potential for high seventh harmonic voltages.
- At bus 10, resonance appears to occur at h=5 and 7, and potentially at h=11.

Inspection of the 69 kV buses in Table 3.4 indicates:

- In cases C, D, and E high values of $|Z_{kk}^{5}|$ and $|Z_{kk}^{7}|$ occur at bus 10. These indicate the potential for high fifth and seventh harmonic voltages at bus 10. Also in these cases, the Q value at resonance is significantly different than the base case results. The common additional capacitors in these cases which are at bus 2 and bus 3 have very severe effect on the resonance in the system.

In summary, the results in Table 3.4 in combination with the IEEE Standard 519 can be used to identify problematic cases. For both buses 9 and 10, the harmonic current injection limit is 0.07 per unit at h = 5, 7; and the harmonics voltage limit in 0.03 per unit.

Using

$$|V_k^h| = |Z_{kk}^h||I_k^h|, \tag{3.1}$$

and

$$|V_k^h| \leq 0.03 \text{ per unit} \tag{3.2}$$

$$|I_k^h| \leq 0.07 \text{ per unit} \tag{3.3}$$

Therefore $|Z_{kk}^h| \leq 0.429$ per unit. This means that for cases A – F, all cases may result in high fifth and/or seventh harmonic voltage at bus 10. The identified problematic fifth and seventh harmonic voltages at bus 10 are consistent with the analysis shown in Chapter 4.

Chapter 4 Forbidden zones

4.1 Definition of the term 'forbidden zone' as applied to the placement of shunt capacitors

In Chapter 2, the capacitance scan of a transmission system was described. For such a capacitance scan, a 'forbidden zone' may exist. A forbidden zone is that range of capacitor values which causes the harmonic voltage magnitude to equal or exceed the permissible limits as per the IEEE Standard 519 [35] for an injection of the permissible maximum harmonic current as per the IEEE Standard 519 at the bus in consideration. The mathematical approach for finding the forbidden zones proceeds as follows.

Step 1: Determine if the injection of maximum permissible harmonic current as prescribed in Table 2 of [35] times the maximum value of driving point impedance exceeds or equals the maximum allowed limit as per Table 1 of [35],

$$I_{h,519}^{max} Z_{kk,h}^{max} \geq V_{h,519}^{max}. \tag{4.1}$$

Step 2: If the product obtained in (4.1) equals the maximum permissible value of harmonic voltage, then the value of shunt capacitor at that point is at the boundary of the forbidden zone. At the cited boundary,

$$\left| Z_{kk,h}^{limit} \right| = \frac{V_{h,519}^{max}}{I_{h,519}^{max}}. \tag{4.2}$$

Step 3: Find the values of shunt capacitor that corresponds to the limiting value of imped-

ance (4.2). The range of values that lies within these two values is the forbidden zone.

Step 4: Forbidden zones should also be calculated by using steps 1 to 3 for other harmonic orders that are of the interest at the bus. Combining all of these individual forbidden zones together gives the forbidden zone for the bus.

Since the forbidden zones that are obtained for the individual harmonics are combined together, there may be cases where two such forbidden zones overlap each other. There can also be cases where there exists a gap between two forbidden zones. The cited "forbidden zones" are actually ranges of shunt capacitance that are *suspect* of causing harmonic resonance. It is quite possible that a shunt capacitor sized in the "forbidden zone" will not cause difficulty because the specific harmonic in unexcited. Therefore the interpretation of a "forbidden zone" is that this is a range of Q that warrants some scrutiny.

4.2 Results for the test bed system

The forbidden zones for the test bed system described in Chapter 2 were calculated from the capacitance scans in Chapter 3 by using the above approach. The forbidden zones thus obtained are shown in Figure 4.1 and in Table 4.1. The forbidden zones only exist for four out of the ten artifact buses. This is the reason that only four buses are depicted in Figure 4.1.

4.3 Principal observations on the forbidden zones

The forbidden zones only exist for four buses namely bus 2, bus 3, bus 8 and bus 10 out of the ten artifact buses. For buses 2 and 8, the forbidden zone exists after the pro-

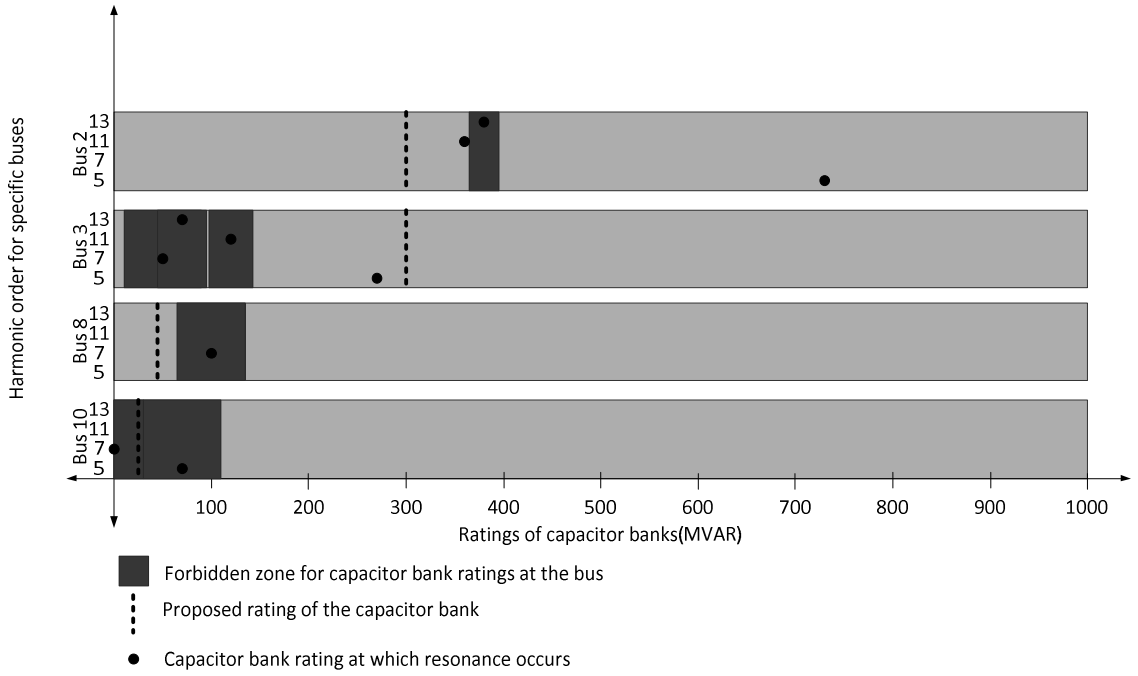

Fig. 4.1 Forbidden Zones for the Test Bed System

Table 4.1 Forbidden Zones for the Test Bed System

Bus	5^{th} harmonic	7^{th} harmonic	11^{th} harmonic	13^{th} harmonic
2	No	No	No	361-391 MVAr
3	No	13-90 MVAr	95-138 MVAr	33-86 MVAr
8	No	66-134 MVAr	No	No
10	30-110 MVAr	0-31 MVAr	0-9.5 MVAr	No

"No" indicates that no forbidden zone was identified

posed maximum size of the shunt capacitor. No special attention is needed for these buses. But care must be taken while considering for future change in sizing as it may causes the shunt capacitor to be in the forbidden zone.

On bus 3 the forbidden zone lies below the maximum proposed shunt capacitor size. In this case, care should be taken that no capacitor step lies within the forbidden zone as it may cause severe resonance issues. Also in bus 3, the forbidden zone overlaps other forbidden zones and there also exists gaps between two forbidden zones. In bus 10, the forbidden zone starts right from the zero shunt capacitor added to a value of about 110 MVAr whereas the proposed capacitor bank size is 24 MVAr. On this bus also multiple forbidden zones overlap.

Chapter 5 Impact of HVDC sources on the test bed system

5.1 HVDC sources in transmission systems

Large HVDC installations act as sources of harmonics. These sources consist of twelve pulse three-phase rectifiers and are thus sources of 11^{th} and 13^{th} harmonics. The IEEE Standard 519 [35] restricts the harmonic current HVDC installations. Harmonic filters are used to limit the harmonic current.

In the WECC transmission system there exist six major HVDC installations. They are as shown in the Figure 5.1. The Pacific DC Intertie which has a line capacity of 3,100 MW [36] and the Intermountain DC Intertie which has capacity of 2400 MW [37] have comparatively high power ratings as compared to the other four. To assess the impact of the HVDC facilities, a harmonic current I_h of 1.0 per unit is injected at the appropriate bus. It must be realized that this is a gross *overestimate* of impact because I_h will be near zero at h=5, 7, and also greatly attenuated at h=11, 13 due to the shunt filters at the AC terminals of the HVDC facility. Here the complete WECC system is considered and is thus not equivalenced so as to consider the effects of HVDC sources which are all outside Arizona.

5.2 Results of HVDC source impacts for the test bed system

For the study purposes, seven cases are considered. The first six cases consider the effects of these six harmonic sources individually (i.e. only one HVDC source exists) and in the last case, all the six HVDC sources inject harmonics in the network simultaneously. The results are shown in the Tables 5.1, 5.2, and 5.3.

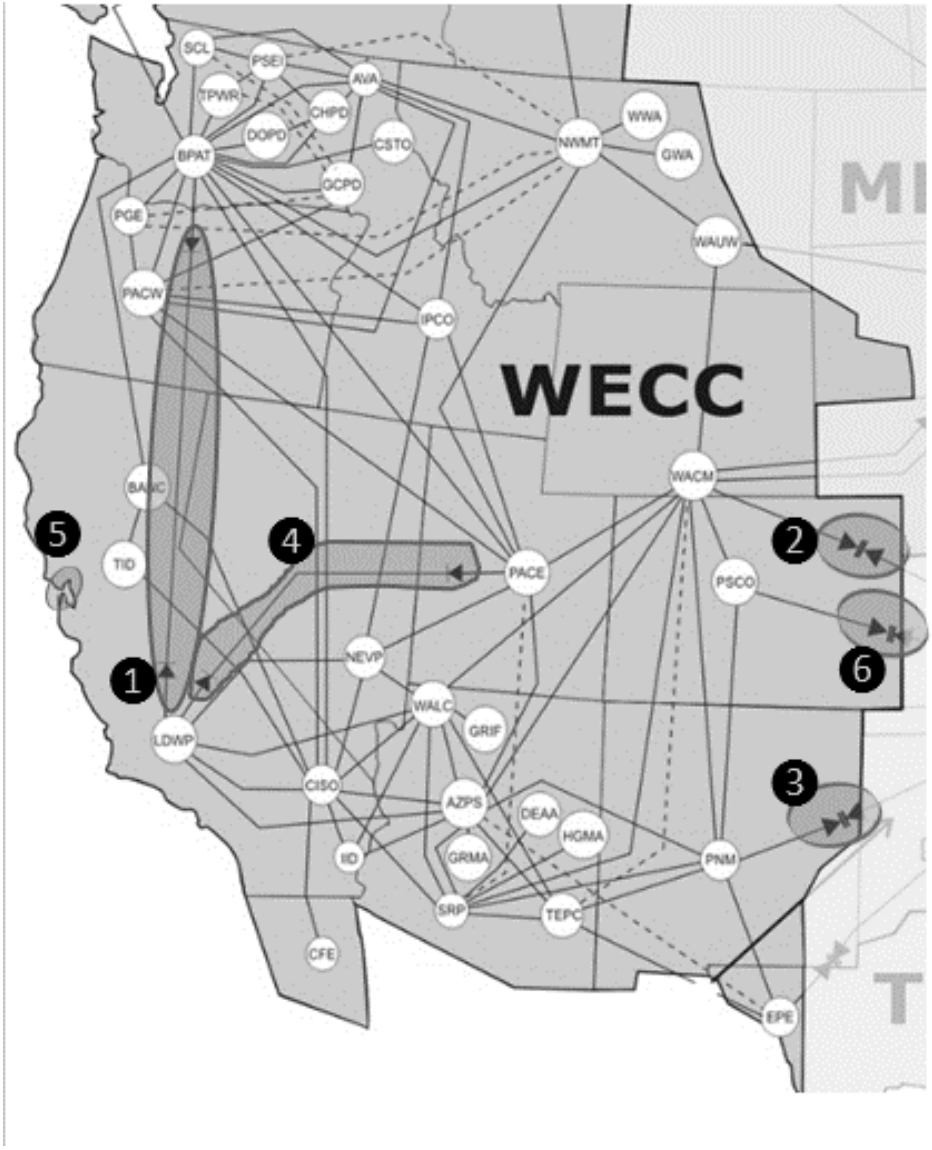

1. Sylmar PDCI
2. Stegall
3. Tres Amigas
4. Intermountain DC tie
5. Trans Bay
6. Virginia Smith (Sidney)

Fig. 5.1 The HVDC Sources in the WECC Transmission Network

Table 5.1 Impact of HVDC Sources at Buses 1, 2 and 3

	Cases	Bus 1	Bus 2	Bus 3
Inject 1.0 per unit harmonic current at these buses individually	PDCI (Sylmar)	$V_{11}=1.798\times10^{-5}$ $V_{13}=6.118\times10^{-6}$	$V_{11}=2.028\times10^{-4}$ $V_{13}=8.068\times10^{-5}$	$V_{11}=2.797\times10^{-6}$ $V_{13}=6.944\times10^{-7}$
	Intermountain (Adelanto)	$V_{11}=3.335\times10^{-5}$ $V_{13}=3.227\times10^{-5}$	$V_{11}=3.713\times10^{-4}$ $V_{13}=4.182\times10^{-4}$	$V_{11}=6.402\times10^{-6}$ $V_{13}=3.711\times10^{-6}$
	Stegall DC	$V_{11}=7.616\times10^{-8}$ $V_{13}=9.917\times10^{-8}$	$V_{11}=1.268\times10^{-7}$ $V_{13}=3.43\times10^{-7}$	$V_{11}=6.302\times10^{-8}$ $V_{13}=6.15\times10^{-9}$
	Clovis	$V_{11}=2.234\times10^{-9}$ $V_{13}=1.614\times10^{-9}$	$V_{11}=3.57\times10^{-9}$ $V_{13}=5.59\times10^{-9}$	$V_{11}=1.751\times10^{-9}$ $V_{13}=9.944\times10^{-11}$
	Virginia Smith (Sidney)	$V_{11}=1.795\times10^{-8}$ $V_{13}=1.611\times10^{-9}$	$V_{11}=2.985\times10^{-8}$ $V_{13}=5.573\times10^{-9}$	$V_{11}=1.49\times10^{-8}$ $V_{13}=9.719\times10^{-11}$
	Trans Bay (Pitts-burg)	$V_{11}=1.855\times10^{-10}$ $V_{13}=2.853\times10^{-12}$	$V_{11}=2.113\times10^{-9}$ $V_{13}=3.831\times10^{-11}$	$V_{11}=3.74\times10^{-11}$ $V_{13}=3.269\times10^{-13}$
	All	$V_{11}=4.328\times10^{-5}$ $V_{13}=2.621\times10^{-5}$	$V_{11}=4.824\times10^{-4}$ $V_{13}=3.377\times10^{-4}$	$V_{11}=7.847\times10^{-6}$ $V_{13}=3.02\times10^{-6}$

All values are in per unit

Voltages greater than 0.1% are shaded

Table 5.2 Impact of HVDC Sources at Buses 4, 5 and 6

	Cases	Bus 4	Bus 5	Bus 6
Inject 1.0 per unit harmonic current at these buses individually	PDCI (Sylmar)	$V_{11}=9.719\times10^{-6}$ $V_{13}=3.387\times10^{-6}$	$V_{11}=9.337\times10^{-4}$ $V_{13}=6.732\times10^{-5}$	$V_{11}=1.875\times10^{-4}$ $V_{13}=1.885\times10^{-5}$
	Intermountain (Adelanto)	$V_{11}=1.836\times10^{-5}$ $V_{13}=1.781\times10^{-5}$	$V_{11}=0.0017$ $V_{13}=3.477\times10^{-4}$	$V_{11}=3.433\times10^{-4}$ $V_{13}=9.959\times10^{-5}$
	Stegall DC	$V_{11}=1.104\times10^{-7}$ $V_{13}=6.591\times10^{-8}$	$V_{11}=5.631\times10^{-7}$ $V_{13}=3.204\times10^{-7}$	$V_{11}=1.783\times10^{-7}$ $V_{13}=1.288\times10^{-7}$
	Clovis	$V_{11}=3.262\times10^{-9}$ $V_{13}=1.072\times10^{-9}$	$V_{11}=1.555\times10^{-8}$ $V_{13}=5.213\times10^{-9}$	$V_{11}=5.066\times10^{-9}$ $V_{13}=2.094\times10^{-9}$
	Virginia Smith (Sidney)	$V_{11}=2.599\times10^{-8}$ $V_{13}=1.071\times10^{-9}$	$V_{11}=1.325\times10^{-7}$ $V_{13}=5.202\times10^{-9}$	$V_{11}=4.2\times10^{-8}$ $V_{13}=2.084\times10^{-9}$
	Trans Bay (Pittsburg)	$V_{11}=9.747\times10^{-11}$ $V_{13}=1.583\times10^{-12}$	$V_{11}=9.725\times10^{-9}$ $V_{13}=3.212\times10^{-11}$	$V_{11}=1.952\times10^{-9}$ $V_{13}=8.873\times10^{-12}$
	All	$V_{11}=2.393\times10^{-5}$ $V_{13}=1.447\times10^{-5}$	$V_{11}=0.0022$ $V_{13}=2.807\times10^{-4}$	$V_{11}=4.473\times10^{-4}$ $V_{13}=8.065\times10^{-5}$

All values are in per unit

Voltages greater than 0.1% are shaded

Table 5.3 Impact of HVDC Sources at Buses 7, 8, 9 and 10

	Cases	Bus 7	Bus 8	Bus 9	Bus 10
Inject 1.0 per unit harmonic current at these buses individually	PDCI (Sylmar)	$V_{11}=0.0014$ $V_{13}=1.582\times10^{-4}$	$V_{11}=1.705\times10^{-4}$ $V_{13}=5.681\times10^{-5}$	$V_{11}=2.99\times10^{-5}$ $V_{13}=2.126\times10^{-6}$	$V_{11}=9.482\times10^{-7}$ $V_{13}=8.319\times10^{-6}$
	Intermoun-tain (Ade-lanto)	$V_{11}=0.0026$ $V_{13}=8.199\times10^{-4}$	$V_{11}=3.266\times10^{-4}$ $V_{13}=3.001\times10^{-4}$	$V_{11}=5.43\times10^{-5}$ $V_{13}=1.13\times10^{-5}$	$V_{11}=1.774\times10^{-5}$ $V_{13}=4.334\times10^{-5}$
	Stegall DC	$V_{11}=8.802\times10^{-7}$ $V_{13}=7.18\times10^{-7}$	$V_{11}=5.018\times10^{-7}$ $V_{13}=4.008\times10^{-7}$	$V_{11}=6.795\times10^{-8}$ $V_{13}=4.733\times10^{-8}$	$V_{11}=4.631\times10^{-9}$ $V_{13}=1.163\times10^{-7}$
	Clovis	$V_{11}=2.435\times10^{-8}$ $V_{13}=1.17\times10^{-8}$	$V_{11}=1.473\times10^{-8}$ $V_{13}=6.513\times10^{-9}$	$V_{11}=2.043\times10^{-9}$ $V_{13}=7.703\times10^{-10}$	$V_{11}=1.35\times10^{-10}$ $V_{13}=1.892\times10^{-9}$
	Virginia Smith (Sidney)	$V_{11}=2.072\times10^{-7}$ $V_{13}=1.167\times10^{-8}$	$V_{11}=1.183\times10^{-7}$ $V_{13}=6.486\times10^{-9}$	$V_{11}=1.602\times10^{-8}$ $V_{13}=7.695\times10^{-10}$	$V_{11}=1.093\times10^{-9}$ $V_{13}=1.886\times10^{-9}$
	Trans Bay (Pittsburg)	$V_{11}=1.459\times10^{-9}$ $V_{13}=7.544\times10^{-12}$	$V_{11}=1.686\times10^{-9}$ $V_{13}=2.677\times10^{-11}$	$V_{11}=3.116\times10^{-10}$ $V_{13}=1.014\times10^{-12}$	$V_{11}=1.019\times10^{-11}$ $V_{13}=3.871\times10^{-12}$
	All	$V_{11}=0.0033$ $V_{13}=6.622\times10^{-4}$	$V_{11}=4.22\times10^{-4}$ $V_{13}=2.43\times10^{-4}$	$V_{11}=7.114\times10^{-5}$ $V_{13}=9.201\times10^{-6}$	$V_{11}=2.281\times10^{-6}$ $V_{13}=3.513\times10^{-5}$

All values are in per unit

Voltages greater than 0.1% are shaded

5.3 Observations

Tables 5.1, 5.2, and 5.3 are actually a measure of sensitivity of harmonic injection from the HVDC facility to the ten study buses. At all these buses, sensitivities are very low. The highest sensitivity of 0.0033 per unit occurs at bus 7 for a 1.0 per unit injection of harmonic current at all the HVDC sources. This is deemed to be low enough to conclude that the HVDC impact on harmonics in the Arizona transmission system are negligible. This conclusion is further supported by noting that Tables 5.1-5.3 are volts for 1.0 per unit current injection at the HVDC terminals. The actual harmonic current injection at the HVDC terminals is very small because these are twelve pulse converters, and 11^{th} and 13^{th} harmonic filters are installed.

Chapter 6 Conclusions and recommendations

6.1 Conclusions

Resonance can cause problematic issues with the normal operation of a transmission network. Addition of capacitors at a bus could create resonance at that bus. The network needs to be examined for resonance conditions that could occur. If these capacitors can be switched from zero to their maximum rating, it is possible that intermediate values may create resonance in the system.

Capacitance scans were done for the Arizona transmission system. A capacitance scan in this context is an evaluation of the driving point impedance at a given bus as the injected capacitive reactive power is varied (or 'scanned'). The capacitance scans were carried at ten buses in consideration for fundamental frequency and 5^{th}, 7^{th}, 11^{th} and 13^{th} harmonics. The ten buses are the buses identified for the placement of shunt capacitors. This considers that the harmonics are injected by three-phase rectifiers. The harmonic current injection up to 13^{th} harmonic was considered. The study done included ten buses rated at 230 and 69 kV. Results appear in Figures 3.1-3.20 (for 230 kV buses) and 3.21-3.50 (for 69 kV buses), all showing capacitor scans. The capacitor scans are plots of driving point impedance $\left|Z_{kk}^{h}\right|$ at bus k, and harmonic h, versus the shunt compensation (MVAr) at bus k. Maxima of $\left|Z_{kk}^{h}\right|$ indicates resonance. In Figure 3.10, for bus 2, the highest value of $\left|Z_{kk}^{h}\right|$ is 1.948 per unit at $h = 13$ for added capacitance of 380 MVAr. This indicates that for 13^{th} harmonic, bus 2 resonates when a shunt capacitor of 380 MVAr is connected at it.

Also studied were the sensitivities of harmonic current injection at six WECC HVDC installations. The electrically nearest of these HVDC installations are the Pacific

DC Intertie and the Intermountain DC Intertie. The sensitivity studies were done for harmonics h =11 and h = 13. Both of these frequencies however, are assumed to be highly attenuated at the HVDC terminals by shunt filters at the HVDC site itself. No significant impact of 11^{th} or 13^{th} harmonic were observed. The highest voltage sensitivity that was observed was 0.0033 per unit at bus 7 when all the HVDC sources are active at the same time.

6.2 Recommendations and future work

The following recommendations are made:

- Problematic cases identified in Figure 4.1 which occurs at buses 2, 3, 8 and 10 should be carefully re-examined.
- In this study, no actual harmonic voltage or current measurements were used. It is recommended to take sample measurements of h =5, 7, 11, and 13 harmonic voltages and currents at some of the ten buses included in the study. It is recommended to use voltage and current measurements to obtain impedance at harmonic h ($|Z_{kk}^h|$), and compare $|Z_{kk}^h|$ with the appropriate graphs in Figures 3.1-3.50.
- Any discrepancies between actual measurements and theoretical calculations should be considered carefully for resolution of differences.
- There was no study of third harmonic voltages or currents. This should be done including measured data. In particular, the identification of the levels and sources of third harmonic should be attempted. It is recommended to correlate measured values of third harmonic currents and voltages with assumed source models. Also,

including h =5 and 7 harmonics from the subtransmission and distribution levels is recommended.

- This study used IEEE 519 maximum harmonic voltage and current values. These maxima were used to obtain the forbidden zones described in Chapter 4. The use of these maxima should be reconsidered to obtain less conservative results.
- Reporting main results to IEEE should be considered. For example, [42].

REFERENCES

[1] C. Amornvipas, L. Hofmann, "Resonance analysis in transmission systems: experience in Germany," *IEEE Power and Energy Society General Meeting*, 25-29 July 2010.

[2] S. M. Halpin, P. F. Ribeiro, J. J. Dai, "Frequency-domain harmonic analysis methods," available at:
https://www.calvin.edu/~pribeiro/IEEE/ieee_cd/chapters/CHAP_6/c6toc/c6_text.htm

[3] Anonymous, "Notes on network admittance and impedance matrices," Indian Institute of Technology, Kanpur, available at:
http://nptel.ac.in/courses/Webcourse-contents/IIT-KANPUR/power-system/ui/Course_home-3.htm

[4] T. Overbye, R. Baldick, "Notes on power system analysis," University of Texas at Austin available at:
http://users.ece.utexas.edu/~baldick/classes/369/Lecture_10.ppt

[5] Anonymous, "Notes on power system matrices," Baylor University available at:
http://web.ecs.baylor.edu/faculty/grady/_14_ELC4340_Spring13_Power_System_Matrices.doc

[6] H. Rafik, B. El-Hana, "Notes on power system analysis," Umm Al-Qura University available at:
https://uqu.edu.sa/files2/tiny_mce/plugins/filemanager/files/4300303/EPS/Electrical_Power_System_Analysis_4._The_Impedance_Model_And_Network_Calculations.pdf

[7] O. Samuelsson, "Notes on power system models," Lund University, available at:
https://www.iea.lth.se/eks/L2_14.pdf

[8] S. Santoso, A. Maitri, "Empirical estimation of system parallel resonant frequencies using capacitor switching transient data," *IEEE Transactions on Power Delivery*, April 2005, vol. 20, no. 2, pp. 1151-1156.

[9] K. Hur, S. Santoso, "An improved method to empirical estimation of system parallel resonant frequencies using capacitor switching transient data," *IEEE Transactions on Power Delivery*, July 2006, vol. 21, no. 3, pp. 1751-1753.

[10] A. P. S. Meliopoulos, F. Zhang, S. Zelingher, "Power system harmonic state estimation," *IEEE Transactions on Power Delivery*, July 1994, vol. 9, no. 3, pp. 1701-1709.

[11] W. Xu, Y. Liu, "A method for determining customer and utility harmonic contributions at the point of common coupling," *IEEE Transactions on Power Delivery*, April 2000, vol. 15, no. 2, pp. 804-811.

[12] B. Blažič, T. Pfajfar, I. Papič, "A modified harmonic current vector method for harmonic contribution determination," *IEEE PES Power Systems Conference and Exposition*, 2004, pp. 1470-1475.

[13] A. Bonner et al., "Modeling and simulation of the propagation of harmonics in electric power networks - part 1: concepts, models and simulation techniques," *IEEE Transactions on Power Delivery*, January 1996, vol. 11, no. 1, pp. 452-465.

[14] R. H. Galloway, W. B. Shorocks, L. M. Wedepohl, "Calculation of electrical parameters for short and long polyphase transmission lines," *Proceedings of the Institution of Electrical Engineers*, December 1964, vol. 111, no. 12, pp. 2051-2059.

[15] P. C. Magnusson, *Transmission Lines and Wave Propagation*, Allyn and Bacon, Boston, 1965.

[16] J. Arrillaga, E. Acha, T. J. Densem, P. S. Bodger, "Ineffectiveness of transmission line transpositions at harmonic frequencies," *Generation, Transmission and Distribution, IEE Proceedings C*, vol. 133, no. 2, pp. 99, March 1986.

[17] J. Arrillaga, B. C. Smith, N. R. Watson, Alan R. Wood, "Power system harmonic analysis," John Wiley & Sons Ltd., Chichester, West Sussex, England, November 2000.

[18] J. C. Das, "Power system harmonics and passive filter designs," IEEE Press, Piscataway, NJ, 2015.

[19] S. A. Papathanassiou, M. P. Papadopoulos, "Harmonic analysis in a power system with wind generation," *IEEE Transactions on Power Delivery*, October 2006, vol. 21, no. 4, pp. 2006-2016.

[20] C. Amornvipas, L. Hoffmann, “Resonance Analyses in Transmission Systems: Experience in Germany,” *IEEE Power and Energy Society General Meeting*, 25-29 July, 2010, pp. 1-8.

[21] D. Tong, V. G. Nikolaenko, N. Ginbey, I. Lau, “ Harmonic propagation in transmission system with multiple capacitor installations*,” International Conference on Power System Technology*, Dec. 2000, vol. 2, pp. 1007-1012.

[22] G. Lemieux, "Power system harmonic resonance - a documented case," *IEEE Transactions on Industry Application*, May/June 1990, vol. 26, no. 3, pp. 483-488.

[23] N. Eghtedarpour, M. A. Karimi, M. Tavakoli, "Harmonic resonance in power systems - a documented case," *IEEE 16th International Conference on Harmonics and Quality of Power,* 2014, pp. 857-861.

[24] R. Yacamini, "Overview on sources of harmonic distortion," *IEE Colloquium on Sources and Effects of Harmonic Distortion in Power Systems* (digest No.: 1997/096), London, 5th March 1997.

[25] Qual-Tech Engineers, Inc., "Harmonics in industrial power systems," available at: www.qualtecheng.com/docs/harmonics/QT-613.pdf

[26] EPRI / Electrotek Concepts, Inc., “Notes appearing on the subject of sources of harmonics,” available at: www.unge.gq/ftp/biblioteca%20digital/Armonicos/some%20sources%20of%20harmonics%20with%20waveforms.pdf

[27] A. K. Akhani, Engineering Articles, blog on sources of harmonics, available at: top10electrical.blogspot.in/2014/09/sources-of-harmonics.html

[28] Anonymous, “Notes on harmonic sources from industrial loads: part II,” available at: www.idc-online.com/technical_references/pdfs/electrical_engineering/Harmonic_Sources_from_Industrial _loads_II.pdf

[29] J. Arrillaga, Neville R. Watson, "Power system harmonics," John Wiley & Sons Ltd., 2003.

[30] "Introduction to PowerWorld simulator: interface and common tools, I14: Equivalents," PowerWorld Corporation, Champaign, IL, available at:
http://www.powerworld.com/files/I14Equivalents.pdf

[31] PowerWorld Corporation, "Steady-State power system security analysis with PowerWorld simulator, S1: power system modeling, methods and equations," Champaign, IL, available at:
http://www.powerworld.com/files/S01SystemModeling.pdf

[32] Anonymous, available at:
http://w3.siemens.com/smartgrid/global/en/products-systems-solutions/software-solutions/planning-data-management-software/planning-simulation/pages/pss-e.aspx

[33] Anonymous, available at:
http://www.powerworld.com/products/simulator/overview

[34] Anonymous, available at:
http://www.geenergyconsulting.com/pslf-re-envisioned

[35] IEEE, "IEEE recommended practice and requirements for harmonic control in electric power systems," IEEE Standard 519-2014, New York, NY.

[36] Bonneville Power Administration, "Pacific Direct Current Intertie (PDCI) upgrade project," available at:
http://www.bpa.gov/transmission/Projects/line-projects/Pages/PDCI-Upgrade-Project.aspx

[37] ABB, "Intermountain Power Project: the second HVDC transmission to Los Angeles," available at:
http://new.abb.com/systems/hvdc/references/intermountain-power-project

[38] Michigan Technological University, "Solving system of linear equations," available at:
http://www.cs.mtu.edu/~shene/COURSES/cs3621/NOTES/INT-APP/CURVE-linear-system.html

[39] Anonymous, Module for forward and backward substitution, available at:
http://mathfaculty.fullerton.edu/mathews/n2003/BackSubstitutionMod.html

[40] Mathuranathan, Gaussian Waves, Solving a triangular matrix using forward and backward substitution, available at:
http://www.gaussianwaves.com/2013/05/solving-a-triangular-matrix-using-forward-backward-substitution/

[41] MathWorks, "Matlab Documentation, mldivide, \," available at:
http://www.mathworks.com/help/matlab/ref/mldivide.html

[42] G. T. Heydt, H. U. Patil, J. Loehr, T. LaRose, "Harmonic resonance assessment for transmission class shunt capacitors," to be submitted to *IEEE Transmission and Distribution Conference and Expo*, Dallas, TX, March, 2016.

APPENDIX A

FORWARD BACKWARD SUBSTITUTION METHOD FOR THE CALCULATION OF X IN $AX=B$

A.1 Forward/backward substitution

Forward and backward substitution is used to solve $Ax=b$ for x (given A and b). The method involves the factorization of A into lower left triangular matrix L and upper right triangular matrix U,

$$A=LU.$$

Then

$$Ax=b \Rightarrow LUx=b.$$

Let $Ux=W$. Then

$$LW=b. \qquad \text{(A.1)}$$

Matrix L and vector b are given, and (A.1) is easily solved for W_1

$$W_1=\frac{b_1}{L_{11}}.$$

Then W_2-W_n are found by forward substitution. This gives the vector W. Then,

$$W=Ux. \qquad \text{(A.2)}$$

And, in (A.2) x_n is found simply by

$$x_n = \frac{W_n}{U_{nn}}.$$

And previous (i.e., rows n-1, n-2, and others) rows of x are found by backward substitution.

This method is shown in detail in [38-40].

A.2 Application in Matlab

Matlab uses LU decomposition in solving $Ax=b$ by using "`A\b`". This "\" function in Matlab also works with sparse matrices. This functionality is useful because the system admittance matrix is a sparse matrix. The algorithm that Matlab follows to solve $Ax=b$ is described above and also in [41].

APPENDIX B

MATLAB CODE USED FOR THE CREATION OF THE CAPACITANCE SCANS

B.1 Matlab code used for the harmonic assessment of single shunt capacitor placement

```
%Removal of Island Buses from the Ybus
p=size(Ybus);
q=p(1);
m=0;
for k=1:1:q
    if Ybus(k-m,k-m)==0
        %B(k-m)=[];
        Ybus(k-m,:)=[];
        Ybus(:,k-m)=[];
        m=m+1;
    end
end
%B
%x=size(B)
%y=size(Ybus)


%Extraction of individual components from Bus Admittance Matrix
A=sum(Ybus);
h1=1;
h=5;
%h=7;
%h=11;
%h=13;
for k=1:1:length(A)
    if imag(A(k))>=0  %Capacitive
        Z=1/A(k);
        Ybus(k,k)=Ybus(k,k)-A(k)+(1/(real(Z)+(imag(Z)*h1/h)*i));
    end
    if imag(A(k))<0   %Inductive
        Z=1/A(k);
        Ybus(k,k)=Ybus(k,k)-A(k)+(1/(real(Z)+(imag(Z)*h/h1)*i));
    end
end
%Ybus
for k=1:1:length(A)
    for l=k:1:length(A)
        if k==l
        else
            if imag(Ybus(k,l))>0 %Inductive
                Z=1/-Ybus(k,l);
                Ybus(k,l)=Ybus(k,l)-Ybus(k,l)-
(1/(real(Z)+(imag(Z)*h/h1)*i));
                Ybus(l,k)=Ybus(k,l);
                Ybus(k,k)=Ybus(k,k)-
(1/Z)+(1/(real(Z)+(imag(Z)*h/h1)*i));
                Ybus(l,l)=Ybus(l,l)-
(1/Z)+(1/(real(Z)+(imag(Z)*h/h1)*i));
            end
            if imag(Ybus(k,l))<0 %Capacitive
```

```
                Z=1/-Ybus(k,l);
                Ybus(k,l)=Ybus(k,l)-Ybus(k,l)-
(1/(real(Z)+(imag(Z)*h1/h)*i));
                Ybus(l,k)=Ybus(k,l);
                Ybus(k,k)=Ybus(k,k)-
(1/Z)+(1/(real(Z)+(imag(Z)*h1/h)*i));
                Ybus(l,l)=Ybus(l,l)-
(1/Z)+(1/(real(Z)+(imag(Z)*h1/h)*i));
            end
        end
    end
end


%Addition of new capacitor banks at the following buses:-
%Bus 1  - 230 kV - 1 x 150 MVAr
%Bus 2  - 230 kV - 2 x 150 MVAr
%Bus 3  - 230 kV - 2 x 150 MVAr
%Bus 4  - 230 kV - 2 x 150 MVAr
%Bus 5  - 69 kV  - add one more 48 MVAr to the existing
%Bus 6  - 69 kV  - add one more 48 MVAr to the existing
%Bus 7  - 69 kV  - add one more 48 MVAr to the existing
%Bus 8  - 69 kV  - add one more 48 MVAr to the existing
%Bus 9  - 69 kV  - add one more 48 MVAr to the existing
%Bus 10 - 69 kV  - convert to 48 MVAr from 24 MVAr

%For this a matrix will be created which will contain the position of
the
%Capacitor bank in the Bus admittance matrix, the voltage of the con-
cerned
%bus and the size of the Capacitor bank in MVAr
A=[408 230 1000;
   417 230 1000;
   409 230 1000;
   410 230 1000;
   693 69 1000;
   698 69 1000;
   440 69 1000;
   688 69 1000;
   695 69 1000;
   898 69 1000];
p=size(A);


for k=4%k=1:1:p(1)
    a=zeros(101,2);
    m=1;

    k
    for Q=0:10:A(k,3)
        m
        Xc=((A(k,2)*10^3)^2)/((Q*10^6)*h);
        Zbase=((A(k,2)*10^3)^2)/(100*10^6);
        Xcpu=Xc/Zbase;
        Ycpun=1/Xcpu;
```

```
        Ybus(A(k,1),A(k,1))=Ybus(A(k,1),A(k,1))+j*Ycpun;
        Zbus=Ybus\speye(length(Ybus),length(Ybus));
        a(m,1)=Q;
        a(m,2)=Zbus(A(k,1),A(k,1));
        Ybus(A(k,1),A(k,1))=Ybus(A(k,1),A(k,1))-j*Ycpun;
        m=m+1;
    end
    l=0;
    for m=2:1:101
        if a(m-l,1)==0
            a(m-l,:)=[];
            l=l+1;
        end
    end
    figure(k)
    plot(a(:,1),abs(a(:,2)),'-b')
    hold on;
    grid on;
    figure(k+p(1))
    plot(a(:,1),angle(a(:,2))*(180/pi),'-b')
    hold on;
    grid on;
end
```

B.2 Matlab code for multiple shunt capacitor bank placement cases

```
%Removal of Island Buses from the Ybus
p=size(Ybus);
q=p(1);
m=0;
for k=1:1:q
    if Ybus(k-m,k-m)==0
        %B(k-m)=[];
        Ybus(k-m,:)=[];
        Ybus(:,k-m)=[];
        m=m+1;
    end
end

%Extraction of individual components from Bus Admittance Matrix and
change
%Ybus to any harmonic order as desired
A=sum(Ybus);
h1=1;
h=5;
for k=1:1:length(A)
    if imag(A(k))>=0  %Capacitive
        Z=1/A(k);
        Ybus(k,k)=Ybus(k,k)-A(k)+(1/(real(Z)+(imag(Z)*h1/h)*i));
    end
    if imag(A(k))<0   %Inductive
        Z=1/A(k);
        Ybus(k,k)=Ybus(k,k)-A(k)+(1/(real(Z)+(imag(Z)*h/h1)*i));
    end
```

```
end

for k=1:1:length(A)
    for l=k:1:length(A)
        if k==l
        else
            if imag(Ybus(k,l))>0 %Inductive
                Z=1/-Ybus(k,l);
                Ybus(k,l)=Ybus(k,l)-Ybus(k,l)-
(1/(real(Z)+(imag(Z)*h/h1)*i));
                Ybus(l,k)=Ybus(k,l);
                Ybus(k,k)=Ybus(k,k)-
(1/Z)+(1/(real(Z)+(imag(Z)*h/h1)*i));
                Ybus(l,l)=Ybus(l,l)-
(1/Z)+(1/(real(Z)+(imag(Z)*h/h1)*i));
            end
            if imag(Ybus(k,l))<0 %Capacitive
                Z=1/-Ybus(k,l);
                Ybus(k,l)=Ybus(k,l)-Ybus(k,l)-
(1/(real(Z)+(imag(Z)*h1/h)*i));
                Ybus(l,k)=Ybus(k,l);
                Ybus(k,k)=Ybus(k,k)-
(1/Z)+(1/(real(Z)+(imag(Z)*h1/h)*i));
                Ybus(l,l)=Ybus(l,l)-
(1/Z)+(1/(real(Z)+(imag(Z)*h1/h)*i));
            end
        end
    end
end

%Addition of new capacitor banks at the following buses:-
%Bus 1  - 230 kV - 1 x 150 MVAr
%Bus 2  - 230 kV - 2 x 150 MVAr
%Bus 3  - 230 kV - 2 x 150 MVAr
%Bus 4  - 230 kV - 2 x 150 MVAr
%Bus 5  - 69 kV  - add one more 48 MVAr to the existing
%Bus 6  - 69 kV  - add one more 48 MVAr to the existing
%Bus 7  - 69 kV  - add one more 48 MVAr to the existing
%Bus 8  - 69 kV  - add one more 48 MVAr to the existing
%Bus 9  - 69 kV  - add one more 48 MVAr to the existing
%Bus 10 - 69 kV  - convert to 48 MVAr from 24 MVAr

%For this a matrix will be created which will contain the position of
the
%Capacitor bank in the Bus admittance matrix, the voltage of the con-
cerned
%bus and the size of the Capacitor bank in MVAr
A=[408 230 1000 150;
   417 230 1000 300;
   409 230 1000 300;
   410 230 1000 300;
   693 69 1000 48;
   698 69 1000 48;
   440 69 1000 48;
   688 69 1000 48;
   695 69 1000 48;
```

```
   898 69 1000 24];
p=size(A);

%B=[1 1 0 0 0 0 0 0 0 0];
%B=[0 0 0 0 1 1 0 1 0 0];
%B=[1 1 1 1 1 1 1 1 0 1];
%B=[1 1 1 1 1 1 1 1 1 0];
%B=[0 1 1 1 0 0 0 0 0 0];
%B=[0 1 1 0 0 0 0 0 0 0];
%B=[0 1 1 0 0 0 0 0 1 0];
%B=[0 0 0 0 1 0 0 0 0 1];
B=[0 0 0 0 1 0 0 0 0 0];
r=size(B);

for k=1:1:r(2)
    if B(k)==1
        Xc=((A(k,2)*10^3)^2)/((A(k,4)*10^6)*h);
        Zbase=((A(k,2)*10^3)^2)/(100*10^6);
        Xcpu=Xc/Zbase;
        Ycpun=1/Xcpu;
        Ybus(A(k,1),A(k,1))=Ybus(A(k,1),A(k,1))+j*Ycpun;
    end
end

for k=10
    a=zeros(101,2);
    m=1;


    for Q=0:10:A(k,3)
        m
        Xc=((A(k,2)*10^3)^2)/((Q*10^6)*h);
        Zbase=((A(k,2)*10^3)^2)/(100*10^6);
        Xcpu=Xc/Zbase;
        Ycpun=1/Xcpu;
        Ybus(A(k,1),A(k,1))=Ybus(A(k,1),A(k,1))+j*Ycpun;
        Zbus=Ybus\speye(length(Ybus),length(Ybus));
        a(m,1)=Q;
        a(m,2)=Zbus(A(k,1),A(k,1));
        Ybus(A(k,1),A(k,1))=Ybus(A(k,1),A(k,1))-j*Ycpun;
        m=m+1;
    end


    figure(1)
    plot(a(:,1),abs(a(:,2)),'-b')
    hold on;
    grid on;
    figure(2)
    plot(a(:,1),angle(a(:,2))*(180/pi),'-b')
    hold on;
    grid on;
end
```

APPENDIX C

SELECTED PHASE ANGLE PLOTS FOR CAPACITANCE SCAN RESULTS

C.1 Selected phase angle plots for capacitance scan results obtained from Matlab

The figures C.1-10 show some of the phase angle plots that were taken from the capacitance scans conducted at the ten buses. These phase angle plots were utilized to verify the resonance point that was observed on the magnitude plots shown in the Chapter 3. The plots were plotted by varying the capacitance bank rating in steps of 10 MVAr. The resonant point was thus chosen based on proximity to zero degrees.

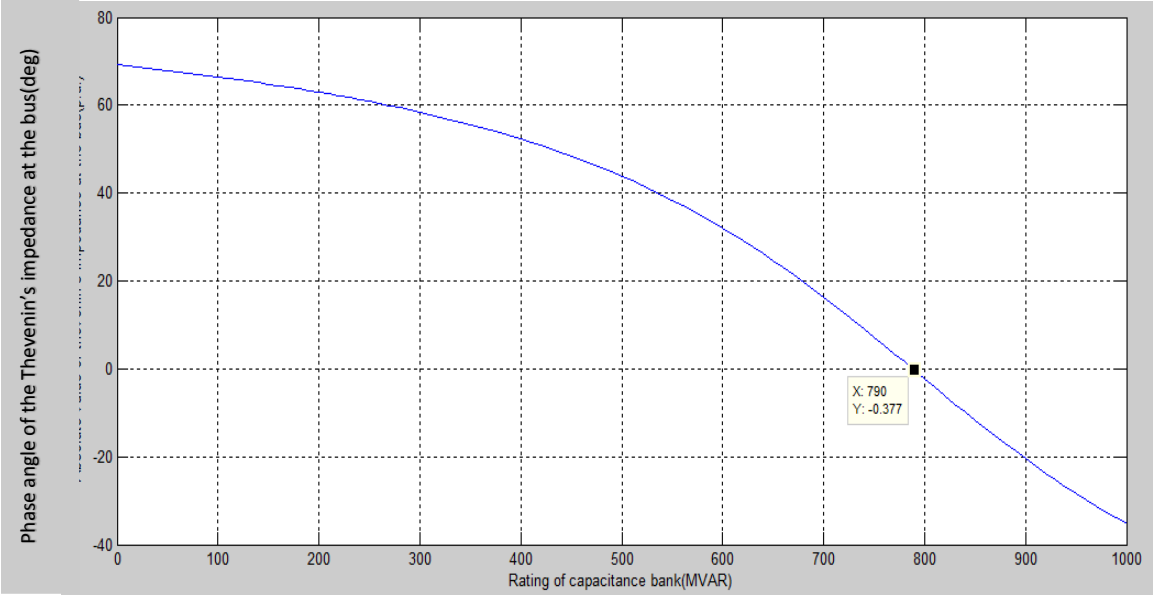

Fig. C.1 Phase Angle Plot of Capacitance Scan at Bus 1 for Harmonic Order 5

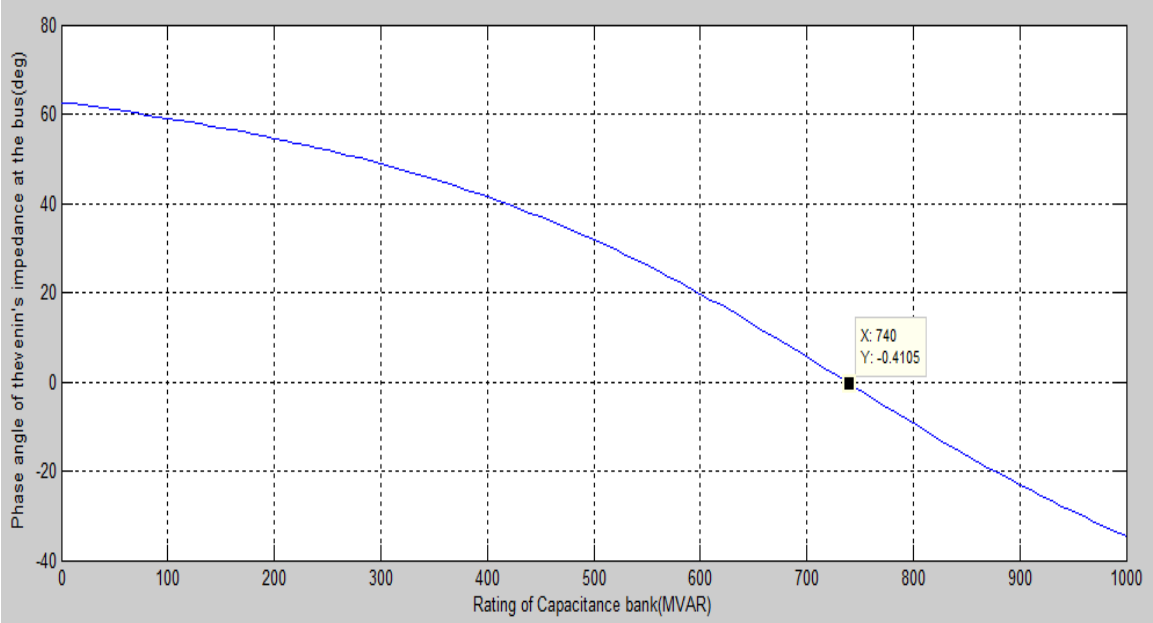

Fig. C.2 Phase Angle Plot of Capacitance Scan at Bus 2 for Harmonic Order 5

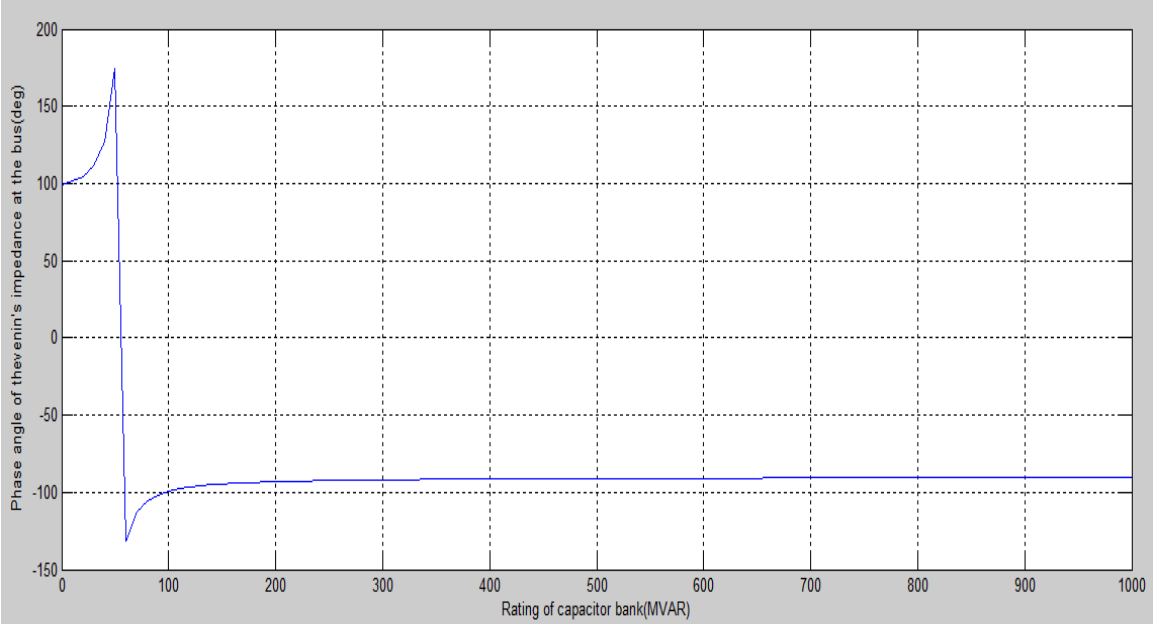

Fig. C.3 Phase Angle Plot of Capacitance Scan at Bus 3 for Harmonic Order 7

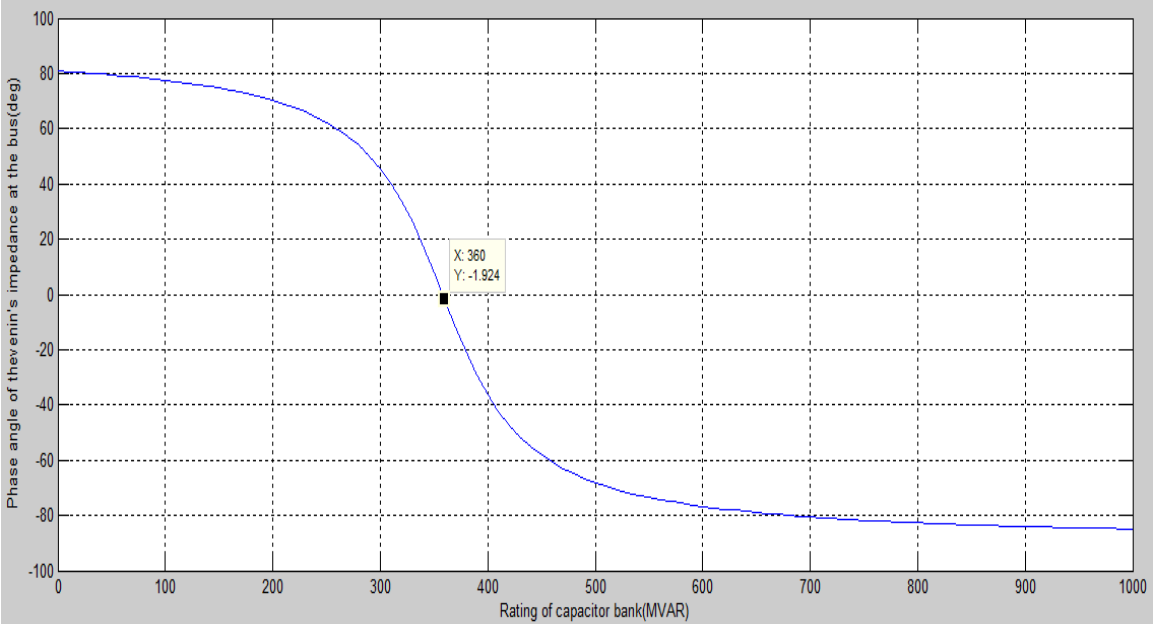

Fig. C.4 Phase Angle Plot of Capacitance Scan at Bus 4 for Harmonic Order 7

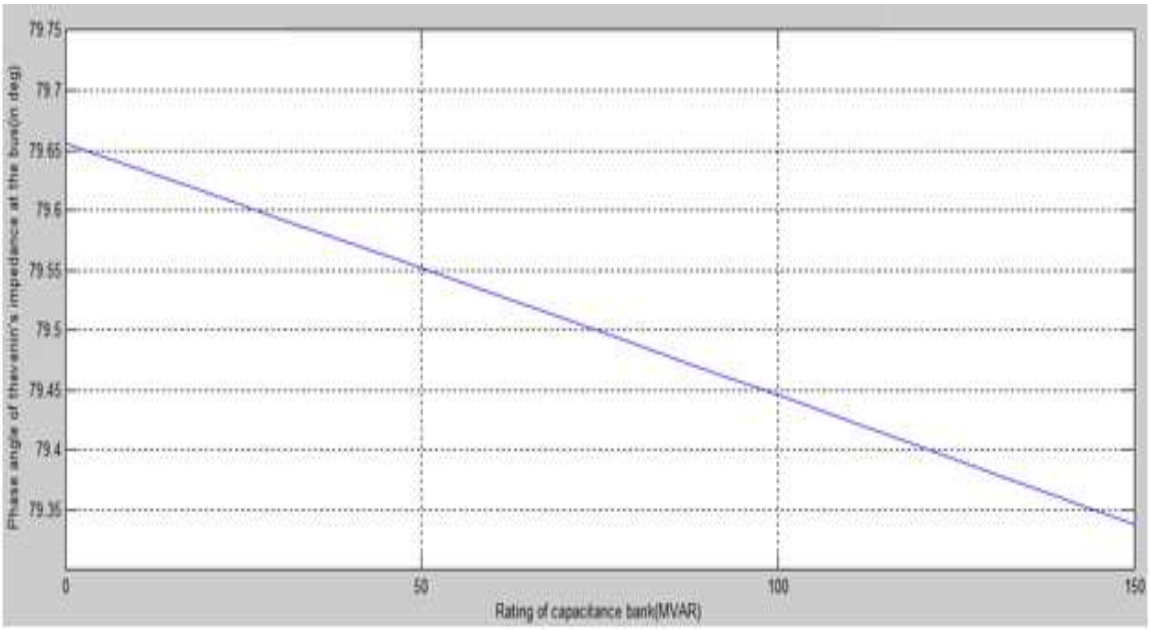

Fig. C.5 Phase Angle Plot of Capacitance Scan at Bus 5 for Fundamental Frequency

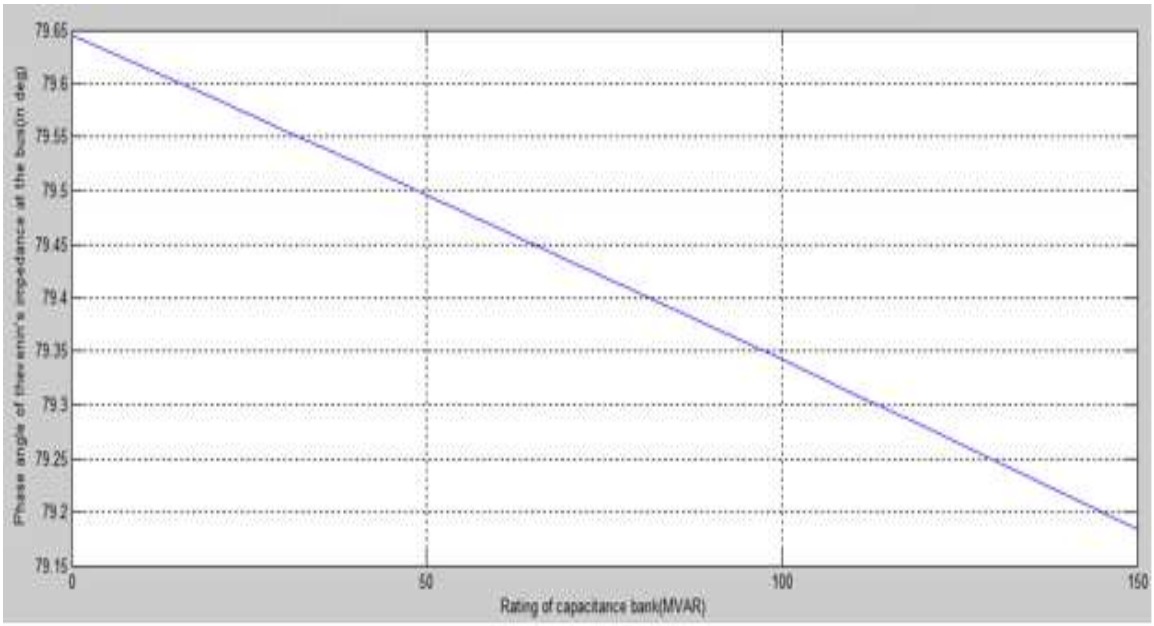

Fig. C.6 Phase Angle Plot of Capacitance Scan at Bus 6 for Fundamental Frequency

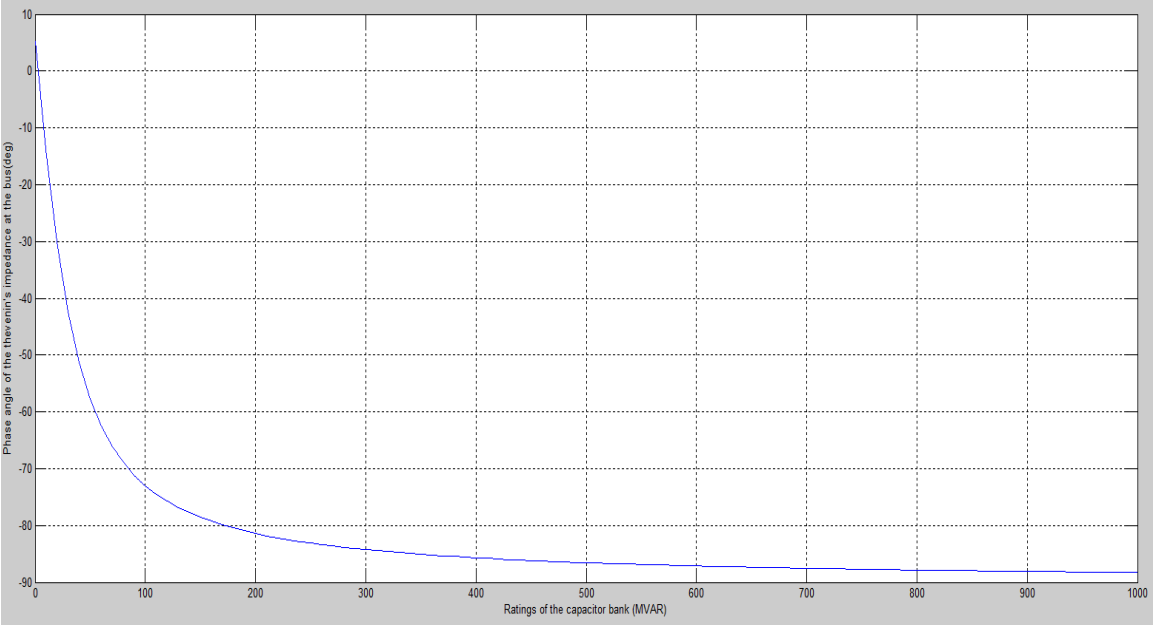

Fig. C.7 Phase Angle Plot of Capacitance Scan at Bus 7 for Harmonic Order 11

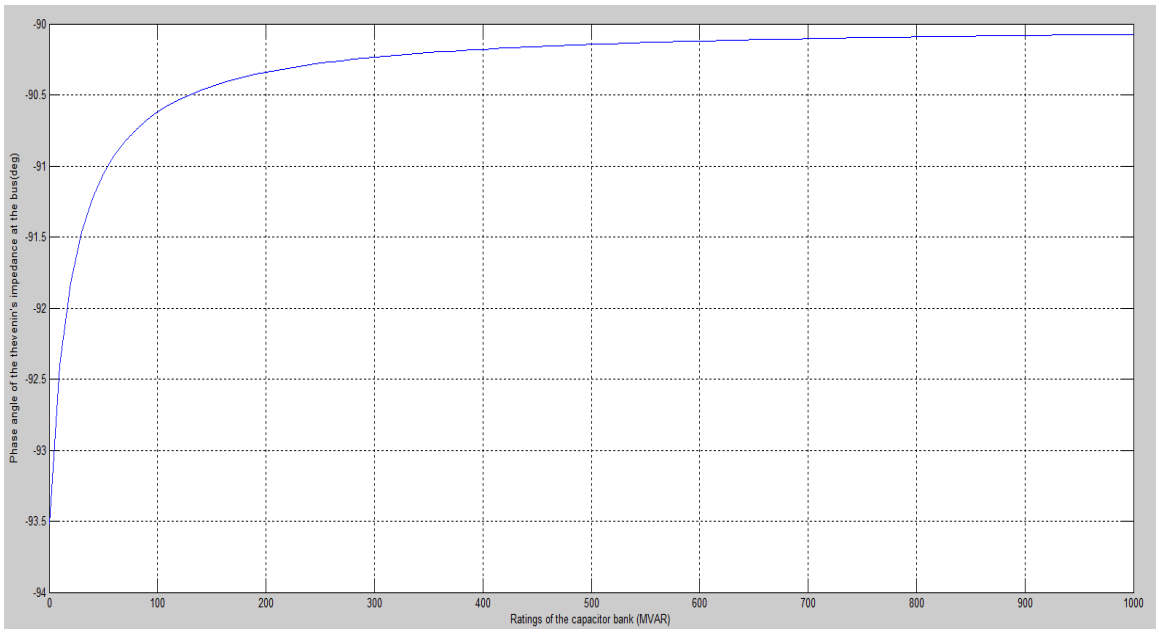

Fig. C.8 Phase Angle Plot of Capacitance Scan at Bus 8 for Harmonic Order 11

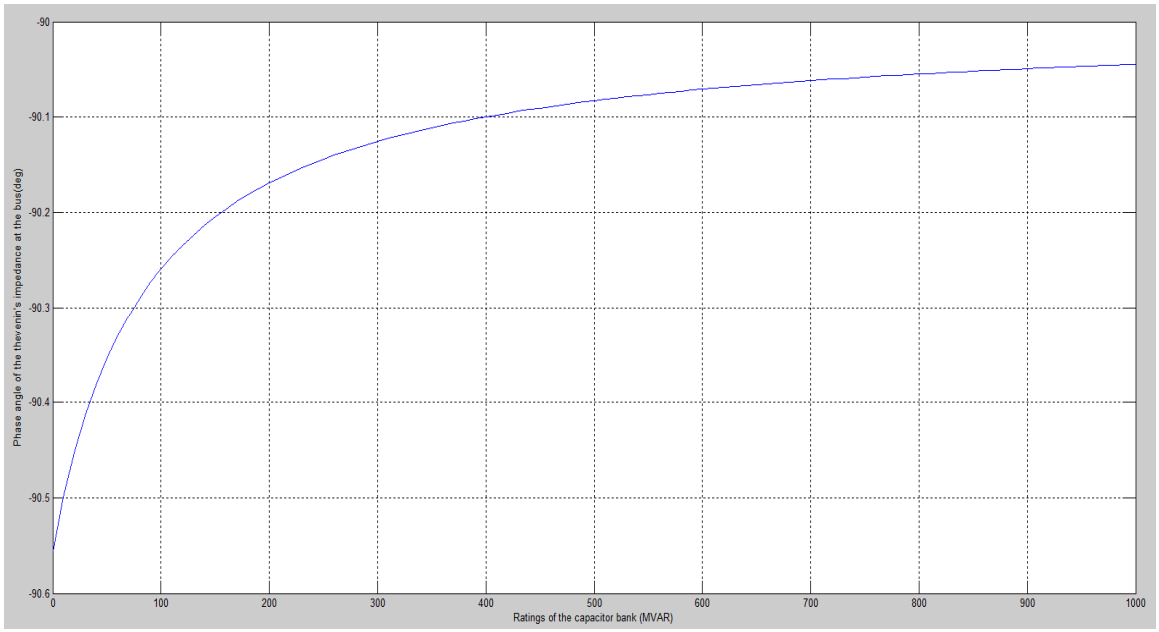

Fig. C.9 Phase Angle Plot of Capacitance Scan at Bus 9 for Harmonic Order 13

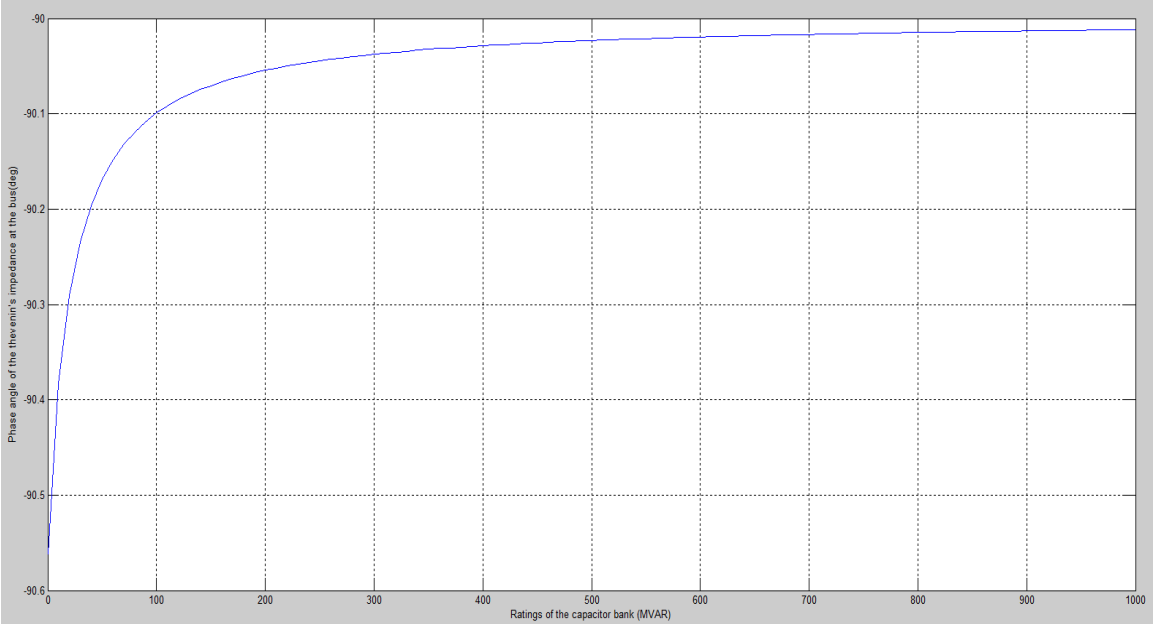

Fig. C.10 Phase Angle Plot of Capacitance Scan at Bus 10 for Harmonic Order 13

APPENDIX D

MATLAB CODE FOR EVALUATION OF IMPACT OF HVDC SOURCES

D.1 Matlab code used for evaluation of impact of HVDC sources

```
%Extraction of individual components from Bus Admittance Matrix and
change
%Ybus to any harmonic order as desired
A=sum(Ybus);
h1=1;
h=13;
for k=1:1:length(A)
    if imag(A(k))>=0  %Capacitive
        Z=1/A(k);
        Ybus(k,k)=Ybus(k,k)-A(k)+(1/(real(Z)+(imag(Z)*h1/h)*i));
    end
    if imag(A(k))<0   %Inductive
        Z=1/A(k);
        Ybus(k,k)=Ybus(k,k)-A(k)+(1/(real(Z)+(imag(Z)*h/h1)*i));
    end
end

for k=1:1:length(A)
    for l=k:1:length(A)
        if k==l
        else
            if imag(Ybus(k,l))>0 %Inductive
                Z=1/-Ybus(k,l);
                Ybus(k,l)=Ybus(k,l)-Ybus(k,l)-
(1/(real(Z)+(imag(Z)*h/h1)*i));
                Ybus(l,k)=Ybus(k,l);
                Ybus(k,k)=Ybus(k,k)-
(1/Z)+(1/(real(Z)+(imag(Z)*h/h1)*i));
                Ybus(l,l)=Ybus(l,l)-
(1/Z)+(1/(real(Z)+(imag(Z)*h/h1)*i));
            end
            if imag(Ybus(k,l))<0 %Capacitive
                Z=1/-Ybus(k,l);
                Ybus(k,l)=Ybus(k,l)-Ybus(k,l)-
(1/(real(Z)+(imag(Z)*h1/h)*i));
                Ybus(l,k)=Ybus(k,l);
                Ybus(k,k)=Ybus(k,k)-
(1/Z)+(1/(real(Z)+(imag(Z)*h1/h)*i));
                Ybus(l,l)=Ybus(l,l)-
(1/Z)+(1/(real(Z)+(imag(Z)*h1/h)*i));
            end
        end
    end
end

%Reading the line data
B=xlsread('LINE DATA.xlsx');
m=1;
for n=1:1:length(B)
    if B(n,11)<0 && B(n,3)>=500
        if B(n-1,1)==B(n,1) && B(n-1,4)==B(n,4)
            C(m,:)=B(n-1,:);
        end
```

```
        if B(n+1,1)==B(n,1) && B(n+1,4)==B(n,4)
            C(m,:)=B(n+1,:);
        end
        C(m+1,:)=B(n,:);
        m=m+2;
    end
end
xlswrite('LINECAPACITANCEDATA.xlsx',C);



%Locating series capacitor compensated lines in the WECC system Ybus
and
%modifying the Ybus
D=xlsread('WECCYbusorder.xlsx');
x=1;
r=0.00001;
y=length(Ybus);
for n=1:2:length(C)
    for m=1:1:length(D)
        if C(n,1)==D(m,1)
            k=m;
        end
        if C(n,4)==D(m,1)
            l=m;
        end
        a=Ybus(k,k)
        b=Ybus(l,l)
        c=Ybus(k,l)
        d=Ybus(l,k)
        Ybus(k,k)=Ybus(k,k)+Ybus(k,l)+1/(C(n,10)+(j*C(n,11)*h))+1/(r);

Ybus(l,l)=Ybus(l,l)+Ybus(k,l)+1/(C(n,10)+(j*C(n,11)*h))+1/(j*(C(n+1,11)
/h));
        Ybus((y+x),(y+x))=1/(r)+1/(j*(C(n+1,11)/h));
        Ybus(k,l)=Ybus(k,l)-Ybus(k,l)-1/(C(n,10)+(j*C(n,11)*h));
        Ybus(l,k)=Ybus(l,k)-Ybus(l,k)-1/(C(n,10)+(j*C(n,11)*h));
        Ybus(k,(y+x))=-1/(r);
        Ybus(l,(y+x))=-1/(j*C(n+1,11)/h);
        Ybus((y+x),k)=-1/(r);
        Ybus((y+x),l)=-1/(j*C(n+1,11)/h);
        a=Ybus(k,k)
        b=Ybus(l,l)
        c=Ybus(k,l)
        d=Ybus(l,k)
        x=x+1;
    end
end
x

%Creation of harmonic current injection vector
I=sparse(length(Ybus),1);
I(4432)=1;      %Sylmar1 bus
I(4433)=1;      %Sylmar2 bus
I(4367)=1;      %Adelantx bus
```

```
I(4368)=1;      %Adelanty bus
I(18011)=1;     %Stegall DC bus
I(18392)=1;     %Clovis bus
I(18005)=1;     %Sidney Dc bus
I(6023)=1;      %Trans bay HVDC cable terminal at Pittsburg bus

%Calculation of harmonic voltages at the required buses
V=Ybus\I;

V1=abs(V(1636))
V2=abs(V(1646))
V3=abs(V(1637))
V4=abs(V(1638))
V5=abs(V(1922))
V6=abs(V(1927))
V7=abs(V(1669))
V8=abs(V(1917))
V9=abs(V(1924))
V10=abs(V(2136))
```